USE OF TRANSIENT EFFECTS IN THE REPETITIVE DETERMINATION OF A VARIETY OF CHEMICAL SPECIES IN SOLUTIONS

By

ADEL HANNA ESKANDER-HANNA II

Bachelor of Science
Cairo University
Cairo, Egypt
1963

Master of Science
Ain Shams University
Cairo, Egypt
1968

Master of Science in Chemistry
Clarkson College of Technology
Potsdam, New York
1971

Submitted to the Faculty of the Graduate College
of the Oklahoma State University
in partial fulfillment of the requirements
for the Degree of
DOCTOR OF PHILOSOPHY
July, 1976

USE OF TRANSIENT EFFECTS IN THE REPETITIVE DETERMINATION OF A VARIETY OF CHEMICAL SPECIES OF SOLUTIONS

Horacio A Mottola
Thesis Adviser

Zuhair F. Al-Shaieb

E J Eisenbraun

John E. Moore

Norman N Durham
Dean of the Graduate College

ACKNOWLEDGEMENTS

I wish to express my gratitude to Dr. H. A. Mottola for his patience, guidance, and deep understanding throughout the course of the present investigation, and also for his assistance in the preparation of this thesis. Further appreciation is expressed to Dr. V. V. S. Eswara Dutt for his valuable suggestions related to the present work. I also acknowledge the help I have received from the members of my committee, Dr. T. E. Moore, Dr. E. J. Eisenbraun, and Dr. Z. Al-Shaieb, who have read the whole of the manuscript and made many helpful suggestions.

I am also grateful to Dr. O. C. Dermer, who has read this manuscript and has contributed to its form. The author wishes to express his gratitude to Mr. Lesley Hoy, formerly in the School of Electrical Engineering, for his great aid in using the Hewlett Packard calculator-plotter, for programming it, and giving his valuable advice. Thanks are also due to Mr. V. Gupta in the same department for his continuous help related to the use of the calculator-plotter. I am also grateful to Mr. Zubin Bharda for his help in drawing the graphs of the draft copy; Misses Jane Hanson, Pam Whitney and Nanida Damani for their help during the last days.

I wish to thank my colleague Phil Bush for his kind and unselfish cooperation during my stay in this institution, my fellow graduate students, the glass blower, Mr. Adkins, and those working in the

machine shop, especially Messrs. Hall and Friedle.

I thank the National Science Foundation for partial financial support during the course of this study; the Gulf Oil Corporation for a fellowship during the summer of 1973; the Continental Oil Company for a 1976 Summer fellowship; the Smith Kline & French Laboratories for supplying three pure phenothiazines; Dr. Cooper in the Oklahoma State University Medical Center for providing the pharmaceutical preparations, and the Chemistry Department for safeguarding financial support during my stay. I am indebted to Mrs. Janet Sallee for the excellent typing of this manuscript.

Finally, I am deeply grateful to my mother, my sisters, Aida and Enayat, and my brother Eskander for their unselfish contributions to my well-being; and lastly but not least; it is with deep meditation that I dedicate this manuscript to the memory of my late father.

TABLE OF CONTENTS

TABLE OF CONTENTS (Continued)

TABLE OF CONTENTS (Continued)

TABLE OF CONTENTS (Continued)

LIST OF TABLES

LIST OF TABLES (Continued)

LIST OF FIGURES

LIST OF FIGURES (Continued)

CHAPTER I

INTRODUCTION

The analytical signal may be defined as the response of the measuring device to the presence of the analyte, and its profile is related to time in order to distinguish a steady state from a transient one. Steady state signals have plateau profiles which correspond to equilibrium, or equilibrium-imposed, values. It should be pointed out, however, that these signals may be made transient by instrumentally imposed conditions. Unlike steady state signals, transient signals have peak profiles that correspond to nonequilibrium values, and they are caused either by the presence of transient species or by transiently imposed conditions.

Thus, one interprets the analytical signal from the viewpoint of the physical property which is related to the concentration of the analyte and the instrumental technique which is used to display the signal. In such an interpretation, both factors can be reproduced, in principle, under exactly the same experimental conditions. However, in practice, some signals can be retraced, while others cannot.

Retraceable signals are those which can be retraced when the response of the measuring device is reversed in time, i.e., when the original state is created before the signal is generated with the same analyte sample. It follows, therefore, that both the concentration of the chemical species and the response of the measuring device must have

attained stationary states. Thus, destruction of an appreciable amount of the analyte does not give retraceable signals, nor does the use of an instrumental technique which irreversibly (or even reversibly) removes the analyte from the observation unit. It follows that transient signals may be obtained by formation of transient species, transient depletion of stable chemical species, or formation of stable chemical species followed by their removal from the detection zone by instrumentally imposed conditions.

Transient signals have had widespread use in analytical chemistry with the improvement of detecting devices, auxiliary electronic circuits, and electronic readout systems which constitute an important part of the majority of contemporary analytical instruments. These signals provide a fast and accurate means for determining a variety of chemical species in solution, and potentially in other media. The time for determination is reduced greatly, typically down to seconds, in contrast to most determinations using steady state signals.

Recently, Dutt and Mottola [1] have reported the production of transient signals in some redox reactions--in one system, by monitoring the absorbance of transiently depleted ferroin. The reactions involved in this system may be represented by the following reaction cycle

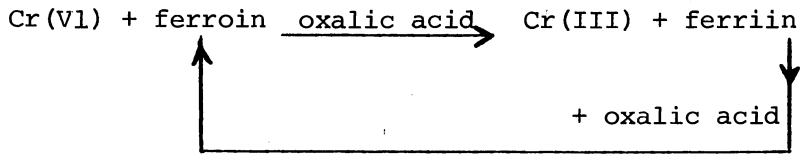

(1)

The signals produced, like other transient signals, have peak profiles in which the peak heights are directly proportional to the concentration of chromium (Vl). Dutt and Mottola have also shown that these signals

are produced by the formation of transient species, or transient depletion of other chemical species. This brings about a novel approach to fast continuous determinations where all necessary reagents, except the sought-for species, are continuously circulated through a flow-through system.

In another approach to fast continuous determination, steady state signals are perturbed to give transient signals. This may be viewed essentially as a series process where the rate of removal of the analyte species depends on the flow rate in the flow-through system. Hence, these signals are dependent upon flow rates, unlike transient signals due to transient species with profiles lasting for time periods much less than the washing cycles.

This concept has been developed in chemical autoanalyzers where the peaks recorded by a continuous flow analyzer [2] are the resultants of rise and fall curves which represent the transition between different steady state conditions. The samples are successively aspirated from their individual containers into a tube through which they move until the whole analysis is complete. These signals are considered as transient signals, where 95% or better achievement of the plateau is used before the signal is washed away. However, the greatest disadvantage of the continuous flow concept is that each sample is liable to contamination from the preceding sample; moreover, contamination increases as the rate of sampling is increased.

Recently, Ruzicka and Hansen [3] claimed that they could achieve a maximum sampling rate of 270 samples per hour using a technique they called Flow injection analysis. Their measuring technique was based on the fact that the rise curve of the signal can be used at any time as a

measure of the analyte's concentration. They injected a small volume of sample rapidly into the streaming solution of the reagent, thus forming a segment which was carried into the observation unit. The signals obtained can be treated as transient signals, but unlike the situation in the autoanalyzers, only about 75% of the steady state is attained before the signal is washed away.

It is worth mentioning, however, that as early as 1970 Pungor and coworkers [4] developed a measuring technique by which small aliquots of the electroactive species were injected into a flow-through cell. A rapid increase followed by a decrease of current with respect to time gave a peaked profile signal as the solution was injected into a supporting electrolyte streaming continuously at a constant flow rate. Later in 1974, Pungor and Fehér [5] extended their injection technique to the determination of electroinactive analytes by injection into supporting electrolytes containing electroactive species which react with the analytes. The signals obtained are transient signals having peaked profiles, and the peak areas were related to concentration.

Finally, Anderson [6] has developed a system of sampling rate above 150 samples per hour which is based on the transfer of samples and reagents by centrifugal force. After mixing, the solutions are transferred into a set of cuvettes arranged radially; these cuvettes are spun past a scanning beam of light and the absorbances are displayed as a series of peaks on an oscilloscope.

I.1. Analysis of Transient Signals

In what follows, an attempt has been made to identify transient signals in various instrumental techniques currently in use. Transient

signals encountered in instrumental methods of analysis can be divided into four main categories:

I.1.1. Spectrometric Transient Signals, obtained in analytical spectrometry such as flameless atomic absorption spectrometry, atomic fluorescence spectrometry, and luminescence spectrometry.

I.1.2. Chromatographic Transient Signals, obtained in elution chromatography with differential detection methods.

I.1.3. Signals due to Transient Species, obtained by following the concentration of a chemical species, with respect to time, without perturbing the concentration versus time profile by any technique.

I.1.4. Signals due to Transient Effects, obtained by perturbing the steady state signals generally by continuous flow analysis.

It is worth noting that, in each of these four cases, series first-order reactions and/or processes are operative in both rise and fall curves of the transient signals. In the following discussion, we shall mention in some detail, for each of the four categories, the analysis of these transient signals. We shall also discuss the relative merits of signal peak height and signal peak area measurements.

I.1-1. Spectrometric Transient Signals

The analogy between transient signals obtained in spectrometric methods of analysis, for example flameless atomic absorption spectrometry, and consecutive unimolecular processes can be drawn as follows: Solutions containing metal salts outside the analytical cell (with atoms represented by A) are introduced into the analytical cell by means of micropipettes. After drying and ashing, the residues are vaporized to atoms (represented by A_c), inside the cell. These atoms are dissipated

away from the cell. Each process is unimolecular, as expressed by Equation (2).

$$A(s/l) \xrightarrow{k_1} A_c(g) \xrightarrow{k_2} A_o(g) \qquad (2)$$

where A_o represents metal atoms outside the analytical cell, after passing through the detection zone, and k_1 and k_2 are the specific rate constants for vaporization and escape from the analytical cell, respectively.

Fuller [7] has investigated the kinetic parameters associated with the production of spectrometric transient signals due to the atomization of copper in a graphite furnace. An analysis of absorbance versus time profiles for these signals shows the following regions:

(a) a region between start of the atomization process and first detection of metal atoms;

(b) a region before the furnace reaches its preset temperature; and,

(c) a constant temperature region having the peak and the tail of the transient signal.

Fuller has experimentally verified that first-order kinetics are followed over region c of the signal's profile; i.e., the values of absorbance versus time for all results were fitted to first, second and third order rate equations and were found to agree with first-order kinetics. Therefore, the rate of formation of copper atoms can be expressed by:

$$R[Cu]_{formation} = k_1[Cu]_{unvaporized} = k_1([Cu]_o - [Cu]_{vaporized}) \qquad (3)$$

where $[Cu]_o$ and $[Cu]_{vaporized}$ are the amounts of copper at t = 0 and t = t, in the analytical cell, respectively. This equation can be integrated between t = 0 and t = t to give:

$$[Cu]_{vaporized} = [Cu]_o (1-e^{-k_1 t}) \quad (4)$$

The rate equation for the change in amount of copper atoms in the graphite furnace is:

$$\frac{d[Cu]}{dt} = R[Cu]_{formation} - R[Cu]_{removal} \quad (5)$$

where the R's represent the rates of formation and removal of copper atoms, respectively. It follows, therefore, that the rate equation expressed by Equation (5) can be rewritten as:

$$\frac{d[Cu]}{dt} = k_1[Cu]_0 e^{-k_1 t} - k_2[Cu] \quad (6)$$

which can be solved for [Cu] to yield:

$$[Cu] = \frac{k_1}{k_2-k_1}[Cu]_0 (e^{-k_1 t} - e^{-k_2 t}) \quad (7)$$

Equation (7) obtained by Fuller is identical with Equation (8) describing the concentration of an intermediate in consecutive molecular processes. Integration [8] of the differential equations relating A and A_c with respect to time yields Equation (8):

$$[A_c] = [A]_o \times \frac{k_1}{k_2-k_1} (e^{-k_1 t} - e^{-k_2 t}) \quad (8)$$

where $[A]_o$ is the initial concentration of A at time equal to zero.

Fuller calculated values of k_1 by plotting $\log_{10}$ (absorbance) versus time for region c of the signal's profile, from the slopes of the straight lines. These $\log_{10}$ (absorbance) versus time plots were made for different initial amounts of copper and different preset temperatures, and as expected for the same initial amounts larger k_1 values were obtained at higher temperatures. On the other hand, similar k_1 values were obtained for different initial amounts of copper at the same preset temperature. The same author has also calculated values of k_2 and p, where p is a constant relating [Cu] to absorbance, by a process of successive approximations. A comparison of the theoretically predicted results according to Equation (7), and the calculated values of k_1, k_2, and p with the experimentally observed results showed very good agreement.

In a subsequent publication [9] Fuller has successfully derived some quantitative relations describing pre-atomization heating losses, effects of inert gas flow rate, and signal integration. In all cases, very good agreement was obtained between the theoretical and experimental data.

Fuller [9] has shown that the percentage of copper recovered decreases greatly above a certain temperature and the comparison between the theoretically predicted and experimental values was very good. He also shows that the percentage of copper recovered decreases with increase of ashing time as theoretically predicted.

Under stopped gas flow conditions [10] k_2 approaches zero, and the maximum peak height is obtained, in other words, no copper atoms are dissipated away from the analytical cell. However, this situation is an

ideal one and has not yet been achieved in practice. At any rate, operation under stopped flow conditions was first proposed by Kahn and Slavin [10]. These authors thus obtained an improvement (over flow conditions) in the signal by a factor of 2 as compared to a factor of 1.7 reported by Fuller [9].

Finally, peak area measurements were more accurate than peak heights for small peak height values. In general, as has been confirmed by others [11], the integral method of recording yields linear working curves and good precision. This is possibly due to the fact that the integration method is independent of the duration of transfer of analyte atoms into the analytical cell, unlike the peak height method.

I.1-2. Chromatographic Transient Signals

The following discussion is intended to point to certain analogies between series or consecutive processes and changes producing the signals.

The normal trace produced by a gas-liquid chromatograph consists of a plot of the detector's response versus time. Detection may be accomplished with a thermal conductivity cell, which detects the difference in thermal conductivity between the pure carrier gas and the carrier gas containing the sample in gas-liquid chromatography. This difference in thermal conductivity generates the familiar signal, which is maximum at the peak maximum.

When the sample enters the chromatographic column it is equilibrated between the stationary phase and the mobile phase mainly either by adsorption or partition, and this equilibration may be represented by:

$$(A_M)_I \underset{k_{-1}}{\overset{k_1}{\rightleftharpoons}} (A_S)_I \tag{9}$$

where k_1 and k_{-1} are the specific first-order rate constants, A_M and A_S are the amounts of solute A in the mobile and stationary phases, respectively, and the subscript (I) designates the first theoretical plate.

Under elution conditions, this equilibration is transient and the flow of the mobile phase inside the chromatographic column is the driving force which moves the solute A through the column. This movement under flow conditions may be visualized as another process as:

$$(A_S)_I \xrightarrow{k_2} (A_M)_{II} \tag{10}$$

where k_2 is a specific first-order rate constant, and the subscript (II) designates the second theoretical plate.

Considering the number of theoretical plates in the chromatographic column as equal to N, hence the number of equilibrium steps given by Equation (9) is also equal to N. Thus the whole chromatographic process, for simplicity, may be visualized as N steps of the series processes given by Equations (9) and (10).

Series or consecutive processes also occur at the detector where the familiar peaked signal is generated. At the base line, the difference, for example, in the thermal conductivity between the pure carrier gas and the carrier gas containing the solute is initially zero. This difference, which is related to the concentration of the eluted solute, starts increasing at the beginning of the rise curve, and reaches its maximum value at the peak maximum. This maximum corresponds theoreti-

cally to a plate where the solute desorbed from it exceeds the equilibrium concentration in the next plate. After the peak maximum and following the fall curve, the difference starts decreasing until it reaches the base line again. Thus, if the flow rate is kept constant during the recording of the chromatogram, a plot of ln (detector response) against time should give a straight line for the rise curve, if first-order kinetics are followed; similar plots should also give straight lines for the fall curves.

A quantitative analysis of an ideal chromatogram can be obtained by measurement of the areas of all the peaks. This ideal chromatogram refers to the chromatogram in which all peaks are symmetrical Gaussian curves, and in which the peak height for any component is proportional to the peak area. The concentration C_x of any component x is given by the equation:

$$C_x = a_x A_x / \Sigma(a_1 A_1 + a_2 A_2 + a_3 A_3 + \ldots) \qquad (11)$$

where the areas are the A's and the a's are calibration constants which relate each peak area to the amount of component [12]. In the case of an ideal chromatogram, the calibration constants a_1, a_2, etc. cannot all have the same value; this is unlike the case of an ideal detector where these constants would either all be the same or bear a simple relationship to the molecular structure of each component. Real chromatograms and most real detectors differ from the ideal in the following ways: the detectors are linear over only a limited range, their responses frequently not simply related to the weight or molecular weight of components; and peaks are often unsymmetrical.

As for spectrometric transient signals, the relative precision of

the two types of measurement, peak areas or heights, depends to some extent on the shape of the peaks. However, peak area measurements are more precise than peak height measurements.

Steady-state signals may be encountered in column chromatography by frontal analysis [13] where the column is saturated with the solvent and washed continuously with a relatively large volume of the analyte solution. Displacement-development chromatography [13] superficially resembles the frontal analysis process in that the chromatogram has a series of horizontal plateaus. In displacement-development, however, the sample is washed with a mixture of the solvent and a strongly adsorbed substance. It should be noted that both frontal and displacement analyses generally provide poorer separations of multicomponent samples than the elution techniques, but they have certain advantages in preparative- and production-scale separations, concentrating trace impurities, and purifying large volumes of gases or liquids.

I.1-3. Transient Signals Due to Transient Species

Recently, Dutt and Mottola [1] have demonstrated the production of transient signals in redox systems by monitoring the absorbance of transiently formed intermediate species with time. The signal profile shows a peak that is related to the concentration of some species for example, chromium (VI). Oxidation of ferroin with Cr(VI) produces ferriin which is reduced back to ferroin with excess oxalic acid. This reaction may be considered as a series of first-order reactions [8] in which ferriin concentration is a function of both the forward and backward rate constants, corresponding to its formation and decay, and to its initial concentration. The peak profile becomes less pronounced as

the rate constant of the decay reaction becomes larger, and accurate determinations from peak heights become doubtful. However, the rate of the forward reaction can be made large and the backward reaction as slow as feasible, so as to increase sensitivity and directly relate peak height to concentration. In the above case, Cr(VI) can be determined by injection into a solution containing ferroin and oxalic acid. A transient signal is obtained whose height is directly proportional to the Cr(VI) concentration.

If one considers the case

$$A \xrightarrow{k_1} B \qquad B \xrightarrow{k_2} C \tag{12}$$

the concentration-time relations for substances A, B, and C may be visualized most effectively using dimensionless parameters and variables. These variables, α, β, and γ, are essentially concentrations of A, B, and C relative to the initial value of A. The remaining variable is $\tau = K_1 t$; the value $\kappa = K_2/K_1$ is a parameter. This visualization can be made by considering plots of α, β, and γ as functions of τ for various values of κ, the ratio of the rate constants. It is of interest to note that the concentration of the intermediate B, as measured by β, goes through a maximum given by:

$$\beta_{max} = \kappa^{\kappa/(1-\kappa)} \tag{13}$$

which becomes less pronounced as κ gets larger. As far as C is concerned, its rate of formation is characterized by an "induction period" whose duration is equal to the time for B to reach its maximum value. At any rate, generally a plot of another function $\delta = \beta + 2\gamma$ versus τ

is a useful measure of the extent of reaction and is more closely related to what is usually measured in a reaction than is β or γ alone [8].

The above case corresponds to an intermediate B, which decays into another species C. Useful analytical information can be taken from the peak height more simply than from the induction period of C, which is arbitrarily taken as the time to reach the point of inflection on the C versus t curve. This is because the induction period corresponds to the value $d^2C/dt^2 = 0$ ($dB/dt = 0$) and it is a well known fact that noise increases with differentiation. In addition, sharp peaks are needed for accurate repetitive determinations which make the measurements of peak heights more reliable.

With respect to peak height as compared to peak area measurements, the advantages of peak area measurements are reduced as the rate of rise of the curve increases considerably. However, the relative merits of the two types of measurements are comparable to those for spectrometric transient signals.

I.1-4. Transient Signals Due to Transient Effects

The following analysis deals with the kinetic parameters associated with the transient state, occurring between steady states, in the continuous flow analyzers [14].

A strip chart record tracing of a physical property versus time in continuous flow analysis shows the following characteristics. For a certain period of time no effect is noted; then the detector senses the change in physical property of the analyte and displays it along a line called the rise curve. If time in of sample-period is sufficiently pro-

longed, a sample steady state is achieved, after which the inlet is removed, and thus a period of-time out of sample has begun. A fall curve thus follows, and if the latter time is prolonged, the base line will again be reached.

Thiers and coworkers [14] have shown, by using different graphic expressions, that during the transient state in continuous flow analysis, the rise curves follow first order kinetics as expressed by Equation (14).

$$\frac{dc}{dt} = k_1(C_{ss} - C_t) \tag{14}$$

where C_{ss} is the final steady state concentration of the analyte, and C_t is its apparent concentration at any given time. The fall curves, however, follow kinetics which are first order with respect to the apparent concentration itself C_t.

$$\frac{dc}{dt} = - k_2 C_t \tag{15}$$

It has also been experimentally demonstrated by Thiers et al. [14] that all the rise curves, for any given concentration, are only parts of the one basic rise curve. It follows, therefore, that the initial slope of a rise curve, and the point it reaches after any given time, is as good a measure of concentration of the analyte as the final steady state. On the other hand, since all fall curves in a given system have the same fundamental shape, they should be superimposable upon each other by movement parallel to the time axis.

The familiar sample peaks are formed from the intersection of the rise and the fall curves during a given time, t_{in}, time in sample.

These curves can be considered to represent series processes with rate constants describing the rise and fall curves, respectively. Thus, these curves are expected to overlap when samples are aspirated one after the other, and such overlapping should be additive in concentration of the analyte. The same authors have shown that two characteristic parameters of continuous flow analysis, namely the half-wash time $W_{1/2}$, and the lag phase time L, can be used to quantitatively correlate some characteristic properties. The first parameter is obtained from the slope of the straight portion of the log C_t versus time plot, while L is calculated from the time at which the extrapolated crosses the time axis.

The percentage of C_{ss} reached at any given time may be calculated from the expression:

$$\frac{t_{in} - L}{W_{1/2}} \qquad (16)$$

Obviously if t_{in} is sufficiently long for 100% of sample steady state to be reached, variations in t_{in} will have no effect on the peak maximum. It is therefore clear that the percentage of sample steady state achieved is affected by the value of t_{in}, and not by the value of t_{bs}, time between successive samples. On the other hand, the observed percent interaction between successive samples can be expected to be affected only by t_{bs} and not by t_{in}.

The previous treatment has been developed by Thiers and coworkers [14] for the analysis of the kinetic parameters associated with the Technicon Autoanalyser's signals. A continuous flow analysis, using an injection technique, has been developed by Pungor et al. [4] where volt-

ammetrically active compounds were injected into a flow of supporting electrolyte.

A theoretical treatment of the voltammetric signal obtained by Pungor et al. [4] showed a very good agreement with the experimental results. This treatment can be summarized as follows:

(A) At a constant flow rate V, the rise curves follow first-order kinetics as expressed by the equation:

$$\frac{dc}{dt} = k_1 \left[\frac{M}{W\tau} - \frac{CV}{W}\right] \tag{17}$$

where W is the volume of the stirring unit, M is the amount of sample injected into the streaming solution, τ is the time elapsed between injection and first detection, and C is the concentration of the voltammetrically active compound at time t.

(B) The fall curves of these signals follow first-order kinetics with respect to one concentration term only:

$$\frac{dc}{dt} = - k_2 \left(\frac{CV}{W}\right) \tag{18}$$

The analogy between Equations (17) and (18) and Equations (14) and (15) for the continuous flow analysis has thus become clear with $\frac{CV}{W}$ standing for C_t and $\frac{M}{W\tau}$ standing for C_{ss}.

The simplicity of the peak height measurements makes it an obvious choice, especially if about 95% of the steady state, or above, has been attained. Thus peak height measurements are applicable in continuous flow equipment such as the Technicon Autoanalyzer, and the signal heights can be related precisely to concentrations. However, signals obtained in the Flow Injection Analysis by Ruzicka [3] have been related to the

amounts injected through their heights, though about 75% of the steady state has been achieved. This is due to the fact that peaks are narrow, and they present greater difficulties in exact determination of their areas.

As previously mentioned, Pungor et al. have shown that a linear relation exists between peak areas and the amounts of injected species. Their work has also shown that peak area measurements are more precise than peak height measurements since the signal's profiles are rather broad.

CHAPTER II

SOME APPLICATIONS OF TRANSIENT SIGNALS IN ANALYTICAL CHEMISTRY

The signals obtained in flameless atomic absorption, emission, and atomic fluorescence spectrometry are transient signals having peaked profiles [15, 16]. In the first case, these signals are produced by the absorption of electromagnetic radiation followed by the dissipation of the absorbing species away from the light path. Thus, atomic absorption spectroscopy with continuous sampling devices does not give transient signals. In principle, however, the signals produced by atomic fluorescence spectroscopy are transient following the nature of the process, i.e., absorption followed by emission within 10^{-8} - 10^{-9} seconds.

All processes of luminescence [17] involve these steps: absorption of energy, change in energy state, and emission of the absorbed energy, all of which may be brought about by a wide variety of processes. Luminescence may thus be defined to cover such forms of light emission as caused by chemical, biological, cathodic, and photonic processes. Luminescence is subdivided into fluorescence, in which the excited state exists for less than 10^{-8} second, and phosphorescence, in which the excited state lasts for more than that time. The signals obtained in analytical fluorescence spectrometry are transient signals as in chemiluminescence [18]. In phosphorescence measurements, the signals are

also transient [19]. Fluorescence is more extensively used because it can be measured under a wider range of conditions than can phosphorescence.

The analytical signals in chromatographic techniques may be discussed in terms of retention and equilibrium with respect to linear elution chromatography at linearly isothermal conditions where the distribution of the solute molecules is approximately at equilibrium at the band centers. By comparison, nonlinear isotherms are encountered in nonlinear elution chromatography, which leads to fronting or tailing in band shapes. Since analytical separations are carried out under linear isothermal conditions, whenever possible, which produce symmetrical band shaped signals, the signals from linear elution will be considered transient in the present context [13].

The analytical signals obtained by Pungor et al. [4] in their voltammetric study of active substances injected into electrolyte flowing streams are transient. The signals obtained have peak profiles due to the abrupt injection of the electroactive substance which causes the current to increase suddenly and then decrease to the base line. The same authors [5] have shown that the injection technique can be applied to many amperometric and biamperometric situations.

In continuous flow analysis [2] the signals obtained are transient signals due to the intersection of rise curves and fall curves. The Flow Injection Analysis technique reported by Ruzicka and Hansen [3] also produces transient signals in the present context. All these signals, including those reported by Pungor et al. [4, 5] are obtained by perturbing the steady-state signals by the continuous flow of reagents, and this has been discussed earlier.

The above presentation is an outline of transient signals obtained in instrumental methods of chemical analysis, and does not include transient signals produced due to transient species as described in Chapter I. However, the purpose of the following review is to report in some detail the applications of transient signals in chemical analysis. Only a very brief note about chromatographic applications will be mentioned within the scope of the present review, and one should refer to the current literature for a review of these.

II.1. Spectrometric Applications

Applications of transient signals in analytical spectrometry will be discussed under two main headings: flameless atomic absorption and atomic fluorescence methods, and molecular fluorescence and phosphorescence methods. Some applications of atomic emission spectrometry are also included under the first heading, and only applications of chemiluminescence are cited with respect to molecular fluorescence methods because of its extensive use in analysis.

II.1-1. Flameless Atomic Absorption and Atomic Fluorescence Methods

In atomic absorption and atomic fluorescence spectrometry there are two useful specifications: sensitivity and detection limit. The sensitivity is defined as the concentration of the analyte atoms in solution of the amount in weight units per sample weight, usually in ppm, that produces an absorbance of 0.0044, which is equal to 1% absorption. The concentration of the analyte that gives a signal-to-noise ratio of 2 is the detection limit.

The work of Donega and Burgess [20] illustrates the analytical potentiality of the electrothermal heating of the sample on a tantalum boat in an enclosed chamber to produce the atomic vapor. Direct determination of copper, chromium and manganese with detection limit of about 10^{-12}g; molybedenum, nickel, and silicon in about 10^{-9}g; and platinum in about 10^{-7}g, has been achieved.

The behavior of the carbon filament atom reservoir in the atomic absorption and atomic fluorescence of trace metals extracted from aqueous solutions into a variety of organic solvents has been studied by Aggett and West [21]. They found that the behavior of the systems of silver, cadmium, copper, lead, and zinc is virtually identical to that of the aqueous solutions of the metals. The atomic fluorescence method provided lower limits of detection than the atomic absorption method.

Anderson, Maines, and West [22] have studied the effects of 62 ions present in 1000-fold amounts on the determination of 10^{-9} - 10^{-11}g of Ag, Bi, Cd, Cu, Hg, Mg, Pb, Tl, and Zn by atomic fluorescence spectroscopy. These authors found that the matrix effects can be minimized in atomic absorption by illuminating a certain space above the carbon filament.

Sequential atomization from a graphite rod was utilized for the rapid determination of copper and silver in used lubricating oils, gold, lead, ores, and other mining samples [23]. The current is first increased to give a cavity temperature sufficient to atomize the silver, then it is further increased so as to atomize the copper. The determination of several elements can be accomplished by atomizing such elements as arsenic, lead, and silver while elements such as copper, iron, nickel, and chromium remain on the graphite.

Talmi and Morrison [24] have described the use of an induction furnace in atomic absorption and emission spectroscopy for the direct analysis of solid microsamples of geological, metallurgical, or evaporated solutions of biological solutions. All elements of Groups IB, IIB, IIIA, excluding thalium, IVA excluding carbon, VA, VIA excluding oxygen and polonium and the first transition period have been determined by atomic emission. The absolute sensitivities of the furnace are inferior by one or two orders of magnitude to those given by other atomizers. However, the larger samples allowed compensates for this disadvantage. Also, it is possible by this method to determine such elements as iodine and other nonmetals which are difficult to determine by atomic absorption and emission spectrometry.

The use of a tungsten filament atom reservoir in flameless atomic absorption spectroscopy has been illustrated by the work of Cantle and West [25] for the analysis for Zn, Cu, Pb, and silver. In this work, greater sensitivity and fewer matrix effects were obtained than with the carbon filament atom reservoir.

Massman has reported in 1968 [16] the use of graphite cells in trace determination of several elements by atomic absorption and fluorescence analyses. The detection limits obtained are in the range 10^{-10} to 10^{-12} g for atomic absorption and are generally lower for atomic fluorescence analysis.

The primary advantage of atomic fluorescence compared with atomic absorption or atomic emission spectrometry is its inherent sensitivity. However, in the absence of an intense stable source of excitation for all elements this cannot be realized. The number of its applications available in the literature is small, compared with atomic absorption

spectrometry. This is because atomic fluorescence is a relatively new technique and further developments are necessary before it is regarded as a routine or preferable method.

II.1-2. Molecular Fluorescence and Phosphorescence Methods

The chemiluminescence of luminol in aqueous alkaline hydrogen peroxide is catalyzed by many metal ions as reported by Weber and coworkers [26]. This catalytic effect is not only observed down to very small quantities of the metal ions, but is also sharply dependent on the valence state of the metal. Both these properties have been used in qualitative and quantitative analytical applications of the luminol reaction as a chemiluminescent method in trace-metal analysis. Some metal ions, such as those of vanadium, zirconium, and cerium, exhibit inhibiting effects on chemiluminescent reactions catalyzed by other metal ions and have been determined accordingly.

An example of catalytic action is that utilized by Seitz, Suydam, and Hercules [27] where the luminol chemiluminescent reaction permitted the determination of trace concentrations of Cr(III) down to 0.025 ppb in the presence of other metal ions. Interference from other metal ions was effectively eliminated by adding EDTA, which forms the trivalent-chromium complex much more slowly than the other metal ion complexes.

Ferrous iron, among the common metal ions, is probably the only ion which catalyzes the luminol-oxygen reaction to the extent that a detection limit of about 0.005 ppb has been reported [28]. In some cases an activator may be used to increase selectivity and sensitivity as in the determination of Mn(VII), where a sensitivity of 0.08 ppb

[29] has been achieved.

The chemiluminescence of luminol in aqueous solution is dependent on three factors. One of these has already been mentioned, namely, metal catalysis; the other two are: presence of hydrogen peroxide, or any oxidant, and pH. Each of these factors can thus be assessed by the use of a sensitive photomultiplier to measure the intensity of light produced. Several analyses for inorganic compounds, oxidants or inhibitors, are based on their action on the luminol system. For example, active chlorine has been determined, in industrial brines and in municipal drinking water [30] by its oxidizing action on the luminol-hydrogen peroxide reation, down to about 0.5 ppm.

Cyanide ions in sea water have been determined by their inhibiting effect on the chemiluminescence of the luminol-hydrogen peroxide-Cu(II) system at concentrations as low as 3 ppm [31].

Several organic compounds such as amino acids, hematin compounds, and organic phosphorus compounds modify the chemiluminescent reactions either by reducing or amplifying the light reaction. Amino acids exhibit catalytic effects on the luminol-hydrogen peroxide system and inhibiting effects on the luminol-hydrogen peroxide-copper amine system [32]. Hematin exhibits a catalytic action on the former system, where it may be determined at about 0.06 ppb [33].

Determination of aliphatic alcohols [34] has been attempted by the effect of the alcohol on the pH at which luminescence is observed. It has been observed that many other organic compounds modify the chemiluminescent reactions and have been determined accordingly.

There are also quite a few special applications of chemiluminescence. In forensic chemistry, for example, blood stains can be identi-

fied even when diluted $1:10^7$ times [35]; in dosimetry, where irradiation of water in the presence of the luminol system produces hydorgen peroxide which forms the basis for the determination of doses below 1000 rads [36]; in microbial analysis, where the microorganisms activate the chemiluminescent reaction, permitting the determination of 10^3 - 10^5 cells of bacteria per ml of water [37]; and in polymer chemistry, where oxyluminescence may be employed [38] for estimating the stability of a polymer toward oxidative degradation.

Chemiluminescence is just one type of luminescence, and has been selected as the subject of the above discussion because of its very rapid progress compared to research made on other types. Other types of luminescence are named by the source of the excitation energy, such as bioluminescence and thermoluminescence.

The intensity of phosphorescence of some species such as polynuclear aromatic hydrocarbons is enhanced by the presence of some heavy atoms such as halogen atoms [39]. The effect of halogen substitution on the luminescence of aromatic hydrocarbons is of considerable importance to chemists. One generally observes that as the substituent series F, Cl, Br, I is traversed, phosphorescence is increasingly favored relative to fluorescence. Paramagnetic ions are also effective quenchers of phosphorescence in many instances since the acetylacetone complexes of paramagnetic transition metal ions are not phosphorescent whereas the same complexes of their diamagnetic ions are phosphorescent. This heavy-atom effect has been utilized in phosphorescence measurements to increase both their selectivity and sensitivity. However, because of the long lifetime of phosphorescence, molecules can easily lose their energy by radiationless processes, mainly by collisional deactivation.

This is the reason for performing the measurements almost exclusively at liquid nitrogen temperature, although some attempts were made at room temperature with rigid transparent organic glasses [40].

As a consequence of its selectivity and sensitivity, phosphorimetry has been mainly applied in the areas of biology and medicine. Several drugs such as procaine and cocaine were determined in urine and blood [41] with detection limits of about 10^{-8} g/ml. Detection limits of 10^{-9} g/ml have been achieved in the determination of sulfonamides in blood such as sulfamerazine, sulfapyridine, sulfamethazine, and sulfacetamide [42]. Phosphorimetry has also been applied in the assay for biologically active molecules such as purines and pyrimidines [43], where different lifetimes have been determined; in the analysis for amino acids and proteins [44], which give different emission spectra; and in the determination of many other compounds like nucleic acids, nucleotides, enzymes, and nucleosides [45].

The phosphorescence characteristics of 52 pesticides, including several degradation products, were surveyed by Moye and Winefordner [46]; 32 pesticides have been determined with detection limits ranging from 10^{-7} to 10^{-11} g/ml for isolan and p-nitrophenol, respectively. In the analysis of pesticides by phosphorimetry, the method is considerably more sensitive than other analytical methods such as gas chromatography, fluorometry, and absorption since in phosphorimetry the detection limits are lowered by a factor of 1000.

Finally, the use of phosphorescence lifetimes has been demonstrated by Drushel and Sommers [47] in the identification of nitrogen compounds separated from petroleum. The same authors [47] have also presented a phosphorimetric assay of about 100 aromatic compounds containing sulfur,

nitrogen, and oxygen.

There are several methods of achieving selectivity in the measurement of mixtures of phosphorescent compounds: excitation resolution, emission resolution, phosphoroscopic resolution, and time-resolved phosphorimetry. The first three methods depend upon varying the excitation wavelength, the emission wavelength, and the time of measurement respectively. Time-resolved phosphorimetry is based on the fact that two molecules which differ by approximately a factor of 10 in their decay times and whose concentrations are about equal give a combination of two straight lines when the logarithm of the phosphorescence intensity is plotted against time.

II.2. Chromatographic Applications

The great importance of chromatography arises from its speed, resolving power, and ability to handle small amounts of material. A further advantage for many chromatographic applications may be the simplicity of technique and equipment. The resolving power of chromatography is illustrated in the separation of 175 compounds from human urine by ion-exchange chromatography [48]. Speed of chromatographic separation may be illustrated by the resolution of 10 isomers of heptane in less than 60 seconds by gas-liquid chromatography [49]. Some forms of chromatography are able to achieve routine separations and analysis below the nanogram level [50].

II.3. Transient Signals Due to Transient Species

Transient signals produced in other methods than those given earlier can also be used in analytical determinations with various degrees of

accuracy based on the physical or chemical change and its measurement.

For example, oxidation of chlorpromazine hydrochloride [51], a thiazine, in acid solution gives an intense red color due to a free radical or semiquinone, which is further oxidized to a colorless sulfoxide. Monitoring the absorbance of this red color with time will produce a transient signal; the peak height can be used to determine the concentration of the thiazine in a rapid and simple manner. Thus, more than twenty phenothiazine derivatives which are used in medicine at the present time as major tranquilizers and neuropletics can be quantitatively determined utilizing these transient signals.

Other examples which can be cited are diphenylamine and its derivatives, diphenylbenzidine and its derivatives, and 3,3'-disubstituted benzidines such as the dimethyl or dimethoxy compounds. These compounds show certain common features in their reactions [52]. For example, the colorless reduced form of the indicator is oxidized to a deeply colored form, the first two giving blue or violet oxidation products and the third group giving yellow or red color. They also show an intermediate between the reduced and the oxidized forms. These intermediates are either inherently unstable or are unstable to excess oxidant, and are irreversibly destroyed with the formation of insoluble products, which are yellow or green for the first two groups, and brown for the third group. These facts are not in dispute, but their utilization in producing transient signals deserves a brief explanation. By optimizing the experimental conditions such as concentration of indicator and acidity these intermediates are made more transient and their absorbance time profiles show transient signals. In this way quantitative determination of oxidants such as dichromate and vanadium (V), hexacyanoferrate

(III), cerium (IV), and other oxidants of potentials higher than the indicator's formal potential can generally be made.

Oxidation-reduction indicators of formal potential less than 0.76 volt [53] have limited applications in general, but they are in use in biological work as a means of measuring the oxidation-reduction potentials of particular systems. The range of formal potential under consideration, different from previous indicators with formal potentials more than 0.76 volt, is such that the indicators are only of use with strong reductants such as chromium (II), vanadium (II), titanium (III), tin (II), and ascorbic acid, solutions of which are unstable in the presence of oxygen. However, reduction of some indicators to give colored unstable intermediates may be utilized to produce transient signals of analytical significance by optimization of the experimental conditions. Procyanine, which belongs to the azines, is reduced in acid medium to a green semiquinone which is further reduced by excess reductant to a colorless product.

To summarize, the systems mentioned are those producing transient species; then the experimental conditions are optimized to give transient signals. In practice, one of the reactants to be determined is injected into a uniformly stirred solution containing excess of the other reactants while the formation and decay of the transient species is monitored with time.

This novel approach to nonequilibrium, or Kinetic-based determination has been recently reported by Dutt and Mottola [1]. In one system, the oxidation of ferroin, tris (1, 10-phenanthroline) iron (II), by chromium (VI), in the presence of a large excess of oxalic acid produces a transient signal under optimal experimental conditions. Thus,

chromium (VI) has been determined in concentrations as low as 0.09 μg/ml when injected into a mixture containing all the other reactants where the absorbance of transiently depleted ferroin is monitored with time. The same authors have also indicated the potentiality of the method in fast continuous determinations of a variety of chemical species in solution.

II.4. Transient Signals Due to Transient Effects

The transient signals obtained in continuous flow analysis have been used extensively in the determination of a wide variety of chemical species in solution. It is sufficient to say that the number of publications about the use of Technicon Autoanalyzer exceeds one thousand. There were three symposia in 1969, 1970, and 1971 held by Technicon, from which the following applications are arbitrarily selected [54].

In the field of clinical chemistry and chemical research, various processes have been automated: determination of fatty acids, human serum albumin, ATP, glucose in plasma and urine, and total and inorganic sulfate in serum and urine. Also possible are in vivo monitoring of inorganic ions, multiple blood parameters, and biochemical analyses. The Autoanalyzer has also been used in hematological applications such as optical techniques of particle counting; and in immunological applications such as diagnostic complement fixation techniques in microbiology, and diagnostic services in the public health laboratory. In biochemical research, processes such as combined amino acid and peptide analysis of physiological fluids, and resin deproteinization of animal and plant physiological extracts for free amino acid analysis have also been automated.

Industrial analysis has also a large share in the use of continuous flow analysis. Agricultural applications include determination of insecticidal organophosphates and carbamates, soil analysis, and determination of fermentation products. In environmental science, automated analysis has aided in such areas as air quality monitoring, choice of analytical parameters in water and water analysis, and chemical oxygen demand. Applications in the pharmaceutical industry include methods such as steam distillation and assay of diazotizable aromatic amines, automatic dispensing analysis for the assay of individual tablets, and enzymatic determination of penicillin G. Finally, processes of importance in areas of metallurgy and inorganic analysis, such as analysis of cement materials and allied silicates and analysis of steel, have also been automated.

Pungor et al. [4, 5] have applied their techniques for the determination of different compounds with the proper selection of the streaming solution or the injected solution. Polarographic determination of calcium and magnesium by injection of their solutions in a continuously flowing solution of EDTA have been made. Phenol has also been determined voltammetrically by injection of a given amount of potassium bromate-bromide mixture in an acidic solution of supporting electrolyte, then into acidic phenol solutions of different concentrations.

Ruzicka and Hansen [3] have applied their flow injection analysis system to the spectrophotometric determination of phosphate, based on the measurement of molybedenum yellow as well as molybedenum blue. They have also applied it in the potentiometric determination of ammonia using an ion selective electrode as a detector. The main advantages of their continuous flow analyzer is that a sampling rate of over 200

samples per hour can be achieved with a very high degree of accuracy and precision.

Bergmeyer and Hagen [55] have developed a new method for the continuous enzymatic analysis for glucose. In their system, water-insoluble carriers containing fixed enzymes can be used continuously, and with a single defined activity more than 10,000 determinations can be made. A buffer solution was continuously pumped and the samples were fed, by a novel applicator, into the continuous flow system. After the oxidation of glucose in aqueous solution catalyzed by the fixed enzyme, an oxygen-sensitive electrode was used as the detector.

The development of fast analyzers through centrifugal transfer for mixing of samples and reagents has been developed in Oak Ridge National Laboratory. The potentiality and applicability of this technique is described in Anderson's article [56].

Finally, transient signals have also been produced in flame atomic absorption spectrometry with the use of one-shot sampling devices with laminar burners. An interesting injection technique is that developed by Sebastiani, Ohlo and Reimer [57] in which the samples are sucked into the burner. The characteristics of this technique have been recently investigated by Berndt and Jackwerth [58], who found that reduction of the amount of sample aspirated improved both the sensitivity and the limit of detection; the relative standard deviation was about 0.05.

CHAPTER III

OBJECT OF INVESTIGATION

The present study dealt with the application of some transient effects to the determination of microgram amounts of a variety of chemical species in solution. The analytical potentiality of these effects stems from the fact that experimental conditions can be adjusted so that continuous determination of a single species can be made by injecting a small volume (0.02-0.1 ml) into a flow-through cell into which an excess of the other reagents is continuously circulated. Also, the approach provides a very rapid method for determinations by employing techniques by which certain properties can be measured "instantaneously", for example, spectrophotometry. Injection of the sought-for species into the cell offers an attractive alternative to conventional analyzers, where the determination times are reduced considerably. On the average, 60 samples per hour can be processed by conventional analyzers; on the other hand, 180 to 360 samples per hour can be processed by the present technique.

Considering that the species A is transformed (oxidized, complexed, etc.) to a short lived intermediate C (by using a large excess of an oxidizing agent, a complexing agent, etc.) and this intermediate C rapidly decays, or is forced to disappear from the detection zone, consecutive pseudo-first order kinetics are followed as given by:

$$A + B \xrightarrow{k_1} C \qquad (20)$$

$$C + Y \xrightarrow{k_2} \text{Products} \qquad (21)$$

Since all reactants except the sought-for species, say A, are present in large excess, the apparent order is the order with respect to A. By monitoring C, for example spectrophotometrically, a transient signal is obtained whose height is proportional to the amount of the injected species A. The peak height is proportional to the absorbance value and depends upon κ, the relative value of the rate constants, i.e., k_2/k_1. For a 99% recovery of the equilibrium signal, i.e., formation of C before its disappearance from the detection zone, values of k_1 should be at least 1000 times k_2 (see Appendix D.1).

In this study, this novel technique was applied to the determination of a variety of chemical species in aqueous solutions such as metal ions, phenothiazines, and oxidants. Chemical reactions of the type represented by Equations 20 and 21 were studied in order to establish the experimental parameters which would lead to an increase in the sensitivity of the determination. Also, different approaches to the problem of measuring and recording the transient signals have been examined.

The kinetics of the reactions chosen have also been studied: computational methods as well as curve fitting methods have been used. The rate constants k_1 and k_2 of Equations 20 and 21 have been determined, except in the case of the zinc and cadmium determinations where only the rate constants k_2 have been determined because of the rapidity of the reaction did not allow. In cases where k_1 and k_2 have been determined, the computed k values were substituted in the model equation describing the formation and decay of the transient species in order to simulate a

signal. The simulated signal is changed by change of the k values until the best fit between the simulated signal and the experimental one is found. The mechanisms of the reactions chosen in the present investigation have not been studied (per se) by the present author; however, these reactions have been extensively studied in analytical titrimetry and complexometry (see Chapter VI).

Finally, it should be noted that some instrumentally generated transient signals referred to as "Transient Signals due to Transient Effects" in Chapter I have been investigated and are reported elseshere [59]. In these signals, with relation to Equations 20 and 21 the injected species A reacts with a complexing agent B to form C, and C is transiently depleted by the continuous flow of a large excess of B into the flow-through cell. In other words, the monitored species C disappears from the detection zone by washing it out of the zone, and not because of its transient nature.

To summarize, this novel approach to fast determinations offers several attractive characteristics such as minimal consumption of reagents, easy to assemble set-up, and no special equipment is necessary.

CHAPTER IV

EXPERIMENTAL APPARATUS

IV.1. Spectrophotometric Unit

The spectrophotometric unit used in the present study consisted of an especially assembled modular unit [60]. It was made up of the following parts:

(a) A six-volt light source (MP-1021) operated from a regulated power supply (MP-1026);

(b) A Jarrel-Ash, 1/4 meter monochromator covering the 180 to 860 nm wavelength range, with an aperture of f/3.5;

(c) A cell holder housing designed to accommodate a variety of conventional cell holders. This part contained all necessary connections for magnetic stirring, external cell flow circulation, electrical connections for measuring of stirring velocities, and temperature control of cells;

(d) A cell holder base with magnetic stirring, described and reported earlier [61]; and

(e) A UVPIN silicon photodiode (UD 500) from United Detector Technology, Inc.

A diagram of the layout of the spectrophotometric unit is presented in Figure 1 (MP stands for McKee-Pedersen Instruments, Danville, CA. 94526).

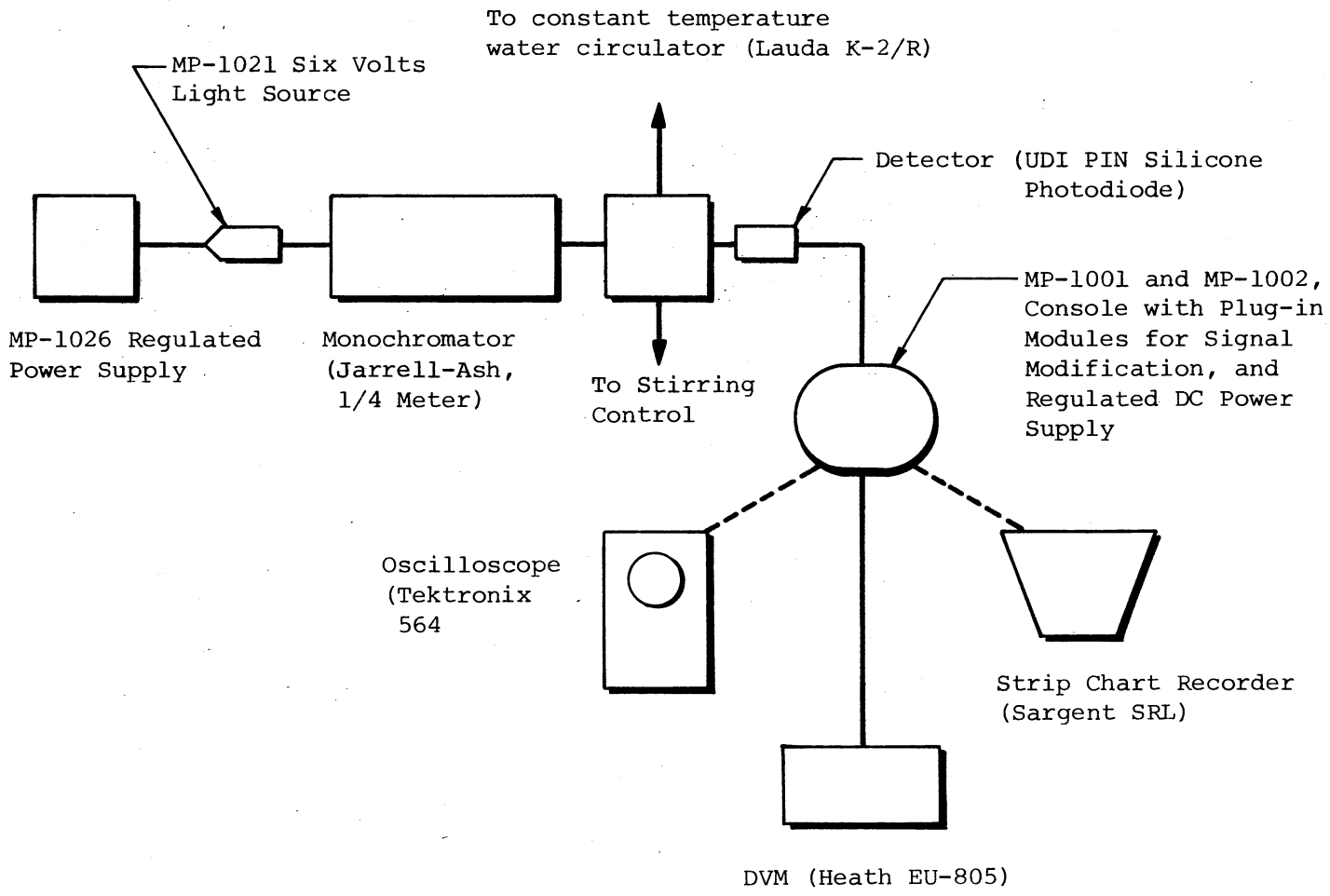

Figure 1. Block Diagram of the Spectrophotometer Arrangement

IV.2. Flow-Through Unit

The flow-through unit used in the present study was primarily that described by Dutt and Mottola [1]. It consisted of the following parts:

(a) An Erlenmeyer flask (125 ml or 250 ml capacity) fitted with a rubber stopper perforated to accommodate a thermometer, circulation tubing, and a combination electrode. This served as a reservoir for the reagent(s) solution(s).

(b) A peristaltic pump (Masterflex SRC Model 7020 speed controller and 7014 pump head); and

(c) A flow-through cell cylindrical made from pyrex glass, and equipped with $ 12/80 with two arms, one serving as the sample injection port, and the other as connection to the reagent solution's external circulation system.

The reagent solution was magnetically stirred at a constant temperature, 25 ± 0.2^{o}C, by a Stir-Kool of Thermoelectrics Unlimited, Inc. Cell temperatures mainly controlled by a Lauda/Brinkman Model K-2/R thermostat-circulator where water at a temperature 25 ± 0.2^{o}C was continuously circulated into the cell jacket, and around the reagent reservoir. Stirring of solution in the flow-through cell has been achieved at 15-20 μamp reading on the stirrer's measuring device magnetically [61]. Later on a solid state submersible stirrer was used [59].

IV.3. Injection Unit

In the early stages, a simple device consisting of a syringe and a teflon tubing was used to inject the sample. As the pressure at which the sample was injected varied, poor precision was obtained. It became

then preferable to adjust the injection pressure, and a push-button repetitive dispenser was used with more success. However, the problem of moving the teflon tubing into the flow-through cell, i.e., change in injection height and position, has not yet been eliminated. This led to designing a stand with a special holder for the dispenser which led to better precision. Of course, improvement of precision can be achieved by employing a mechanically controlled sample injection. The injection unit which has been used in the present investigation is shown in Figure 2.

IV.4. Measurement and Recording Unit

Transient signals were obtained after injecting small aliquots of the sought-for species into the flow-through cell. These signals were traced either on a Sargent recorder model SRG, or on a Tektronix Type 564 Storage Oscilloscope. Some transient signals were also recorded on the Heath Log/Linear Current Module EU-20-28 as percent transmittance. This Heath module served to relate directly the transmittance of the transient species to its concentration. The mV traces obtained by the other two recording devices were found to be linearly related to absorbance.

Several approaches to the problem of treating the transient signal have been examined in the present study. These may be cited under two main headings:

(1) Measurement of peak heights by;

  (a) A millimeter ruler
  (b) Precision peak reader

(2) Measurement of peak areas by;

Another View of Push-button Dispenser Handle

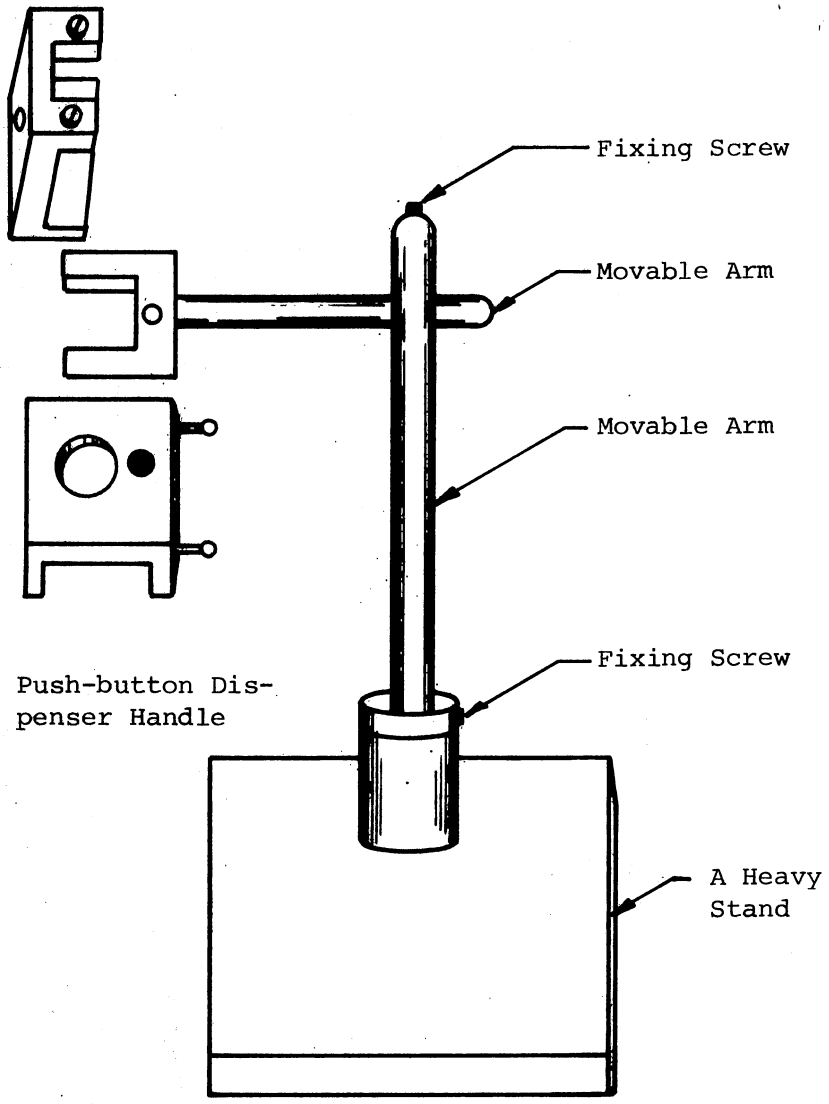

Figure 2. The Injection Unit. (This Stand and a Push-button Repetitive Dispenser)

(a) The difference integrator
(b) Analog integrator circuit

As generally accpeted, the integral method of recording yields, in most cases, linear working curves and good precision. However, if base line drifts are present, this can lead to serious errors and thus the methods in (1) would be preferable. But, since base line drift and noise levels were satisfactory under the present experimental conditions, all the above mentioned approaches have been examined. Schematics of the circuits applied to measure peak heights are shown in Figures 3 and 4; those to measure peak areas in Figures 5 and 6.

Finally, a rather indirect way of measuring the time elapsed between injection and reaching the peak value was the application of a differentiator circuit as represented in Figure 7. The signal was stored on the oscilloscope where its profile crosses the time axis at the peak value, and thus time could be calculated to the order of one tenth of a second.

IV.5. Kinetic Analysis of Transient Signals

Kinetic analysis of transient signals, as such, refers to the computation of the pseudo rate constants for the rise curves and fall curves of the signals and curve fitting for the experimental and computed data related to the signal profile.

For this analysis, a Hewlett Packard programmable calculator Model 9820A with 429 register, interfaced with Hewlett Packard x-y plotter Model 9862A have been used. The plotter has a peripheral central function block which scales data automatically, generates words as well as numbers, and sets up both axes complete with labels and tick marks--all in previously designated units. The 9820A programmable calculator is

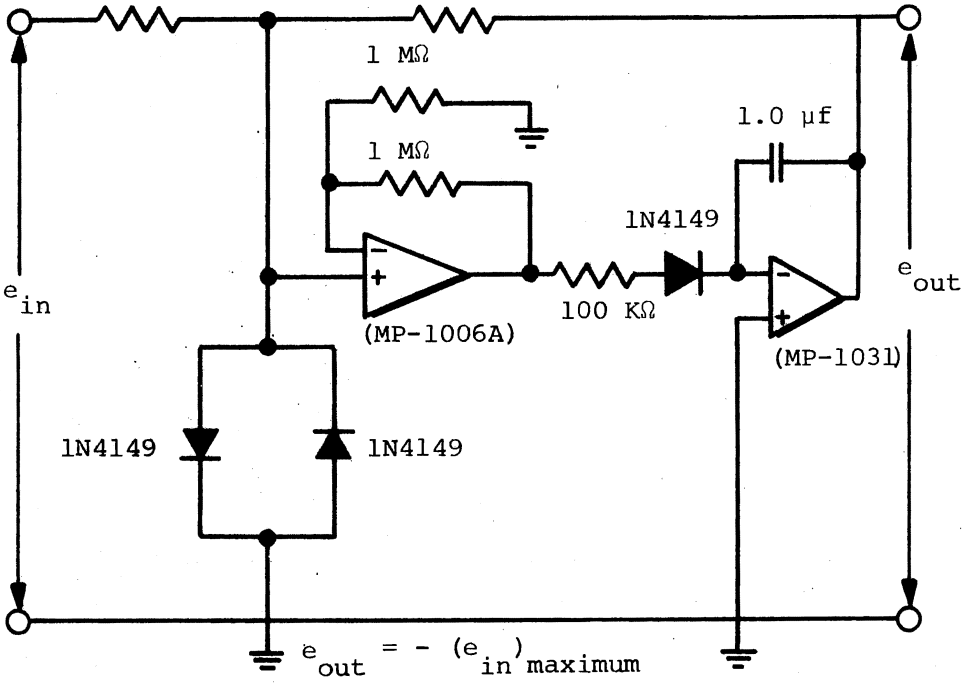

Figure 3. Precision Peak Reader and Memory

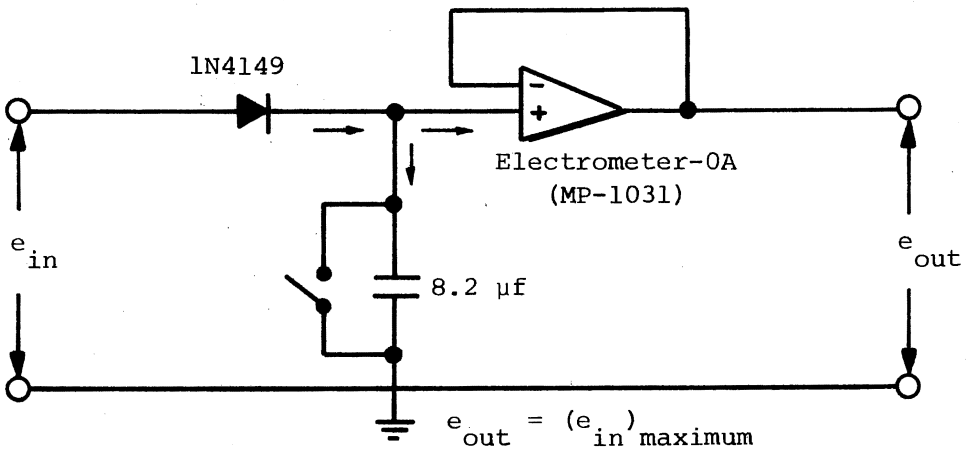

Figure 4. Precision Peak Reader

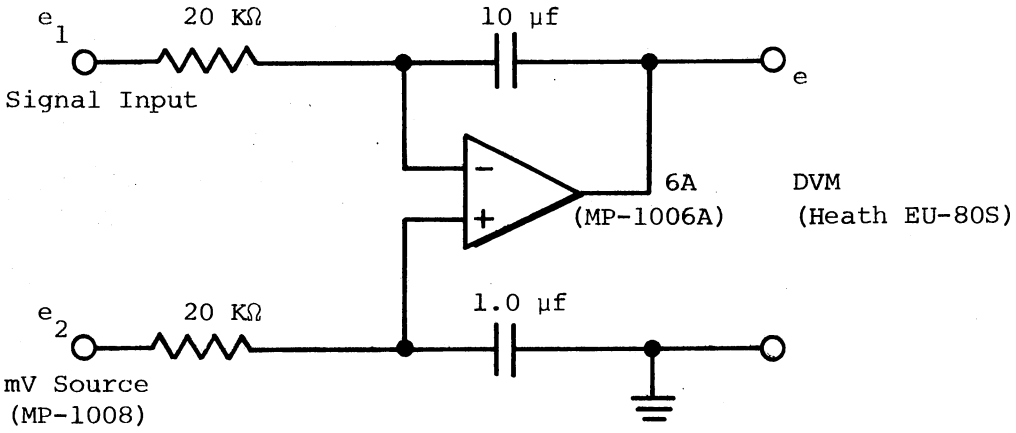

$$e = \frac{1}{T}\int^{t} (e_2 - e_1)dt; \quad (RC = R'C' = T)$$

Figure 5. The Difference Integrator

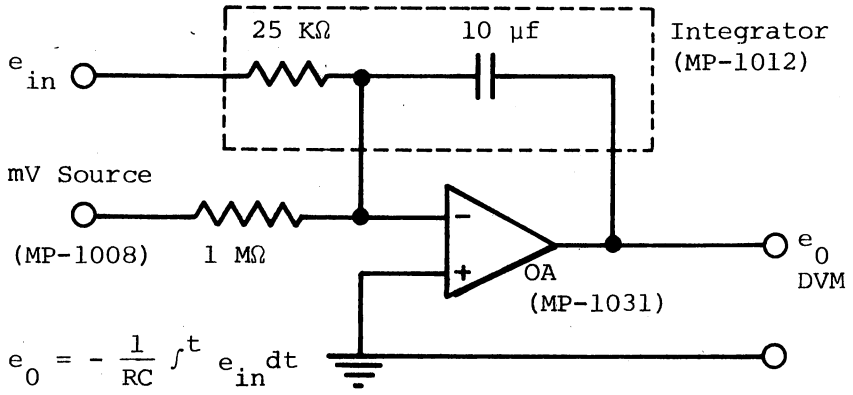

Figure 6. Analog Integrator Circuit

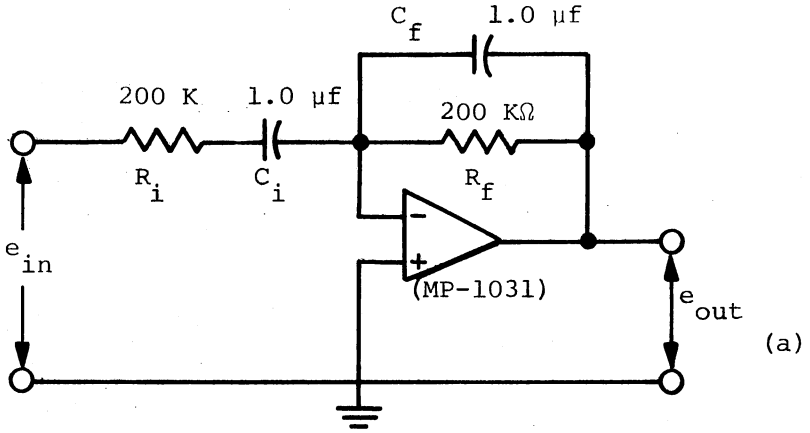

$$e_{out} = - R_f C_i \frac{de_{in}}{dt} \qquad \frac{1}{R_i C_i} = \frac{1}{R_f C_f} = 20\ \pi F$$

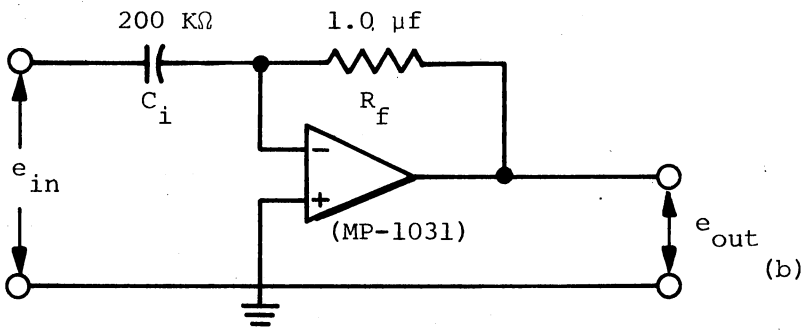

$$e_{out} = - R_f C_i \frac{de_{in}}{dt}$$

Figure 7. Differentiator Circuit. (a) Frequency Limited, (b) Simple

programmed through algebraic language; where mathematical problems are keyed in the same form one would write them on paper.

Also, the IBM system/360 at the University computer center, with its Calcomp 565 digital plotter, has been used to calculate and plot data related to kinetic analyses.

CHAPTER V

EXPERIMENTAL PROCEDURE

V.1. Reagents and Solutions

All chemicals used were of the A. R. grade, and all solutions were prepared in distilled-deionized water.

V.1-1. Acids

Stock solutions, 5.0M, were prepared from the concentrated acids.

-Sulfuric acid, H_2SO_4, DuPont Reagent.

-Perchloric acid, $HClO_4$, 'Baker Analyzed' Reagent.

-Glacial acetic acid, CH_3COOH, Fisher A.C.S. Reagent.

-Phosphoric acid, H_3PO_4, 'Baker Analyzed' Reagent.

V.1-2. Oxidizing Agents

Stock solutions of the following oxidants were prepared, 10^{-2}M.

-Ceric sulfate, $Ce(SO_4)_2 \cdot 4H_2O$, Fisher Certified Reagent.

-Ammonium meta-vanadate, NH_4VO_3, Fisher Purified.

-Potassium peroxydisulfate, $K_2S_2O_8$, Fisher Certified Reagent.

-Potassium iodate, KIO_3, 'Baker Analyzed' Reagent.

-Potassium periodate, KIO_4, 'Baker Analyzed' Reagent.

V.1-3. Complexing Agents

Stock solutions, 2.0×10^{-3}M, of the following complexing agents

have been prepared.

-Eriochrome Black T, 'Baker Analyzed' Reagent.

-Disodium ethylenediamine tetraacetate, Fisher A.C.S. Certified.

-Trans 1,2 diaminocyclohexane-N,N,N',N'-tetraacetic acid, Aldrich Reagent.

-Diethylenetriaminepentaacetic acid, Aldrich Reagent.

V.1-4. Metal Ions

Stock solutions 10^{-2}M, of the following metal ions have been prepared; diluted solutions were freshly prepared from the stock solutions.

-Zinc nitrate, $Zn(NO_3)_2 \cdot 6H_2O$, 'Baker Analyzed' Reagent.

-Cadmium sulfate, $CdSO_4$, 'Baker Analyzed' Reagent.

-Potassium dichromate, $K_2Cr_2O_7$, 'Baker Analyzed' Reagent.

-Ferrous sulfate, $FeSO_4$, Fisher Certified Reagent.

V.1-5. Phenothiazines

Stock solutions containing 1.0 mg/ml were prepared, stored in amber-colored bottles, and kept refrigerated. Dilute solutions were freshly prepared from these stock solutions.

-Chlorpromazine hydrochloride, $C_{17}H_{19}ClN_2S \cdot HCl$, SK&F.

-Prochlorperazine dimaleate, $C_{20}H_{24}ClN_3S \cdot 2C_4H_4O_4$, SK&F.

-Trifluoperazine dihydrochloride, $C_{21}H_{24}F_3N_3S \cdot 2HCl$, SK&F.

Tablets of the following pharmaceutical compounds were dissolved in distilled water using an ultrasonic cleaner and the solutions filtered off through Whatmann No. 42 filter paper, then transferred into dark bottles, and refrigerated.

-Thorazine (SK&F, Chlorpromazine hydrochloride), 100 mg.

-Phenergan (SK&F, Promethazine hydrochloride), 12.5 mg.

-Sparine (Wyeth, Promazine hydrochloride), 50 mg.

-Compazine (SK&F, Prochlorperazine dimaleate), 10 mg.

SK&F stands for Smith, Kline and French Laboratories, Philadelphia, PA., 19101.

V.2. Procedure

The oxidant, or complexing agent, was placed into the reagent reservoir in addition to other reagents, and the mixture stirred at a constant temperature for 15 minutes. After the temperature of the thermostat had become constant at 25°C, water was circulated into the Stir-Kool, and then to the cell jacket; meanwhile, reagents were also circulated through the flow-through system.

After the base line had been stable for half an hour, the wavelength at which maximum absorbance occurred was determined by repetitive injection of six equal aliquots (0.02 ml) of the metal ion, or phenothiazine solution into the flow-through cell and readings made at a known wavelength. This injection process was repeated for different wavelengths, and the corresponding peak heights were measured by a millimeter ruler. The wavelength at which maximum absorbance was obtained, the highest measured peak, was then selected for measurements.

Several experimental variables were studied in order to optimize the experimental conditions, and ascertain the effects of various factors on the signal's profile. These variables were acid concentration, oxidant concentration, nature of acids, nature of oxidants, stirring speed, flow rate, temperature, nature of complexing agents, pH, nature

of metal ions, and number of repetitive injections. Finally, it ought to be mentioned that repetitive injection of the sample containing the sought-for species into a continuously circulating reagent mixture have been reported by Mottola, Dutt, and the present author [59]. Practical application of this approach was illustrated in the determination of iron(II) in aqueous solutions with Ferrozine.

CHAPTER VI

RESULTS AND DISCUSSION

VI.1. A Review of Methods of Analysis for Phenothiazine Drugs

The phenothiazines commercially available today probably form the largest group of chemically related drugs. Owing to their relatively low toxicity, high physiological activity, and versatile pharmacological action they are widely used in medicine today, particularly for the treatment of psychiatric disorders. Reviews on the use of phenothiazine derivatives in therapeutics and of analytical methods for their determination have been presented by Blazek [62], Cimbura [63], and Tompsett [64].

The available methods for the analysis for phenothiazines in biological samples can be divided into three main categories: direct screening tests for presence of the family, extraction techniques, and identification and estimation methods for individual compounds. Many tests of the first type have been described [65]; most are based on the oxidation of phenothiazines with various oxidizing agents to form colored products. The most common of the direct screening tests are the Bromination-Acidulation test [65] and the FPN (mixture of ferric chloride, perchloric and nitric acids) test [66]. The Bromination-Acidulation test consists in the treatment of a solution of a phenothiazine with bromine water and sulfuric acid under controlled condi-

tions, where upon an "immediate" violet color is obtained. The FPN test consists of mixing the phenothiazines with the FPN reagent; in a positive test, purple, red or pink colors are developed in 10 seconds. In both tests false positives have been encountered and further confirmatory tests are required.

The literature contains numerous reports pertaining to the extraction of phenothiazines and their metabolites, and to review them is outside the scope of this study [67]. The methods reported for identification and estimation of phenothiazines in biological samples, and in their pure forms, include visible and U.V. spectrophotometry, thin-layer chromatography (TLC), paper chromatography (PC), gas-liquid chromatrography (GLC), and luminescence spectrometry.

The photometric determinations like the screening tests, are based on the oxidation of phenothiazines with various oxidizing agents. For example, uranium nitrate, mercuric nitrate, ferric chloride, and phosphotungstic acid and sulfuric acid will oxidize phenothiazines to produce intense pink, purple or blue colors which, however, tend to fade [63].

Haue and Natelson [68] utilized the reaction between acidic solutions of phenothiazines and 1M-arsenic acid to oxidize the phenothiazine and measure the absorbance of the stable color formed. Egorov et al. [69] used two color reactions to draw up a systematic analytical scheme for the identification of some phenothiazine derivatives. The first consisted of adding slowly a 10M-KOH solution to an ice-cooled solution of phenothiazine in concentrated H_2SO_4 where different colors were produced with different compounds, while the second consisted of heating the phenothiazine with 10% $CuSO_4$ solution and 0.1N-HCl where distinctive colors were produced. Thiocyanato complexes of Cobalt(II) form blue

compounds with phenothiazines which are sparingly soluble in water; these compounds were quantitatively extracted with ether, and assayed by colorimetry, where Beer's law was obeyed in the concentration range 100-600 µg/ml [70] Picric acid forms well crystallized colored complexes with phenothiazines, which can be extracted with benzene, and the colors used for spectrophotometric estimation in the concentration range (10-60 µg/ml) [71].

The UV absorption pattern of phenothiazine drugs exhibits two maxima, a higher absorption peak in the spectral region between 242-262 nm, and a lower one between 297-322 nm [65]. Sulfoxides corresponding to phenothiazines producible by mild oxidation of phenothiazines exhibit in general, four maxima in the U.V. spectral region [72] and thus give a more characteristic spectral pattern. Wallace and Biggs [73] have oxidized the drugs to sulfoxides with cobalt(III) and found their U.V. spectra to follow Beer's law over the concentration range 0.5-50.0 µg/ml.

A great number of TLC or PC systems have been developed for the separation and identification of hundreds of different drugs, including phenothiazines; most of the data have been summarized in toxicological texts [67]. The results of extensive TLC work were reported by Cochin and Daley [74]. Both ascending and descending paper chromatographic systems were employed to separate and identify many phenothiazines in various solvent systems [75, 76]. Ebel et al. [77] reported the determination of fifteen phenothiazines by reflectance spectrometry; in solutions and on thin layer chromatographic plates; the detection limits were about 1 µg.

Parker et al. [78] applied GLC to the separation and determination of tranquilizers, including many phenothiazines, with a limit of detec-

tion equal to 1 µg. Curry [79] was able to determine nanogram amounts of chlorpromazine hydrochloride and its metabolites by a GLC procedure.

Two extensive reports on the spectrofluorometric measurement and identification of phenothiazine drugs are given in the literature [80, 81]. Mellinger and Keeler [80] reported the determination of oxidized phenothiazines in the concentration range as low as 0.1-0.5 µg/ml; the phenothiazines were oxidized with potassium permanganate in sulfuric acid. The sensitivity of the method reported by Ragland and Kinross-Wright [81] is such that most compounds could be quantitatively determined at concentrations of 0.5 µg/ml. The fluorescence of phenothiazines and the corresponding sulfoxides at room temperatures has been well studied by Martin [82]; however, the luminescence data at low temperatures are few [83]. Recently, Bridges et al. [84] reported the phosphorimetric determination of phenothiazines with detection limits of 0.02-0.1 µg/ml.

From the preceding review, it is evident that there are numerous methods for the analysis for phenothiazines in both biological samples and pharmaceutical formulations. In the following, a brief comment is made on the advantages and disadvantages of the estimation and identification methods.

Generally, the lack of specificity and selectivity are the main disadvantages of the photometric methods; on the other hand the spectrophotometric instruments are relatively inexpensive and can be applied to routine analysis. The U.V. spectrophotometric technique provides a very useful tool for the analysis for phenothiazines and detection limits of 0.25 µg/ml. can be achieved.

The principal value of TLC, and PC, lies in its ability to separate

and to identify to some extent, many of the phenothiazine derivatives, especially in relatively large amounts. Gas-liquid chromatrography represents the most widely used means to date to separate and to determine individual phenothiazines in submicrogram amounts. However, two main disadvantages of GLC are the difficulty in eluting some of the high-molecular weight components, and applying the technique to a routine practice.

The main advantages of spectrofluorometry are its sensitivity and the relative ease of measurement. The limits of detection are generally similar to those attained in GLC, though they vary for different phenothiazines. Phosphorimetric analysis for phenothiazine derivatives have recently been reported to attain detection limits as low as 0.02 μg/ml [84]. Bridges et al. [84] have also reported phosphorescence lifetimes for some commonly-used phenothiazines.

VI.1-1. Determination of Some Phenothiazines Via the Formation of Transient Species

VI.1.1.1. General Discussion. A typical example of the oxidation of phenothiazines is that of the oxidation of chlorpromazine, which may be represented as follows:

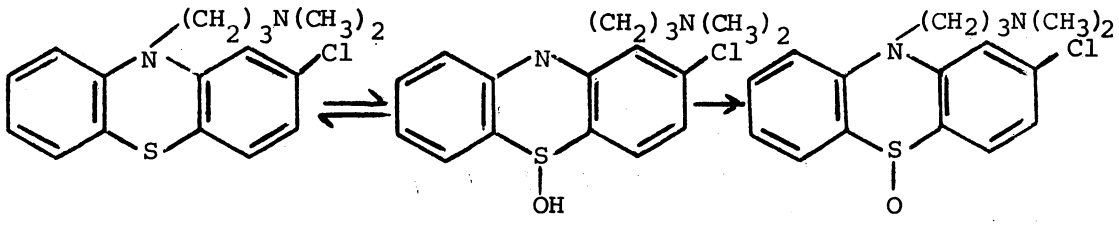

where the free radical is stable in acid solution [85], but is further oxidized irreversibly by strong oxidizing agents to colorless sulfoxide.

Thus, when the absorbance of this free radical was monitored with respect to time, a transient signal corresponding to the formation and decay of the free radical was obtained.

In the present investigation, microgram amounts of some phenothiazines have been determined spectrophotometrically, simply by injection of the phenothiazine into a flow-through cell were a solution of cerium (IV) in sulfuric acid was continuously flowing. A variety of experimental conditions have been studied in order to ascertain the optimal experimental factors for continuous repetitive determination of these phenothiazines in aqueous solutions. The results are shown in Table I.

TABLE I

EFFECTS OF VARIOUS EXPERIMENTAL PARAMETERS ON THE PEAK HEIGHT OF THE SPECTROPHOTOMETRIC TRANSIENT SIGNAL OF CHLORPROMAZINE FREE RADICAL

Experimental Parameter	Range of Change in the Parameter	Percent Relative Change in Peak Height
Cerium(IV) concentration (M)	5.0×10^{-5} - 3.0×10^{-4}	-20
Sulfuric acid concentration (M)	0.70 - 8.11	+43.5
Temperature (^{o}C)	25 - 50	+30.6
Flow rate (ml/min)	0 - 70	+4
Stirring rate (r.p.m.)	450 - 650	+3
Recorder chart speed (inches/min)	1 - 4	-3

Amount of chlorpromazine hydrochloride injected 10 µg (0.02 ml); other experimental parameters: chart speed, 4 inch/min; mV span, 50 mV; stirring rate, 570 rpm; flow rate, 25 ml/min.

These results are basically a comparison of peak heights of the transient signals obtained at different conditions; thus, the percent relative change in peak maximum of the signal was calculated from the expression:

$$\frac{\text{Difference Between Peak Height Values}}{\text{Initial Peak H ight Value}} \times 100 .$$

A negative value shows a decrease in peak height; for example, an increase in cerium(IV) concentration gives rise to a decrease in peak height, while that of sulfuric acid has an opposite effect. Both these observations are in agreement with the stability of the free radical toward strong oxidants and acids, respectively [86]. Variation of the peak height with cerium(IV) concentration and with sulfuric acid concentration are shown in Figures 8 and 9, respectively. The optimum concentrations of cerium(IV) and sulfuric acid were thus chosen as 8×10^{-5} and 1.43 M, respectively, where there was enough cerium(IV) to carry out several injections and the solution was not highly viscous. Temperature changes of 1-2^{o}C have negligible effects on the signal; but larger temperature increases increase the peak height, probably because of a decrease in the ratio of rate constants, i.e., k_2/k_1. Flow rate had a negligible effect on the peak height since the signal profile lasts for about 8 seconds and the rate of the fall curve was independent of the flow rate. Stirring was controlled so that turbulent effects known as eddy currents or whirls were minimal. Constancy of stirring rate was expected to play a vital role on the signal profile because of the transient nature of the signal. Thus large fluctuations in the stirring rate gave rise to signals with high v_x values (Appendix E.1). It was therefore of utmost importance to control the stirring rate so

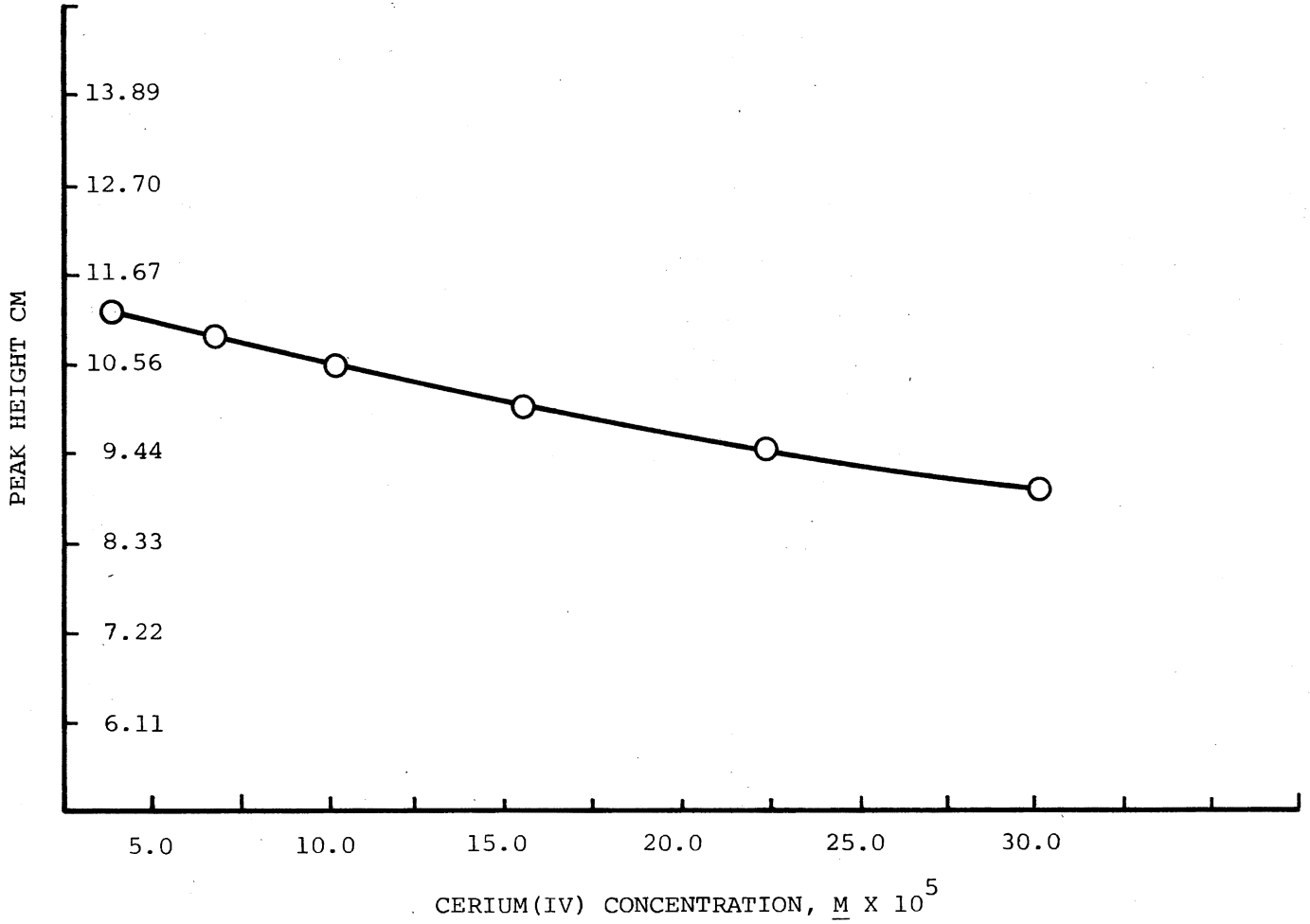

Figure 8. Variation of Peak Height With Cerium(IV) Concentration

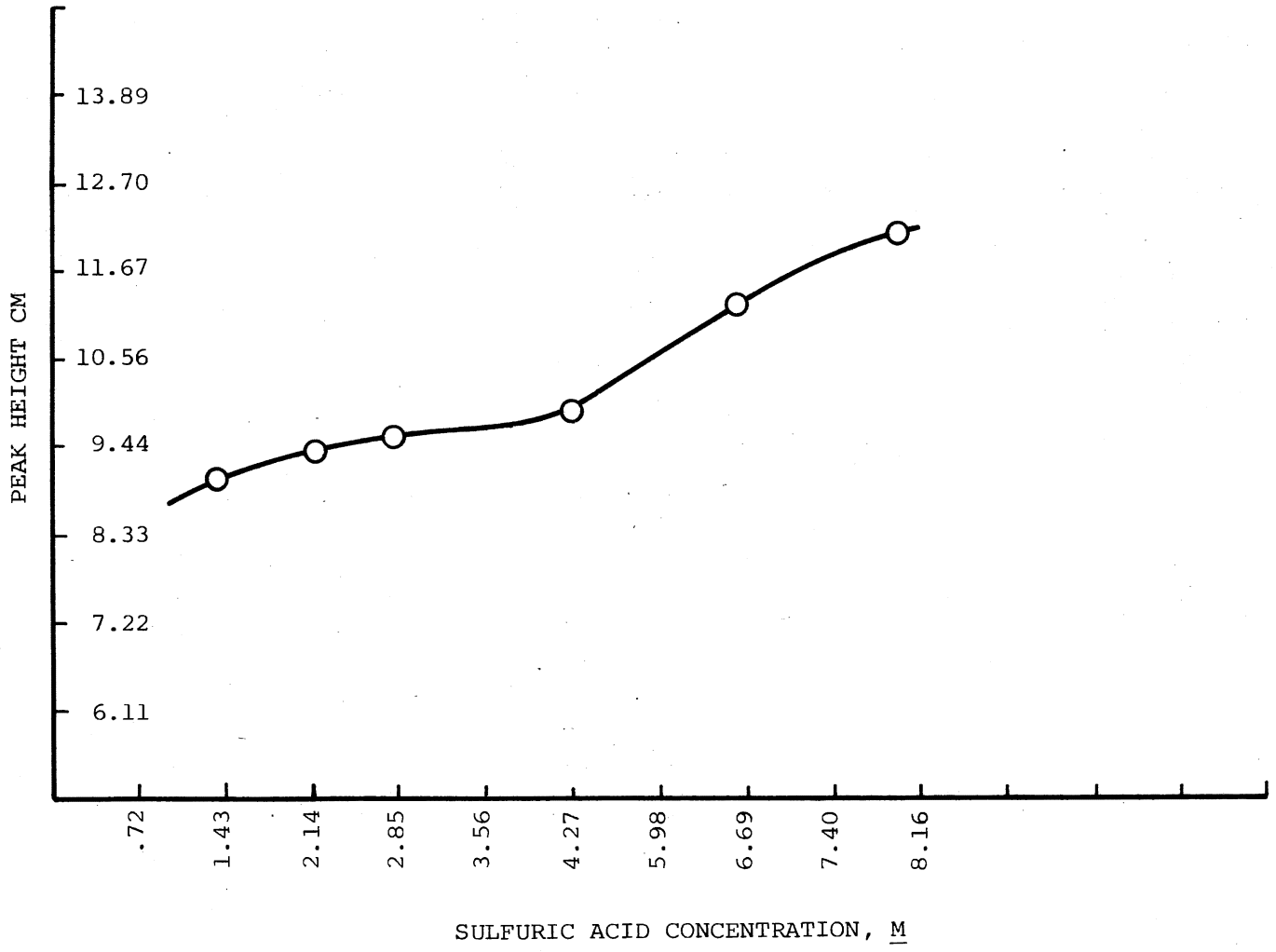

Figure 9. Variation of Peak Height With Sulfuric Acid Concentration

that there were no abrupt changes.

Thus, by the production of colored free radicals by the oxidation of phenothiazines with cerium(IV) in sulfuric acid medium, different phenothiazines have been determined following the procedure reported earlier.

VI.1.1.2. Determination of Phenothiazines Via Transient Signals. Table II shows some pertinent data for the spectrophotometric determination; the wavelength at which maximum absorbance of the free radical takes place is designated by λ_{max}. The values of λ_{max} obtained in the present study are in close agreement to those reported in the literature [68]; they were determined as described in Section V.2.

The limit of detection has been defined as the amount of the phenothiazine which produces a peak height equal to twice the height of a blank signal (when water was injected instead of the drug). Also reported is the range of determination where linearity was observed.

The absorbances of the free radicals obtained by the oxidation of phenothiazines with cerium(IV) in sulfuric acid medium, and at different wavelengths, are shown in Figure 10 (Section V.2.). In reality, these are total peak heights (directly proportional to absorbance) at different wavelengths. It is apparent from Figure 10 that maximum absorbance is at 520 nm for prochlorperazine free radical; a similar plot shows maximum absorbance for chlorpromazine free radical at 525 nm. It follows, therefore, and it was experimentally verified that the free radicals obtained from their pharmaceutical preparations can be monitored at these wavelengths. Other phenothiazine free radicals show maximum absorbance at smaller wavelengths between 475 and 510 nm with peak absorbance at 475 nm for trifluoperazine dihydrochloride. This maximum

TABLE II

USE OF TRANSIENT SPECIES IN THE SPECTROPHOTOMETRIC DETERMINATION OF MICROGRAM AMOUNTS OF SOME PHENOTHIAZINES IN AQUEOUS SOLUTIONS

Compound	λ_{max} nm	Limit of Detection µg	Intercept c, cm	Range of Determination µg	Slope a cm/µg
Chlorpromazine hydrochloride	525(530)	1.3	0.48	2.0 - 28.0	0.77
Prochlorperazine dimaleate	520(530)	1.6	0.52	3.0 - 35.0	0.64
Trifluoperazine dihydrochloride	475	0.3	-0.27	1.5 - 27.0	0.85
Thorazine tablets	525(530)	0.5	-0.40	2.0 - 27.0	0.84
Compazine tablets	520(530)	0.2	-0.10	0.5 - 34.0	0.67
Phenergan tablets	510(520)	3.1	0.48	5.0 - 75.0	0.31
Sparine tablets	500(-)	1.2	0.29	3.0 - 43.0	0.49

For each calibration graph a 125-ml reservoir was used (cerium(VI), 8.00×10^{-5} M; H_2SO_4, 1.43 M); other experimental parameters are described in the text; values of λ_{max} between parenthesis are those reported in reference [68]; values of intercept c and slope a were obtained from the regression line (1 cm = 0.01A).

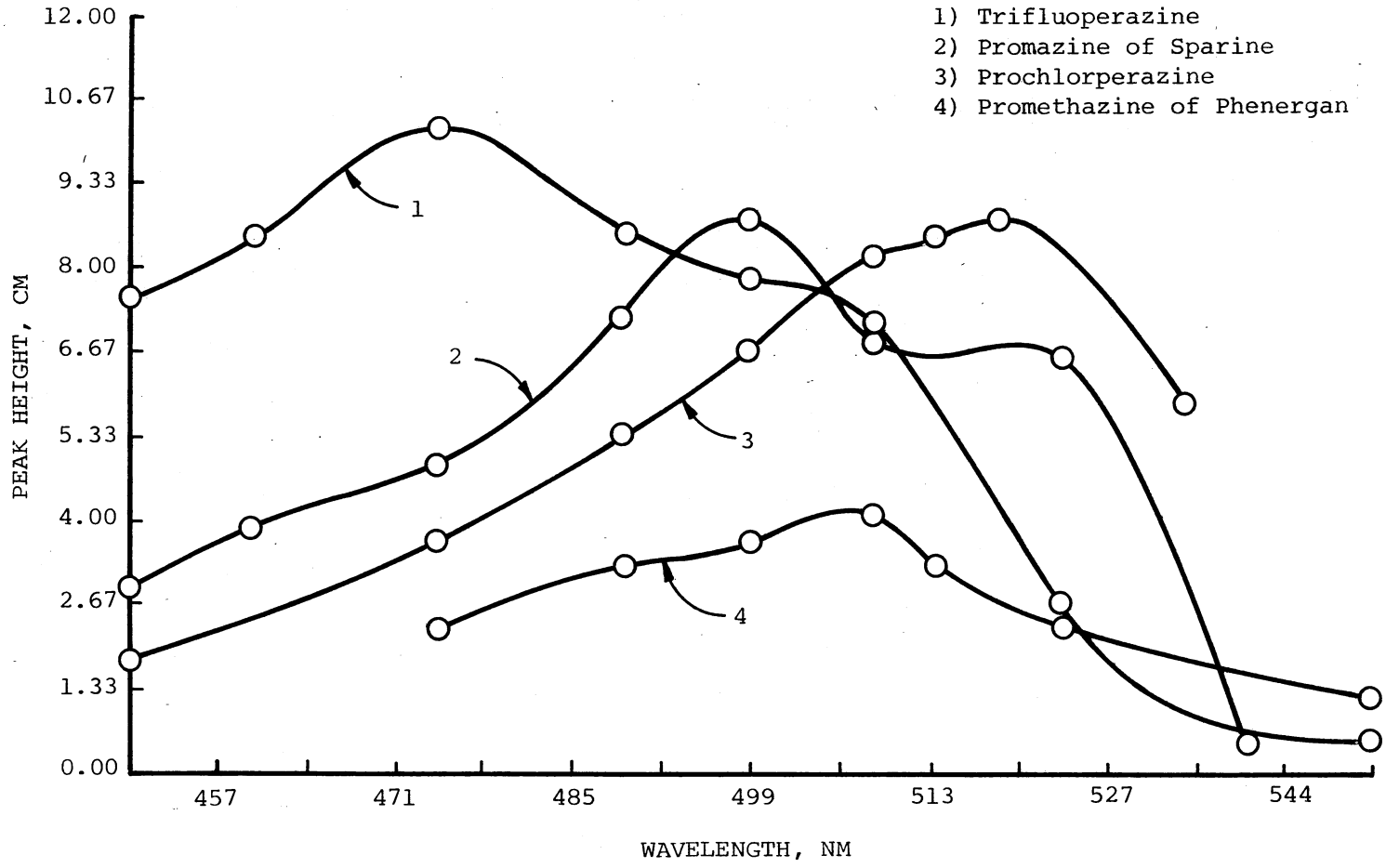

Figure 10. Visible Absorption Spectra of Some Phenothiazines' Free Radicals

may be attributed to the effect of $-CF_3$ in position 2 of the phenothiazine skeletal structure (Appendix A.1).

Plots of the calibration curves for some of the phenothiazines determined are shown in Figure 11; similar linear curves were obtained for Thorazine and Compazine. Linear regression analysis was applied to obtain the slope a, and the intercept c, of each regression line (Appendix D.2.), and the values of a and c are listed in Table II. As can be seen, linearity occurs over the reported range of concentrations which is at least several times lower than the concentrations of the drugs usually given to patients [68]. Using Student's t statistics, $t = \frac{|c|}{s_c}$, the blank effects were found to be statistically insignificant at the values of n, f, and α of 6, 5, and 0.05, respectively (Appendix E). The differences of slope of the standard curves are due partly to the different molecular weights of the parent substances, but mainly to the difference in the molar absorptivities of their free radicals (Table II). Chemical structures of the compounds studied are presented in Appendix A. Promazine hydrochloride, under the Wyeth trade name Sparine, and promethazine hydrochloride, under the SK&F trade name Phenergan, were not obtained in their pure form; however, it is assumed that the amount of the pure compound in each tablet was accurate when the tablets were pooled, and was in accord with the values reported [87].

One of the main objectives of this study was to detemrine repetitively, and automatically if possible, different phenothiazines in aqueous solutions. Therefore, Table III lists the number of injections n made which gave signals having the same profile, the average peak height $\bar{X}$, and the percent relative standard deviation v_x (Appendix E.1).

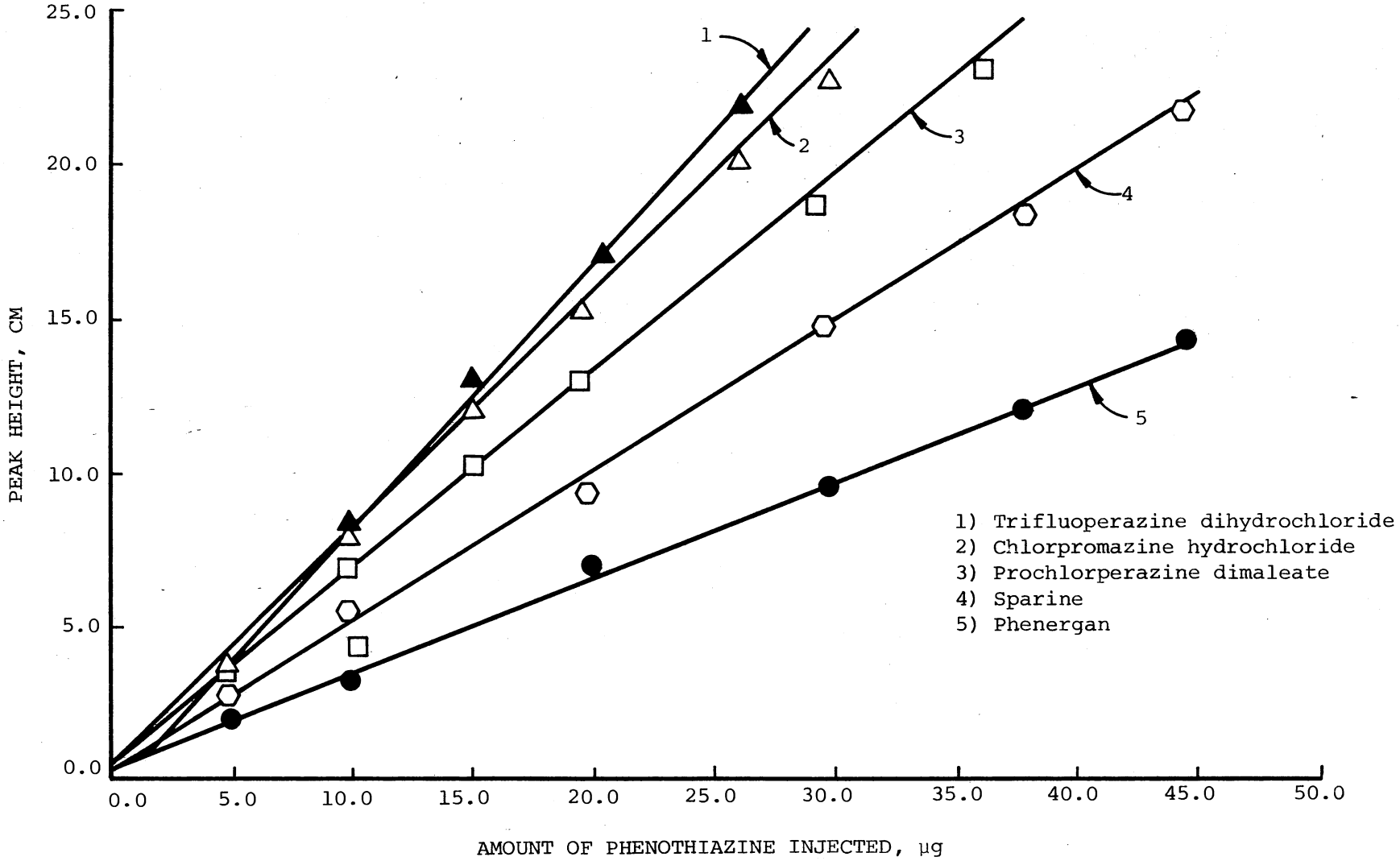

Figure 11. Variation of Peak Height With Phenothiazine Concentration

TABLE III

APPLICATIONS OF TRANSIENT SIGNALS IN THE REPETITIVE SPECTROPHOTOMETRIC DETERMINATION OF MICROGRAM AMOUNTS OF SOME PHENOTHIAZINES IN AQUEOUS SOLUTIONS

Compound	Phenothiazine Present	Number of Injections n	$\bar{X}$, cm	± Confidence Limits at the 95% Level	v_x
Chlorpromazine hydrochloride	Chlorpromacine hydrochloride	25	12.0	0.41	2.80
Prochlorperazine dimaleate	Prochlorperazine dimaleate	33	10.0	0.36	3.41
Trifluoperazine dihydrochloride	Trifluoperazine dihydrochloride	30	13.0	0.37	2.94
Thorazine tablets	Chlorpromazine hydrochloride	30	11.8	0.37	2.86
Compazine tablets	Prochlorperazine dimaleate	30	9.8	0.35	3.57
Phenergan tablets	Promazine hydrochloride	25	5.0	0.41	2.88
Sparine tablets	Promethazine hydrochloride	35	7.8	0.35	3.41

For each determination, a 125 ml reservoir was used (Cerium(IV), 8.00×10^{-5} M; H_2SO_4, 1.43 M); other experimental parameters described in the text; amount of the injected phenothiazine 15 µg (0.02 ml) (1 cm = 0.01A).

The percent relative standard deviation v_x, which is related to the magnitude of the peak height, ranged from 2.80 to 3.57 pph and was on the average equal to 3.04 pph. The confidence limits at the 95% level were comparable to the standard deviations (s_x); confidence limits based on the z values, where z represents the standarized normal measurement were too far apart. Thus, it was reasonably assumed that the ranges based on the t distribution were more nearly correct than those based on the z values.

It is of interest to note that, after the nth injection given in Table III, the signal profile changes gradually and continuously, with more peak broadening as further injections were made, until a signal hardly distinguishable from the blank was finally obtained. Strictly speaking, the peak maximum decreased continuously with a decrease in the rate of the fall of the signal, and with minimum change in the rate of the rise of the signal. The number of injections reported in Table III is the number obtained after applying the Q test in order to discard abnormally large or small peak heights (Appendix E.3). Confidence limits at the 95% level were calculated from the Student's t and they refer to the limits within which we expect the true value of the population mean to occur (Appendix E.1).

To summarize, the spectrophotometric measurement of transient signals by the flow injection technique has been successfully applied to the determination of a number of phenothiazines in both their pure form, and pharmaceutical preparations, to the order of microgram amounts. Different oxidizing agents, other than cerium(IV), such as potassium periodate, potassium peroxidisulfate, potassium iodate, and ammonium metavanadate have been used [88]. None of these gave more sensitive

or more rapidly developed signals, and all of these oxidizing agents have standard electrode potentials higher than that of chlorpromazine [85].

In the present study (Table III), phenothiazines have been determined in their pharmaceutical preparations--Thorazine, Compazine, Phenergan, and Sparine. The values obtained for the active drugs in these formulations agree satisfactorily with the values reported in the specialized references [87]; where the experimentally obtained values correspond to 92-95% of the reported values.

VI.1.2. Interference Studies

VI.1.2.1. Effects of Interfering Compounds. An ampoule of compazine is reported by the manufacturer to contain the following constituents: prochlorperazine edisylate (5 mg/ml), sodium sulfite (1 mg/ml), sodium hydrogen sulfite (1 mg/ml), sodium phosphate (8 mg/ml), and sodium biphosphate (12 mg/ml) [89]. Each of these constituents was added separately, and in combination, to the pure phenothiazine (prochlorperazine dimaleate), in order to study their possible interferences with the spectrophotometric transient signal.

Under exactly the same concentration ratio mentioned above, it was found that the sulfites reduce the peak height to about 73% of its original value. This is due to the simultaneous injection of the reducing agent with the phenothiazine; thus increasing the cerium(IV) concentration is not expected to increase the peak maximum, and this has been experimentally verified.

On the other hand, the phosphates had no effect on the signal height; i.e., effects were comparable with the experimental errors in

the peak maximum. However, when all the constituents present in the ampoule of Compazine were added together, peak height was only reduced to 95% of its original value. These results were obtained using three ampoules, where the amounts of the drug determined are within the ranges reported in the Pharmacopeia of the United States, and the American Medical Association Drug Evaluations [87] (Experimental conditions were in Table II).

VI.1.2.2. Standard Addition Method. The method of standard addition is well established as an evaluation method; it is particularly suited for residual matrix effects, and in trace analysis for the correction of interference effects. In this method, net peak heights were obtained for two solutions: Solution A, containing an aliquot of the pharmaceutical preparation of the phenothiazine; and Solution B, containing the same quantity of the latter solution plus a measured amount of the pure phenothiazine.

After a series of standard additions which were approximately one-half, equal to, twice, four times and six times the original amount, the resulting peak maxima were plotted against the amounts of the pure phenothiazine that were added to the pharmaceutical preparation as shown in Figure 12.

The measurements obtained were based on the averages of six injections where v_x lies between 2.4 and 3.8 pph for longer and shorter peaks, respectively. Figure 12 predicts that the extrapolated lines, intersect the abscissa at amounts equal to 4.50 and 5.39 µg for Thorazine and Compazine, respectively. The actual calculated amounts, as reported by the supplier, are 4.00 and 5.00 µg, respectively.

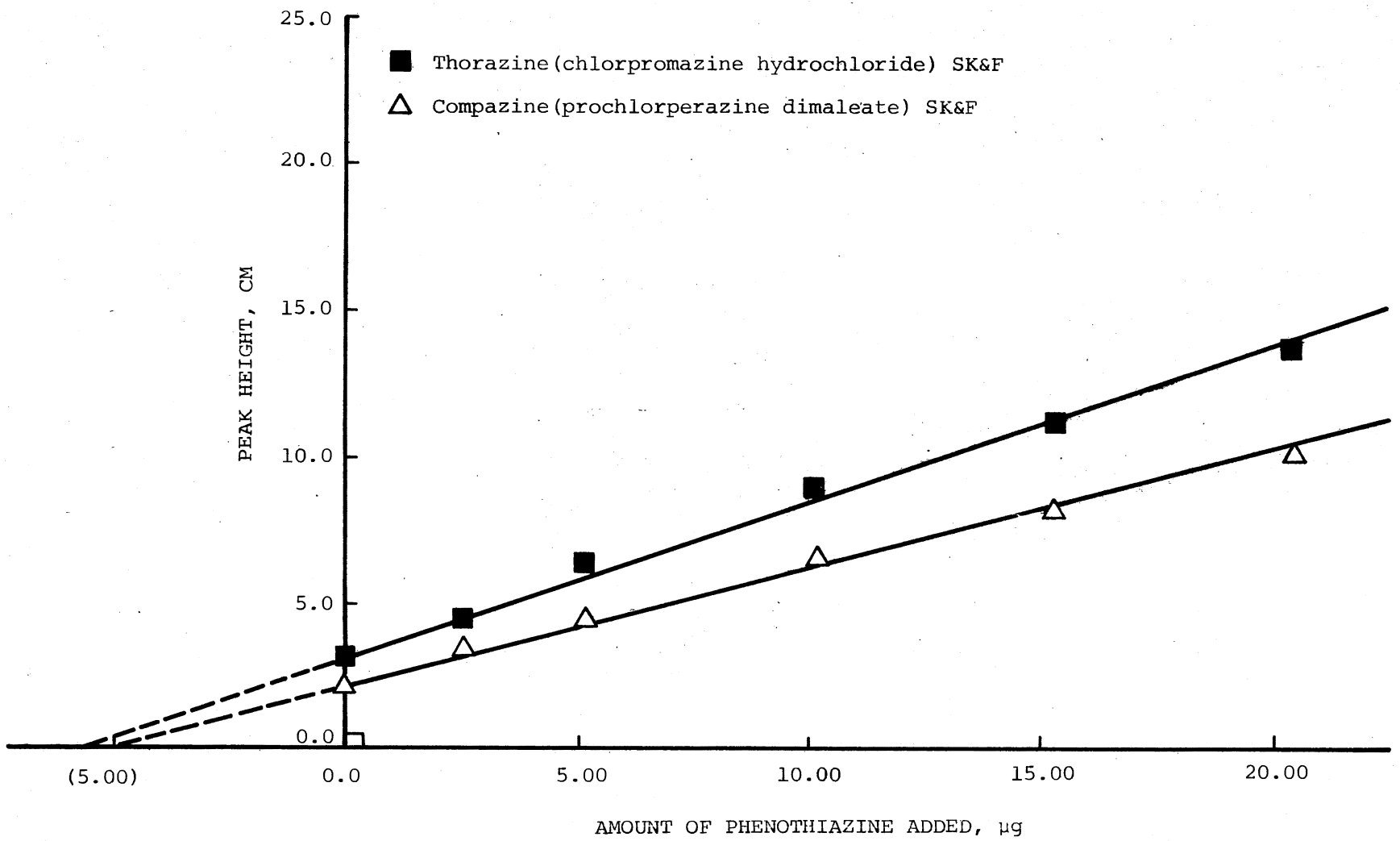

Figure 12. Graphic Representation of the Standard Addition Method

Since the quantity of the test solution found was more than the quantity added, an enhancement effect may be considered operative. In such cases, the true phenothiazine content, as reported by the manufacturer, of the pharmaceutical preparation is found by multiplying the observed drug content by a factor which corrects for the interference. This factor can only be obtained from a large number of data treated statistically, and the present study is not intended to evaluate it.

VI.1.3. Kinetic Studies Related to the Formation and Decay of Phenothiazine Free Radicals

VI.1.3.1. Computation of the Pseudo First-Order Rate Constants.

The mathematical description of the kinetic model is given in Appendix C and definition of the symbols in Section I.1.3. The computation procedure can be summarized as follows: the concentration of the transient species at the peak maximum, $[B]_{max}$, is calculated from Beer's law, and related to β_{max} by the relation:

$$\beta_{max} = \frac{[B]_{max}}{[A]_0}$$

The constant κ can thus be obtained from the computed values of β_{max} (Appendix D.1). By substitution for κ in the equation:

$$\tau_{max} = \frac{1}{\kappa - 1} \ln \kappa$$

τ_{max} can be calculated; then using the relation $\tau_{max} = k_1 t_{max}$, k_1 can be calculated by substituting the values for τ_{max} and t_{max}. Finally, k_2 can be obtained from the expression for κ where $\kappa = k_2/k_1$.

This estimation procedure is referred to as Method I to differentiate it from Method II. In Method II, when t_{max} is accurately known, k_2 can be calculated from the equation (Appendix C):

$$[B]_{max} = [A]_0 e^{-k_2 t_{max}}$$

and k_1 from κ, where the relative value of the rate constants κ is obtained as described earlier.

Both these methods were applied to calculate experimental first-order rate constants k_1 and k_2 for the hydrolysis of hydroxylaminenitrodisulfonate (A) by Candlin and Wilkins [90]. The rate constants were calculated by these authors to be equal to 8.0×10^{-3} and 5.9×10^{-3} min^{-1}, respectively. Referring to the concentration time profiles for A, B, and C where two successive first-order reactions represent the complete hydrolysis of A as:

$$A \xrightarrow{k_1} B + SO_4^{2-}$$

$$B \xrightarrow{k_2} C + SO_4^{2-}$$

estimates of the maximum concentration of B and t_{max} were calculated, by the present author, to be equal to 0.42×10^{-2}M and 1.38×10^{2} min, respectively (from the concentration-time profile for [B] in Figure 3 of Reference 90).

The two methods mentioned earlier were applied to recalculate the first-order rate constants from $[B]_{max}$ and t_{max}. A tabulation of the rate constants values reported by Candlin and Wilkins and calculated by the present author is as follows:

	k_1, min^{-1}	k_2, min^{-1}	% Deviation k_1	% Deviation k_2
Candlin and Wilkins	8.0×10^{-3}	5.9×10^{-3}	0.0	0.0
Method I	8.4×10^{-3}	6.2×10^{-3}	5.0	5.0
Method II	8.5×10^{-3}	6.5×10^{-3}	6.3	10.1

Apparently, both methods gave higher values than those reported but the agreement is very satisfactory in spite of the fact that the rate constants were calculated from estimates of the concentration-time profile, and not from actual experimental data. The percent deviations were calculated from the formula

$$\frac{\text{Calculated Value - Candlin's Value}}{\text{Candlin's Value}} \times 100 \ .$$

Calculation of the concentration values $[A]_0$ and $[B]_{max}$ for some phenothiazines is presented in Table IV. Tables V and VI list the first-order rate constants k_1 and k_2 as calculated by methods I and II, respectively. The initial concentration $[A]_0$ was calculated using the following expression:

$$\frac{\text{Amount Injected in } \mu g \times 10^{-6} \times 10^{3}}{\text{Detection Volume (ml)} \times \text{Molecular Weight of Compound}}$$

which is expressed in mmoles/ml, i.e., in molarity. Since the solution is injected into the flow-through cell, the absorbance of the free radical is represented by the absorbance of a segment of solution in the light path. This segment is referred here as the detection volume and was found to be equal to 2.50 ml. This is the volume of solution occupied by the colored free radical before it starts to decay and was

TABLE IV

CALCULATION OF THE CONCENTRATION VALUES $[A]_0$ AND $[B]$

Compound	Molecular wt. of Compound	Molecular wt. of Free Radical	Initial Concentration $[A]_0$, M	Absorbance at Peak	Molar Absorptivity & $l.mol^{-1}\ cm^{-1}$	$[B]_{max}$, M
Chlorpromazine hydrochloride	356.35	335.89	2.49×10^{-5}	0.158	9.60×10^{3}	1.65×10^{-5}
Prochlorperazine dimaleate	605.91	390.77	1.44×10^{-5}	0.121	8.27×10^{3}	9.50×10^{-6}
Trifluoperazine dihydrochloride	468.34	412.42	1.86×10^{-5}	0.146	1.53×10^{4}	1.17×10^{-6}
Thorazine	356.35	335.89	2.49×10^{-5}	0.167	9.60×10^{3}	1.74×10^{-5}
Compazine	605.91	390.77	1.44×10^{-5}	0.121	8.27×10^{3}	9.50×10^{-6}

Amount of phenothiazine compound injected, 20 µg (0.04 ml); Ce(IV), 8.00×10^{-5} M; H_2SO_4, 1.43M; 125 ml reservoir containing cerium(IV) and sulfuric acid.

TABLE V

CALCULATION OF THE FIRST ORDER RATE CONSTANTS k_1 AND k_2 FOR DIFFERENT PHENOTHIAZINES' FREE RADICALS BY METHOD

Free Radical	$\beta_{max} = [B]_{max}/[A]_0$	$\kappa = k_2/k_1$	$\tau_{max} = (1/\kappa - 1) \ln \kappa$	$t_{max} = \tau_{max}/k_1$	k_1, Sec^{-1}	k_2, Sec^{-1}
Chlorpromazine	0.66	0.21	1.98	1.00	1.98 (1.90)	0.42 (0.40)
Prochlorperazine	0.70	0.17	2.14	0.88	2.43 (2.35)	0.41 (0.40)
Trifluoperazine	0.63	0.25	1.85	1.00	1.85 (1.75)	0.46 (0.44)
Chlorpromazine in Thorazine	0.70	0.17	2.14	1.00	2.14 (2.00)	0.36 (0.34)
Prochlorperazine in Compazine	0.70	0.17	2.14	1.00	2.14 (2.05)	0.36 (0.35)

Amount of phenothiazine injected, 20 µg (0.04 ml); Ce(IV), 8.0×10^{-5} M; H_2SO_4, 1.43 M; t_{max}, measured from an oscilliscope trace, values for rate constants between parenthesis were obtained by curve fitting.

TABLE VI

CALCULATION OF THE FIRST ORDER RATE CONSTANTS k_1 AND k_2 FOR DIFFERENT PHENOTHIAZINES' FREE RADICALS BY METHOD II

Free Radicals	$\beta_{max} = [B]_{max}/[A]_0$	$\kappa = k_2/k_1$	t_{max}, Sec	k_1, Sec^{-1}	k_2, $Sec^{-1} = \frac{-\ln \beta_{max}}{t_{max}}$
Chlorpromazine	0.66	0.21	1.00	1.98 (1.90)	0.42 (0.40)
Prochlorperazine	0.70	0.17	0.88	2.38 (2.35)	0.41 (0.40)
Trifluoperazine	0.63	0.25	1.20	1.54 (1.75)	0.39 (0.44)
Chlorpromazine from Thorazine	0.70	0.17	1.20	1.76 (2.00)	0.30 (0.34)
Prochlorperazine from Compazine	0.70	0.17	1.00	2.10 (2.05)	0.36 (0.35)

Amount of phenothiazine injected, 20 µg (0.04 ml); Ce(IV), 8.0×10^{-5} M; H_2SO_4, 1.43 M; t_{max}, measured from an oscilloscope trace, values for rate constants between parenthesis were obtained by curve fitting.

calculated from the absorbance and molar absoptivity values.

Molar absorptivities were calculated by stabilizing the free radicals for about 30 seconds, except that the molar absorptivity of chlorpromazine free radical was taken from data of Lee and Tan [86]. (9.6×10^3 l.mole^{-1}.cm^{-1} compared to 1.0×10^4 l.mole^{-1}.cm^{-1} obtained in the present study).

The concentration values $[B]_{max}$ were obtained from Beer's law.

It is worth noting that values of k_1 and k_2 obtained by Methods I and II previously mentioned agree well within themselves (±5%) except values of k_1 and k_2 for prochlorperazine free radical by method II. One explanation may be possible if one considers that the t_{max} is slightly smaller than the actual value which gave rise to higher values of k_1 and k_2. However, a comparison of the theoretically predicted results by curve fitting (solid line) and the experimentally observed results as calculated by method I (crosses) shows very good agreement as depicted in Figure 13 for a typical case.

It is of interest to note that the rate constants determined for prochlorperazine dimaleate and its pharmaceutical preparation Compazine are almost identical; similar rate constants have also been obtained for chlorpromazine hydrochloride and its pharmaceutical preparation Thorazine (Table V). Rate constants values for Phenergan and Sparine are not reported here as no studies were carried on the pure compounds.

VI.1.3.2. Curve Fitting of the Transient Signal Profile. The curve fitting is based on computer-simulated data which have no error in themselves other than those introduced by round-off errors. The computer program carries out a self-modeling curve resolution automatically; its input is the data matrix of x (time in seconds) and y

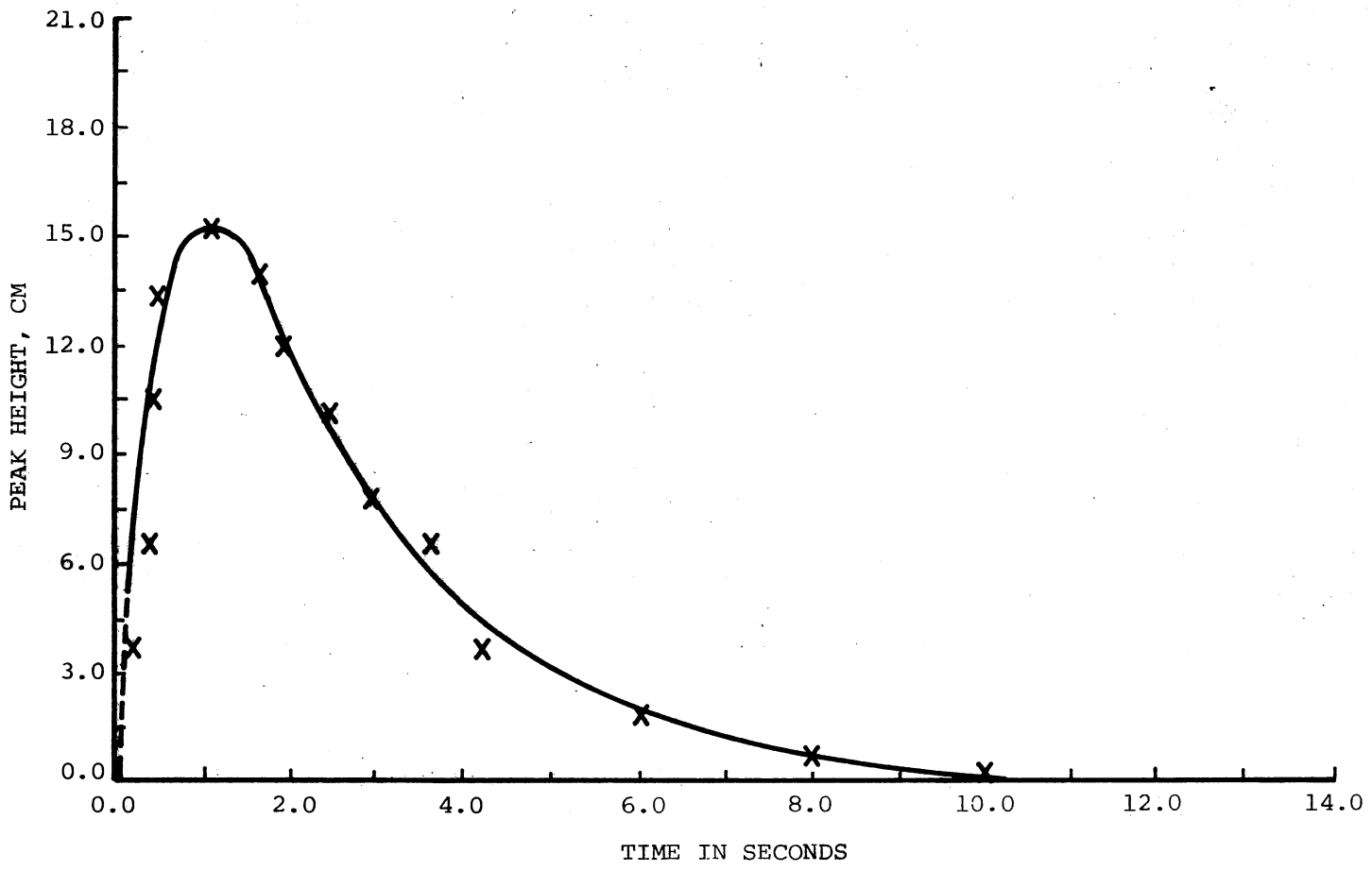

Figure 13. Comparison of the Signal Profile for Chlorpromazine Free Radical Obtained Experimentally (X) With That Predicted Theoretically (—)

(height from base line in centimeters), a range of values of k_1, another range of values for k_2, and a range of values for A (Appendix D.3). Ranges of k_1 and k_2 were taken from the computed values of the rate constants in Tables V and VI; ranges of A were taken between the peak height values experimentally obtained and higher values (intersection of two independent exponential curves).

A typical example of the graphic output is shown in Figure 13 for chlorpromazine free radical spectrophotometric transient signal, where the (x)-marked points are the experimentally obtained data pairs, and the solid line shows the data plotted with the least squares fit of the model: $[A]_0 \frac{k_1}{k_2-k_1} (e^{-k_1 t} - e^{-k_2 t})$. This solid line has been plotted after a search of combinations of k_1, k_2 and A values was made which gave the minimal sum-of-squares error.

It is the relative error, not the absolute error, which is critical in this analytic technique. Large errors are tolerable in regions where both x and y are large. However, even small errors in a region where both x and y are small and can produce considerable noise error in the estimates of x and y and the signal profile. It is wise therefore to avoid including extreme tail areas, near the base line, especially in the fall curve of the signal.

At any rate, a comparison of the transient signal profile experimentally obtained with that theoretically predicted from the equation describing the concentration time profile for the transient species shows a very good agreement. Apart from the dotted line which was not plotted by the plotter using the curve fitting program, it is seen that the best fit was obtained.

Another approach to the selection of different combinations of k_1 and k_2 values which satisfy the relation $\kappa = k_2/k_1$, was made as follows:

$$\text{at } t_{max}, \frac{d[B]}{dt} = 0,$$

hence,

$$0 = \frac{[A]_0 k_1}{k_2 - k_1} (-k_1 e^{-k_1 t} + k_2 e^{-k_2 t})$$

and since $[A]_0$, k_1 and k_2 cannot be equal to zero because its lack of any physical significance, therefore:

$$-k_1 e^{-k_1 t_{max}} + k_2 e^{-k_2 t_{max}} = 0$$

On rearrangement:

$$k_1 e^{-k_1 t_{max}} = k_2 e^{-k_2 t_{max}}$$

which is equivalent to,

$$k_1/k_2 = e^{-k_2 t_{max} + k_1 t_{max}}$$

Taking natural logarithms for both sides:

$$\ln k_1/k_2 = -k_2 t_{max} + k_1 t_{max}$$

which on rearrangement gives,

$$\ln k_1 - k_1 t_{max} = \ln k_2 - k_2 t_{max}$$

By substituting for t_{max} in the last equation, either side of the equation may be plotted for several values of k, covering the range of values for k_1 and k_2 as found in Tables V and VI, where a peaked profile was obtained. The values of k_1 and k_2 taken from the graph were substituted in the equation and a plot was obtained. Several combinations of k_1 and k_2 were tried until the best fit was obtained (each combination has the same value of κ).

This last approach differs from the first approach to curve fitting in that the combinations of k_1 and k_2 were selected a priori to selection of the best fit. Though both approaches are mainly trial-and-error approaches, the first one is basically more sound, statistically speaking, than the second one. Unlike the second approach, the first one is independent of the t_{max} value from which the combinations of k_1 and k_2 are selected. Thus, the first approach was preferred over the second one in the present investigation.

VI.2. A Note on Methods for the Spectrophotometric Determination of Vanadium(V) and Chromium(VI)

As with most transition metals, there is no lack of chromogenic reagents for vanadium, and a large number of spectrophotometric methods appeared in the last few years. From the standpoint of spectrophotometric trace analysis, chromium is one of the most readily determined elements. It can be separated from the other elements fairly easily and determined with very high sensitivity. As with vanadium, the literature contains a very large number of methods, and one may refer, for example, to the April issues of Analytical Chemistry for reviews.

VI.2.1. Determination of Vanadium(V) and Chromium(VI) Via the Formation of Transient Species

VI.2.1.1. General Discussion. At low pH's (1.3-2.0), the dioxovanadium(V) ion, VO_2^+, is the main form of vanadium(V) in aqueous solution, while for chromium(VI) the dichromate ion, $Cr_2O_7^{2-}$, is the principal species. Unlike vanadium(V), chromium(VI) does not give rise to the extensive and complex series of polyacids and anions such as $(H_nV_{10}O_{28})^{(6-n)-}$ [91]. The following standard potentials have been estimated for acidic solutions of vanadium and chromium, respectively [88].

$$VO_2^+ + 2H^+ + e = VO^{2+} + H_2O \qquad (E^0 = 1.00 \text{ volt}) \qquad (22)$$

$$Cr_2O_7^{2-} + 14H^+ + 6e = 2Cr^{3+} + 7H_2O \qquad (E^0 = 1.33 \text{ volt}) \qquad (23)$$

When a solution of either vanadium(V) or chromium(VI) is injected into a strongly acidic solution containing oxalic acid and excess barium diphenylaminesulfonate, a transient signal is produced. This is due to the "instantaneous" oxidation of the barium diphenylaminesulfonate, to the colored product, corresponding to diphenylbenzidine violet, and its destruction by further oxidation.

Diphenylamine-4-sulfonic acid and its salts, for example barium diphenylamine-4-sulfonate, are water soluble, and the course of oxidation is said to be the same as for the unsubstituted compound such as diphenylamine [92]. The reactions for the oxidation of diphenylamine, and its derivatives, were postulated as follows [93].

$$2DPA \longrightarrow DPB + 2H^{+} + 2e \qquad (24)$$

$$DPB \underset{k_{-1}}{\overset{k_1'}{\rightleftharpoons}} DPBV + 2H^{+} + 2e \qquad (k_1 >> k_{-1}) \qquad (25)$$

$$DPB \cdot DPBV$$

$$DPBV \xrightarrow{k_2} \text{Destruction product} \qquad (26)$$

where DPA stands for diphenylamine, DPB for diphenylbenzidine, and DPBV for diphenylbenzidine violet. For comparison with Equations 20 and 21, DPBV is the monitored transient species that corresponds to C, DPB corresponds to A, and B and Y correspond to the reagents vanadate and perchloric acid. The rate constants k_1 and k_2 refer to the formation and decay of DPBV, respectively. Skeletal structures of the different species can be found in Appendis B-3.

Bishop et al. [94] have shown that diphenylamine and its derivatives are oxidized directly to the violet compound (DPBV) without intermediate formation of the diphenylbenzidine derivative (DPB). The benefit in using diphenylbenzidine as an indicator in place of diphenylamine is marginal, because with the latter the diphenylbenzidine is formed from homogeneous solution and appears to be in a colloidal dispersion that reacts more quickly with oxidants. On the other hand, when diphenylbenzidine is used directly, the coagulated precipitate formed is very slow to redissolve and react. This is in accord with the results obtained by Bishop et al. [94] where the rate of formation of DPBV is very large (from diphenylamine) as compared to that from diphenylbenzidine.

It follows therefore that the reaction pertinent to the formation of the diphenylbenzidine violet is as follows:

$$2DPA \xrightarrow{k_1} DPBV + 4H^+ + 4e \qquad (27)$$

where k_1 is the pseudo-first-order rate constant for the formation of DPBV. In relation to Equations 20 and 21, DPBV is the monitored transient species which corresponds to C, and DPA corresponds to A. Thus, Equations 24 and 25 are not treated kinetically, and Equations 26 and 27 are used instead. The earlier discussion only refers to an obsolete scheme and was mentioned only for the sake of completeness.

The major analytical applications of diphenylamine, and its derivatives, is in dichromate and vanadate titrimetry, which are well covered in standard texts [95]. Dichromate as an oxidant is not capable of oxidizing the indicator except in the presence of iron(II), probably owing to an induced effect. Kilthoff and Belcher [96] asserted that oxidation of the indicator itself is normally slow but is induced by the reaction between dichromate and iron(II). These indicators are also subject to such induced reactions in the presence of polyhydric alcohols and sugars [97]. It was found in the present investigation that oxidation of diphenylaminesulfonate anion by dichromate and vanadate did not proceed, or proceeded very slowly. Oxalic acid acting as a promoter [98] considerably accelerates the oxidation of diphenylaminesulfonate by both chromium(VI) and vanadium(V).

In the present study, microgram amounts of vanadate and dichromate have been determined spectrophotometrically via transient signals. This was effected by injection of their solutions into the flow-through cell where a solution of barium diphenylaminesulfonate, perchloric acid, and oxalic acids, was continuously flowing. A variety of experimental factors have been investigated in order to ascertain the optimal experi-

mental conditions for continuous repetitive determination of vanadate and dichromate in aqueous solutions.

VI.2.1.2. Effects of Different Experimental Factors on the Transient Signal

Effects of Various Acids. According to the equations for the oxidation of DPA in acidic media, Equations 24-26, hydrogen ions take an essential part in the oxidation-reduction reactions of diphenylamine. They also participate in the redox reactions of the vanadium(V) and chromium(VI) species, Equations 22 and 23. The optimum concentrations of oxalic acid, barium diphenylamine-sulfonate, and perchloric acid were selected after each reactant concentration was varied separately and the heights of the signals obtained were compared.

Figure 14 shows variation of peak height of the transient signal with change of concentration of perchloric acid. As can be seen, the peak height increases with increase of perchloric acid concentration, until the curve reaches a plateau at about 1.4 M. A concentration of perchloric acid equal to 1.67 M was chosen as the optimum concentration in order to insure minimal variations in the peak height. A graph having a similar profile was obtained for chromium(VI) injections.

The effects of phosphoric acid (K_{a_1}, 1.0×10^{-2}) and acetic acid (K_a, 2.24×10^{-5}) were compared with those of perchloric acid (completely ionized) under the same conditions. Larger signals were obtained in the presence of phosphoric acid. Though perchloric acid gave signal heights similar to those obtained with phosphoric acid in the case of vanadium(V), larger signals were obtained with perchloric acid for chromium(VI). Sulfuric acid was not used because it would cause

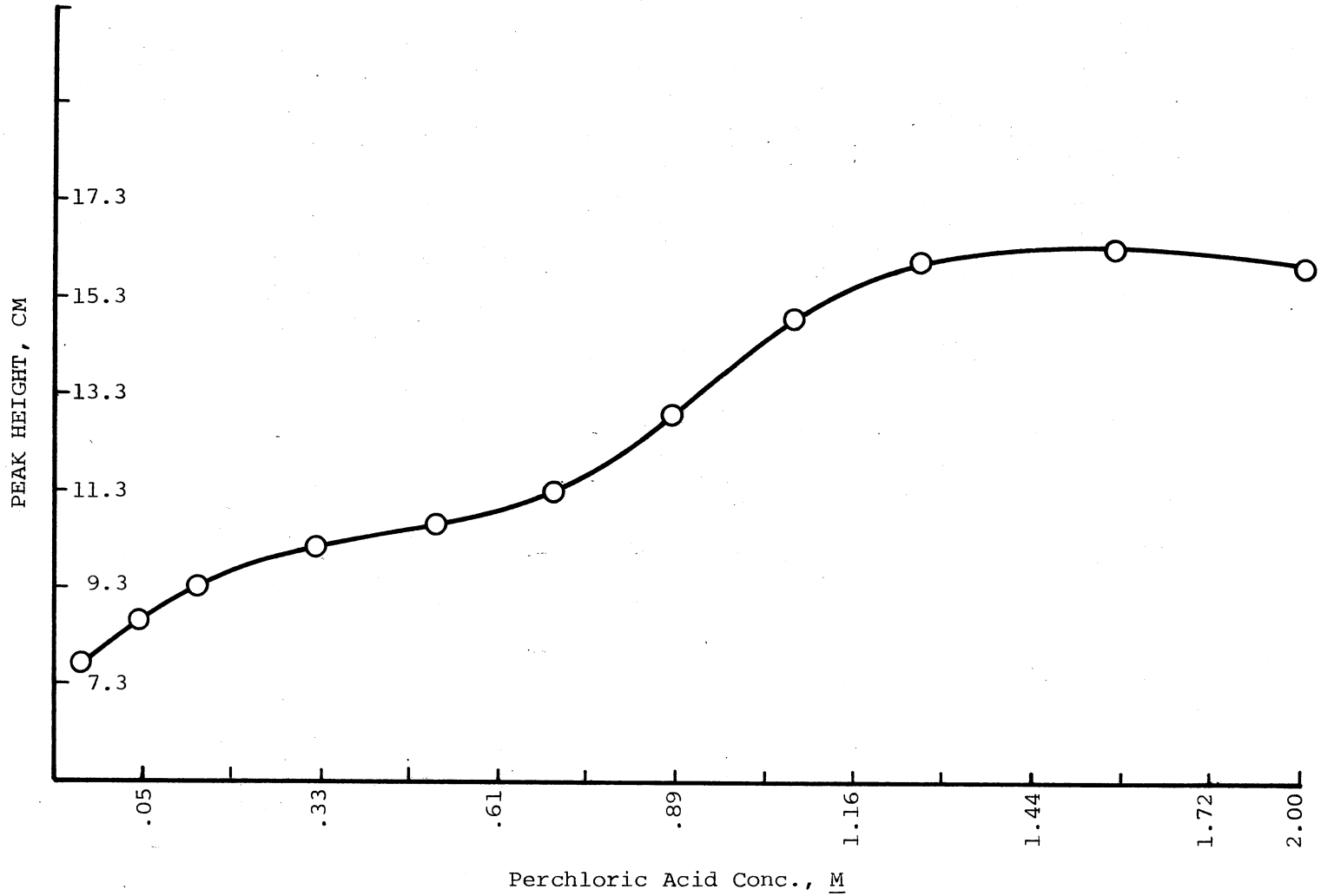

Figure 14. Variation of Peak Height With Perchloric Acid Concentration

precipitation of barium sulfate from the barium diphenylaminesulfonate, hydrochloric acid was not used because it might produce free chlorine by reaction with vanadate and dichromate.

Effect of Oxalic Acid Concentration. The oxidation of diphenylbenzidine (DPB) by vanadate to diphenylbenzidine violet (DPBV) and its further destruction by excess of the oxidant proceeded slowly in the absence of oxalic acid. An example involving induced reactions has been mentioned earlier; the dichromate oxidation of diphenylamine in the presence of iron(II). Iron(II) is said to induce the reaction between chromium (as dichromate) and diphenylamine. A fundamental difference between an induced reaction and a catalyzed one is that the inductor is consumed and is not regenerated. The overall change from chromium(VI) to chromium(III) is a three-electron process and chromium(V) or chromium(IV) can participate as transient intermediates in the reactions. Since vanadate does not react by producing an intermediate species ($V^{5+} \rightarrow V^{4+} - e$), it is suggested that the oxidation of diphenylbenzidine by vanadium(V) in the presence of oxalic acid is not an induced reaction, and is probably a promoted one [98]. Examples of several promoter effects were reported by Dutt and Mottola [98]. They found that the rate of oxidation of ferroin (tris (1,10-phenanthroline) iron(II)) by chromium(VI) in the presence of promoters, including oxalic acid, is only affected in the earlier portions of the reaction, the disappearance of the modified rate appears to be due mainly to complexation of the promoter with chromium(III). Oxalic acid was either decarboxylated or rendered inactive by complexation with some species of chromium(III). In addition, chromium(III)-oxalate complex showed no accelerating effect on the ferroin-chromium(VI) indicator reaction.

To summarize, the effect of oxalic acid does not satisfy the criterion for induced effects, where in the velocity of a redox process is increased during a concurrent rapid reaction between the redox reagent and the inductor. The nature of the rate modifier would indicate that it is concurrently either destroyed or rendered inactive--a behavior which may be better regarded as promotion [98]. It should also be noted that the reaction between oxalic acid and chromium(VI) is not rapid nor is that between oxalic acid and vanadium(V). If the peak maximum is proportional to the ratio of the rate constants (Appendix C), the ratio varies with the concentration of oxalic acid as shown in Figure 15, then becomes independent of oxalic acid concentrations at values above 0.21 M. A graph having a similar profile was obtained for chromium(VI) injections.

Effect of Barium Diphenylaminesulfonate Concentration. Variation of peak height with the sulfonate concentration is represented in Figure 16. The peak maximum varies linearly with DPA concentration until a concentration equal to 1.00×10^{-3} M is reached. At concentrations higher than this concentration, the peak height is independent of DPA concentration, and in essence the ratio of the rate constants is related to the peak height.

The optimum DPA concentration was obviously chosen in the plateau region where the peak maximum is the largest and is independent of DPA concentration. This optimum concentration of DPA is obviously dependent upon the amount of vanadium(V) or chromium(VI) injected.

Effects of Other Experimental Factors. A variety of other experimental factors such as flow rate, stirring rate and recorder chart

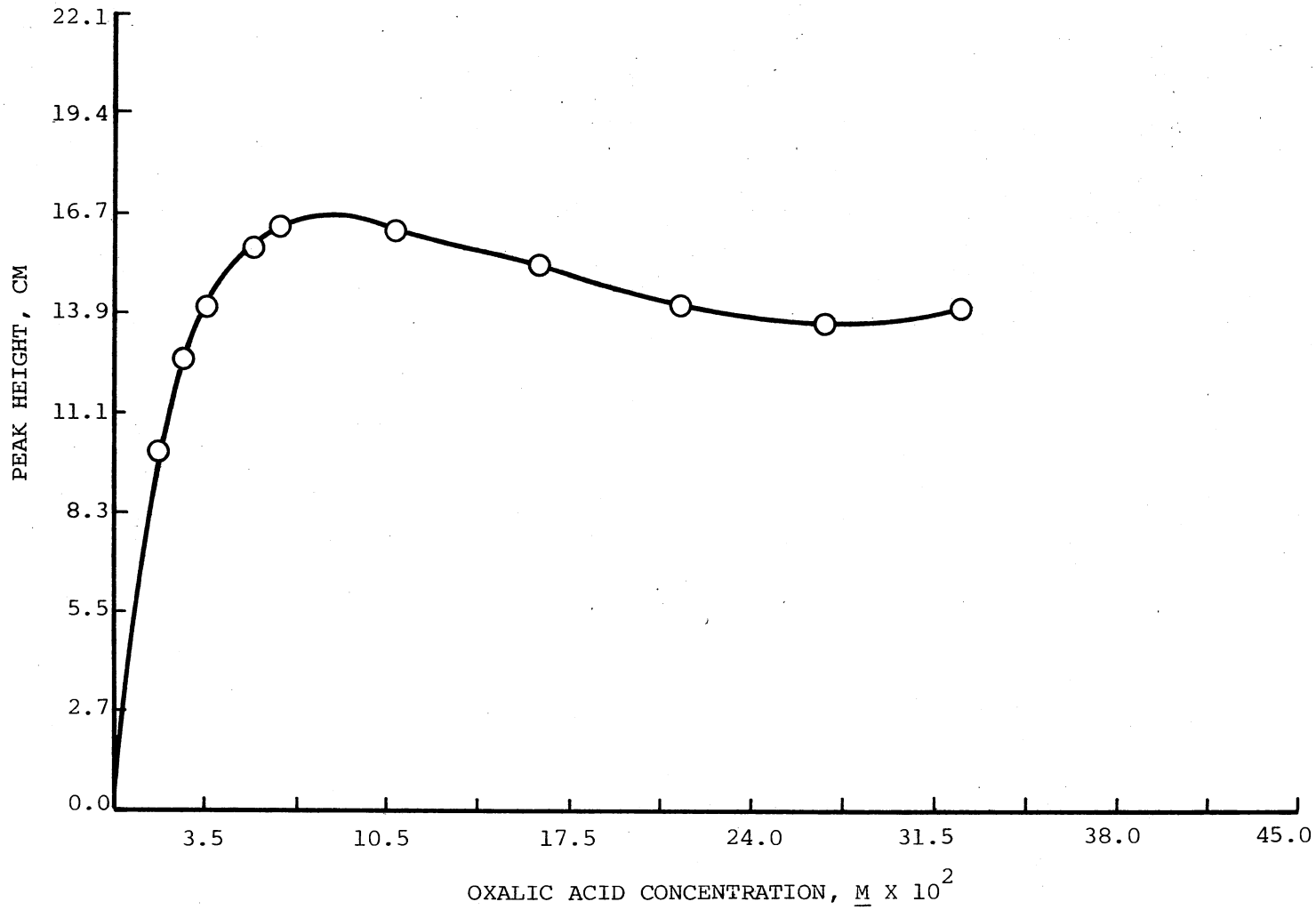

Figure 15. Variation of Peak Height With Oxalic Acid Concentration

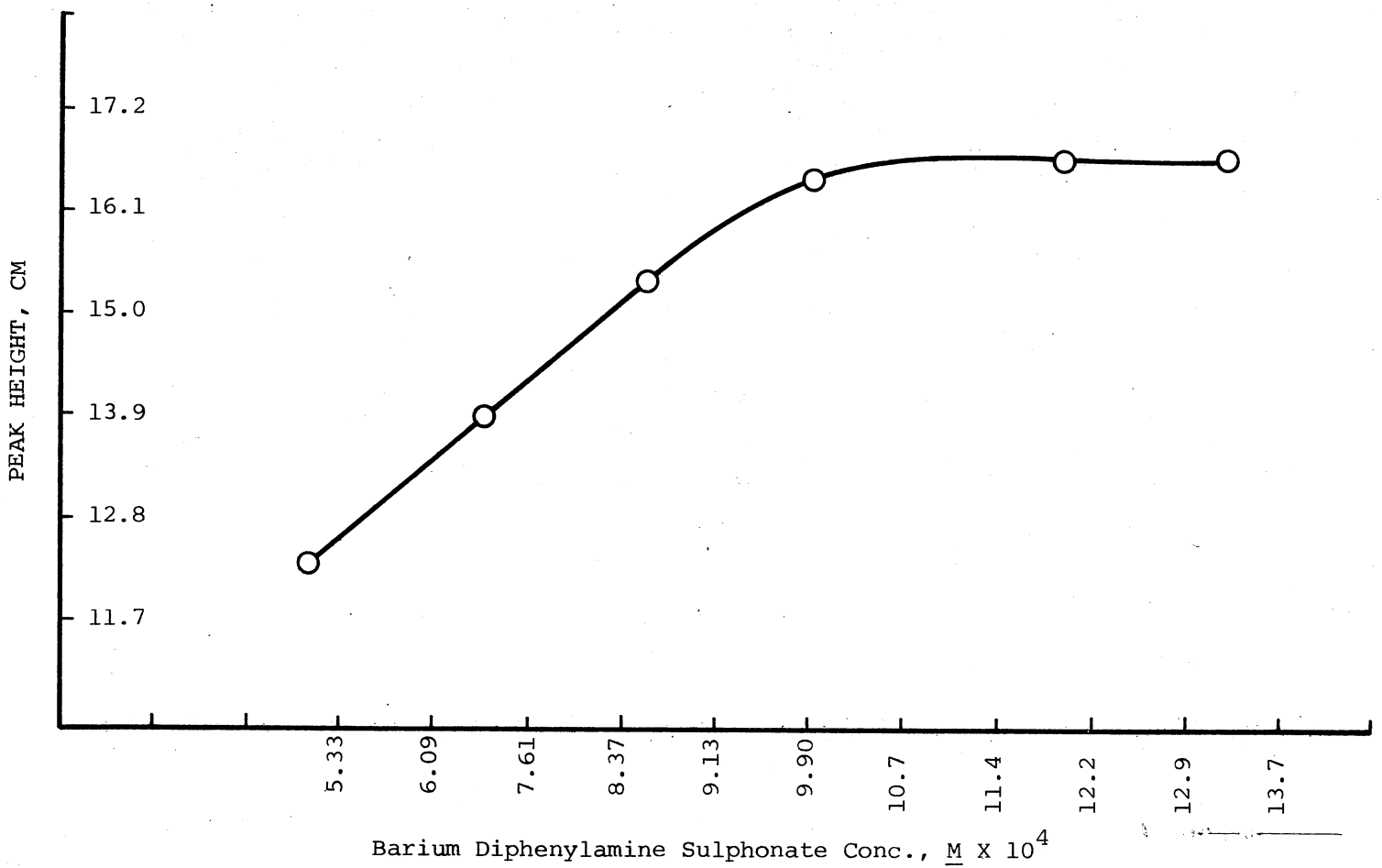

Figure 16. Variation of Peak Height With Indicator Concentration

speed have also been studied in order to ascertain the optimum experimental conditions for continuous repetitive determination of vanadate and dichromate in aqueous solutions. The results are similar to those of Table I, and are basically comparisons of peak heights of the transient signals obtained at different conditions.

The effect of temperature on the transient signal has also been studied. Temperature increase accelerates the formation of the destruction product (Equation 26). This makes the determination via transient signals by monitoring the absorbance of DPBV rather difficult. It should be noted that the destruction product formation and decay is not transient as is the case of diphenylbenzidine violet.

VI.2.1.3. Determination of Vanadium(VI) and Chromium(VI) Via the Formation and Decay of Diphenylbenzidine Violet. Table VII shows some pertinent data for the spectrophotometric determination of vanadate and dichromate via the formation and decay of the transient species diphenylbenzidine violet. In both cases, the formation and decay of DPBV was monitored at 550 nm, where maximum absorbance was observed. The limit of detection has been selected as the amount of oxidant which produces a peak maximum equal to twice the height of the blank signal, and the range of determination corresponds to the linear portion of the working curve under the present experimental conditions.

Plots of the calibration curves for the determination of vanadium and chromium are shown in Figure 17, where linear regression analysis was applied to obtain the slope a and the intercept c of the regression line. Using Student's t statistics, the calculated t value given by $|t| = |c|/s_c$ was found to be smaller than the tabulated t value for the corresponding values of n, f, and α. It is therefore accepted that the

TABLE VII

USE OF TRANSIENT SPECIES IN THE SPECTROPHOTOMETRIC DETERMINATION OF MICROGRAM AMOUNTS OF VANADIUM(V) AND CHROMIUM(VI)

Metal Compound	Limit of Detection, µg	Intercept c, cm	Range, µg	Slope a, cm/µg
Vanadate	0.10	-0.4	0.5-10.0	3.44
Dichromate	0.12	+0.4	0.5-10.0	2.07

For each calibration graph (DPA, 1.04×10^{-3} M; $HClO_4$, 1.67 M; $H_2C_2O_4$, 0.07 M) 150 ml solution; other experimental conditions are given in the text; values of c and a are obtained from the regression line (1.0 cm = 0.0157 A).

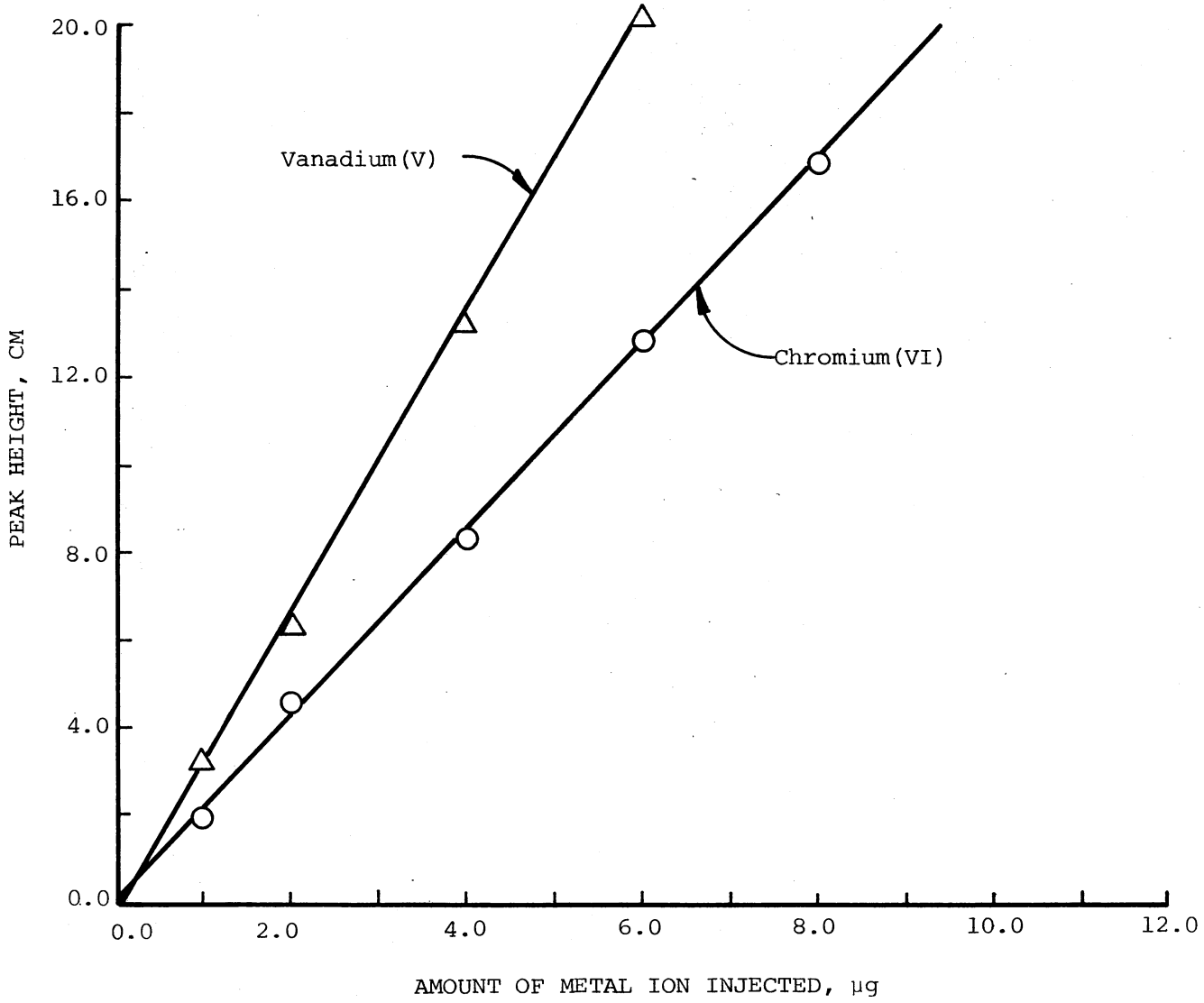

Figure 17. Variation of Peak Height With Metal Ion Concentration

regression line passes through the origin; in fact, if the value corresponding to the limit of detection is excluded from the regression line, this line actually passes through the origin [99]. The differences in slopes of the standard curves are due partly to the different rates of formation and decay of the DPBV species by vanadate and dichromate, as can be seen in Table XI. Also comparison of the slopes, draws that determination of vanadium is more sensitive than determination of chromium.

Data for repetitive determination of these oxidants in aqueous solutions are listed in Table VIII, where n is the number of injections made, $\bar{X}$ is the average peak height, and v_x is the percent relative standard deviation (Appendix E.1). It should be noted that the number of injections can be increased considerably simply by using a large reservoir which contains a larger volume of the reagents.

TABLE VIII

REPETITIVE SPECTROPHOTOMETRIC DETERMINATION OF VANADIUM(V) AND CHROMIUM(VI) VIA TRANSIENT SIGNALS

Metal Compound	Number of Injections, n	$\bar{X}$ cm	±Conficence Limits at the 95% Level	v_x
Vanadate	40	16.8	0.10	3.1
Dichromate	35	10.8	0.07	3.2

For each set of determinations a 50.0 ml solution was used (concentrations as in Table VII; amount of metal injected, 5.0 µg (0.10 ml).

To summarize, the spectrophotometric measurement of transient signals using the flow injection technique has been successfully applied to the determination of vanadate and dichromate in the order of microgram amounts. The percent relative standard deviation, which is related to the magnitude of the peak height, could be even decreased below its values of 3.50 by a mechanically controlled injection device. It should be pointed out that other oxidants, such as cerium(IV) and manganese(VII) are also capable of oxidizing DPA to the transient DPBV; it has been suggested [1] that they can be determined via transient signals.

TABLE IX

VARIATION OF THE PEAK HEIGHT OF THE TRANSIENT SIGNAL FOR VANADIUM(V) AND CHROMIUM(VI) IN PRESENCE OF SOME FOREIGN IONS

Added Ion(X)	Concentration Ratio C_X: C_V (C_X: C_{Cr})		
	1:1	10:1	100:1
Cu^{2+}	16.9(11.2)	17.8(11.8)	-----
Fe^{3+}	16.7(11.1)	17.5(11.6)	-----
Ni^{2+}	16.8(11.1)	16.9(11.2)	17.0(11.3)
Co^{2+}	16.7(11.0)	16.7(11.1)	16.7(11.1)
Cr^{3+}	16.4(10.9)	16.5(10.9)	17.2(11.4)
Mn^{2+}	16.8(11.2)	16.9(11.2)	17.4(11.6)
Mo^{6+}	16.8(11.2)	15.9(10.5)	White ppt.
W^{6+}	16.3(10.8)	8.6(5.7)	Green ppt.

Experimental conditions are given in Table VII; amount of injected metal, 5.0 µg (0.10 ml); peak height for Cr(VI), 11.0 cm; peak height for V(V), 16.6 cm; 1.0 cm = 0.0157 a. No values were taken for Cu^{2+} and Fe^{3+} since the latter is usually extracted or complexed before determination of other elements in steel, and Cu^{2+} is usually present in small amounts.

VI.2.2. Effects of Interfering Ions

The influence of a limited number of ions on the spectrophotometric determination of vanadate and dichromate via transient signals has been studied. This study was limited to the metal ions ordinarily encountered in steels. These ions were added to the vanadate, or dichromate, solution to be injected in varying quantities as shown in Table IX. Transient signals obtained upon injection of these different solutions were compared with those obtained with pure vanadate, or dichromate, aqueous solutions.

Colored ions which have appreciable absorption at 550 nm do not interfere with the spectrophotometric determination except when they are present in appreciable concentrations (100-fold excess); use of double beam spectrophotometers might compensate for the background absorbance of the injected solution.

VI.2.3. Analysis of Steel Samples

Plain carbon steel contains a certain amount of carbon, silicon, sulfur, phosphorus, and manganese. For special purposes, varying amounts of other elements such as chromium, vanadium, molybdenum, tungsten, titanium, nickel, cobalt, copper, and zirconium are added. Generally, a large number of methods are available for the determination of each element; iron itself is rarely determined in steels. The procedure for determination will depend upon the object in view; the more accurate methods are usually less rapid.

For the determination of elements present in small quantities (usually less than one per cent), colorimetric, spectrophotometric, spectrographic and polarographic techniques are widely used. The intro-

duction of EDTA as a masking agent and as a titrant, as well as selective organic reagents, has contributed greatly to the development of simplified methods of analysis. Solvent extraction procedures are used for the removal of major amounts of iron and selective extraction of various elements so as to eliminate interfering substances.

The steel samples used (NBS 34a and NBS 65) for the determination of chromium and vanadium contained all the elements mentioned above except cobalt, titanium, tungsten, and zirconium. Vanadium and chromium were present in very small amounts: 0.007 and 0.275% in National Bureau of Standards Sample No. 34a and 0.003 and 0.05% in NBS Sample No. 65. The main problem lies here in concentrating the solutions obtained by dissolving the steels so that one will be able to determine the amounts of these elements by the injection technique.

Steel samples were first dissolved in sulfuric-phosphoric mixture where phosphoric acid was used to complex the iron and decolorize the solution. Nitric acid was then added to break up the black insoluble carbides of chromium and vanadium which were left after the acid-mixture treatment. Persulfate, and silver nitrate as a catalyst, was added to oxidize chromium, any unoxidized vanadium, and manganese to chromic, vanadic, and permanganic acids, respectively. Hydrochloric acid was used to reduce the permanganic acid, and the resulting solution was divided into two unequal portions. The vanadic and chromic acids in the larger portion were reduced with sulfur dioxide gas and the vanadium (but not chromium) selectively reoxidized with permanganate. Excess permanganate was removed by boiling the solution with very little hydrochloric acid, and the solution was then concentrated by evaporation. A small volume (0.20 ml) of the resulting solution was injected

into the cell for vanadate determination. A smaller volume (0.10 ml) of the other portion was injected into the cell for dichromate determination.

The experimental procedure adopted for the dissolution of steel samples was that given in Vogel [100] and will not be described here as the main features have already been mentioned. It has been assumed that interference by very small amounts of vandium with the determination of chromium was negligible, especially in Sample No. 34a in which the ratio of Cr: V = 39:1. The results of the determinations are given in Table X.

TABLE X

DETERMINATION OF VANADIUM AND CHROMIUM IN NATIONAL BUREAU OF STANDARDS STEEL SAMPLES

Sample No.	Chromium, %		Vanadium, %	
	Present	Found	Present	Found
NBS 65	0.05	0.045,0.046	0.003	0.0027,0.0025
NBS 34a	0.275	0.253,0.250	0.007	0.0064,0.0062

It should be noted that although the determination of vanadium and chromium in steel is possible via transient signals, the chemical system used does not seem to offer substantial advantages over other conventional ways for their determination.

VI.2.4. Kinetic Studies Related to the Formation and Decay of Diphenylbenzidine Violet

Computation of the rate constants k_1 and k_2 for the formation and decay of DPBV was made following the previous discussion (Section VI.1.3.) and the results are given in Tables XI and XII.

TABLE XI

CALCULATION OF THE CONCENTRATION VALUES $[A]_o$ AND $[B]_{max}$ FOR DIPHENYLBENZIDINE VIOLET

Oxidant	Initial Conc. $[A]_o$, M	Absorbance at Peak	$[B]_{max}$, M
Vanadate	9.81×10^{-6}	0.263	5.78×10^{-6}
	3.92×10^{-6}	0.106	2.35×10^{-6}
Dichromate	2.96×10^{-5}	0.172	3.78×10^{-6}
	1.18×10^{-5}	0.074	1.65×10^{-6}

Amount of oxidant injected: 5.0; 2.0 µg (0.10 ml); diphenylamine sulfonate, 1.04×10^{-3} M; $HClO_4$, 1.67 M; oxalic acid 0.07 M; molar absorptivity of diphenylbenzidine violet, 4.50×10^4 l.per mole per cm.

The molar absorptivity of diphenylbenzidine violet was taken from the data reported by Sarver and von Fischer [101]. The initial concentration for DPBV was calculated using the following expression:

$$\frac{\text{Amount Injected (µg)} \times 10^{-6} \times 10^{3}}{\text{Detection Volume (ml)} \times \text{at. wt.} \times F}$$

which is expressed in mmole per ml, i.e., in molarity. From the chemi-

TABLE XII

CALCULATION OF THE PSEUDO-FIRST ORDER RATE CONSTANTS k_1 AND k_2 FOR DIPHENYLBENZIDINE VIOLET BY METHOD II

Oxidant	$\beta_{max} = [B]_{max}/[A]_o$	$\kappa = k_2/k_1$	t_{max}, Sec	k_1, Sec^{-1}	k_2, Sec^{-1}
Vanadate	0.59	0.31	2.1	0.81 (0.78)	0.25 (0.24)
	0.60	0.29	2.0	0.89 (0.83)	0.26 (0.24)
Dichromate	0.13	0.74	1.5	1.84 (1.73)	1.36 (1.28)
	0.14	0.72	1.4	1.95 (1.85)	1.40 (1.33)

Experimental conditions are given in Table XI; values between parentheses were obtained by curve fitting.

cal equations relevant to the oxidation of diphenylamine to diphenylbenzidine violet, it is evident that four vanadate ions are consumed in the production of one diphenylbenzidine violet molecule (Equation 25), and hence F in the denominator is equal to four. On the other hand, in case of dichromate oxidation F is equal to four-thirds and the atomic weight of chromium is substituted for that of vanadium in the previous expression. This is based on the assumption that one dichromate ion consumes six electrons, i.e., two chromium ions consume six electrons when the dichromate ion acts as an oxidant in strongly acidic medium. Consequently, four electrons are furnished by 2 x 4/6 chromium(VI) ions. The molecular weight was calculated from the formula to be 334.42, and the detection volume to be 2.5 ml (Section VI.1.3.1.).

In both cases, the initial concentration $[A]_0$ is equivalent to the diphenylbenzidine violet concentration since the transient signal follows the formation and decay of DPBV itself. Data for the pseudo-first order rate constants for the formation and decay of the transient violet chromophore are given in Table XII. Curve fitting of the signal profile was carried out as in Section VI.1.3.2, and the agreement between the theoretical and experimental data is satisfactory as can be seen in Figure 18.

It should be noted that the pseudo-first order rate constants were calculated by Method II and not by Method I since the two methods give essentially similar results.

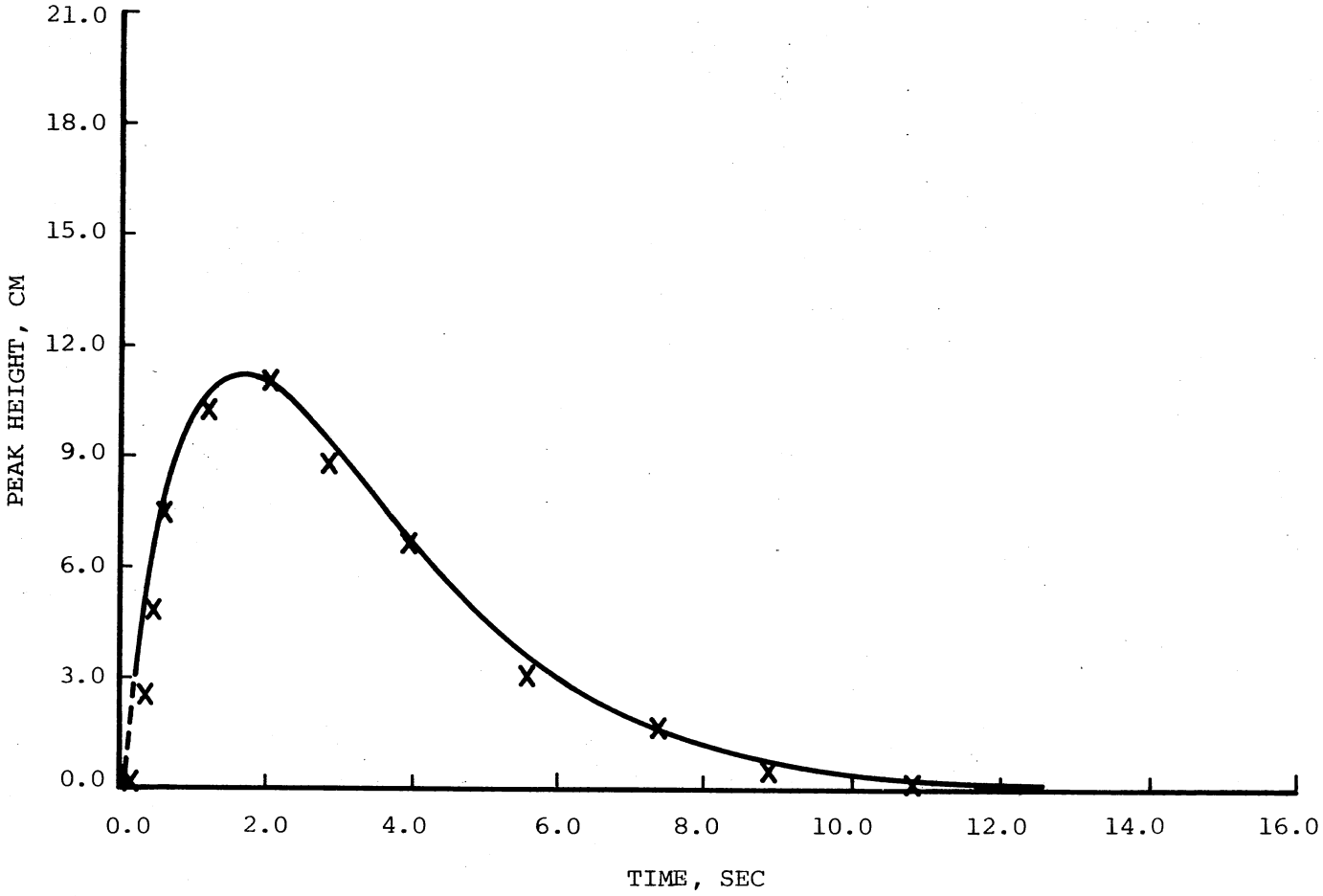

Figure 18. Comparison of the Signal Profile for Diphenylbenzidine Violet Transient Species Obtained Experimentally (X) With That Predicted Theoretically (Solid Line)

VI.3. Determination of Zinc(II) And Cadmium(II) Via the Formation of Transient Signals

VI.3.1. General Discussion

Among the complexing agents used extensively nowadays in analytical complexometry are aminopolycarboxylic acids of which ethylenediaminetetraacetic acid (EDTA) is by far the most important. Trans-diaminocyclohexanetetraacetic acid (DCTA) generally forms somewhat more stable complexes than EDTA does but they are formed and dissociated more slowly [102]. On the other hand, diethylenetriaminepentaacetic acid (DETPA) binds metal ions having a coordination number of 8 better than EDTA does, and therefore has advantages in titrations of larger cations, especially those of the lanthanindes and actinides.

The reactions that take place when a solution of a metal cation and one of a chelating agent are mixed, such as Zn^{2+} and EDTA, respectively, may be simply described by the following equations [103].

$$(\text{pH } 7\text{-}9)\quad Zn^{2+} + HZ^{3-} \rightarrow ZnZ^{2-} + H^{+} \qquad (28)$$

$$(\text{pH } 4\text{-}5)\quad Zn^{2+} + H_2Z^{2-} \rightarrow ZnZ^{2-} + 2H^{+} \qquad (29)$$

where H_4Z stands for the fully protonated EDTA. Since hydrogen ions are liberated during the reaction of metal ions with EDTA, the solution is buffered to prevent a large change in pH.

Owing to the basicity of the ion Z^{4-}, the free energy of complex formation depends on the pH and is measured in terms of the conditional formation constant, which is equal to the equilibrium constant divided by the alpha (α) coefficient. This alpha coefficient is here defined

to be equal to $1 + \sum_{j=1}^{J} \beta_{H_jZ}[H]^j$, where β_{H_jZ} denotes the overall stability constant for j series of steps, and log β_{H_jZ} is equal to $\sum_{j=1}^{J} pK_j$.

In the exceptional case of strongly alkaline solutions (pH ≥ 11), the alpha values approach one ($\alpha_{Z(H)} \geq 1$); at lower pH values they are far greater than one. Thus, the influence of pH on the stability of a complex is extremely important, and its extent can be realized from the values of alpha for different complexing agents at various pH values.

At any given pH value, the $\alpha_{Z(H)}$ value is always greater for DCTA than for EDTA; this arises from the larger value of pK_{a_1} for DCTA (12.35 as compared to 10.26) [103]. Also, the $\alpha_{Z(H)}$ value for DETPA is always greater than for EDTA (pK_{a_1} for DETPA, 10.58). However, metal complexes of polyaminocarboxylic acids are able to take up a proton in strongly acidic solutions and to react with a hydroxyl ion in alkaline solutions. This extra proton attaches itself to a carboxylate ion which therefore does not act as a ligand and the hydroxyl ion either displaces a carboxylate ion or increases the coordination number to 7 or 8.

In analytical complexometry, the solution to be titrated often contains the metal to be determined not as free cation or chelated complex, but also in the form of other complexes, e.g., as ammine complexes, if the solution has been made ammoniacal. To produce a high and nearly fixed pH, ammonium ion--ammonia buffer is added; this forms complexes with the cations present and also prevents precipitation of metal hydroxides. Naturally, the stabilities of the ammine complexes will be lower than those formed by the polyaminocarboxylic acid and reactions take place between the various ammine complexes and the various ionized species derived from the aminopolycarboxylic acid (complexone).

This somewhat complicated state of affairs can describe with the aid of the alpha coefficients for the metal ion $\alpha_{M(A)}$ and complexone $\alpha_{Z(H)}$ and the equilibrium constant for the reaction of the metal complexone (K_{MZ}) where $\alpha_{M(A)} = 1 + \sum_{n=1}^{N} \beta_{MA_n} [A]^n$, ($A = NH_3$).

Changes in colors which can be used to indicate end-points in complexometric titrations are almost always due to complex formation between the indicator and the metal. Metallochromic indicators refer to those organic coloring materails that undergo a change of color when they form metal complexes. Since they have high molar absorptivities, of the order of 10^4 - 10^5 $l \cdot mole^{-1} \cdot cm^{-1}$, they need only be added in concentrations of 10^{-6} - 10^{-5} M to give a color change which is still clearly detectable in a visual form. Eriochrome Black T was referred to in the very first papers on complexometric titration, and even now is one of the most frequently used metallochromic indicators [104]. The following structural formulas describe the red species that occur in solutions below pH 6, and its divalent metal complex [104].

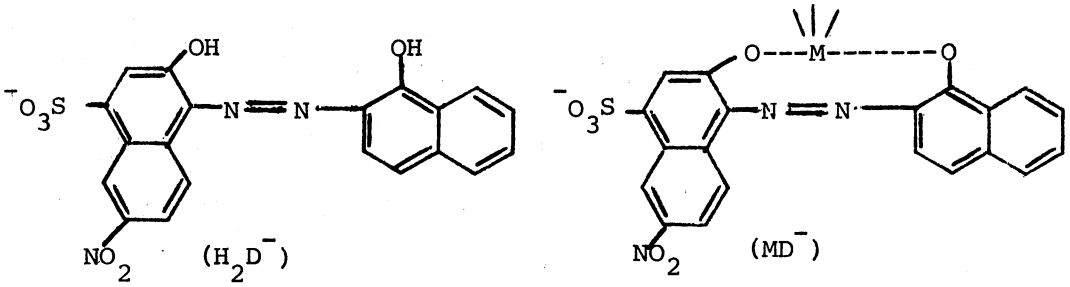

At about pH 6.3, the red species H_2D^- changes to blue HD^{2-}, and finally into the fully deprotonated yellow-orange form D^{3-} at pH 11.5. The metal complexes are red or violet, and the change in color when they are formed is especially sharp if the pH lies between 7 and 11, since

this is the region in which the indicator exists in the blue form HD^{2-} and the color changes to red on the addition of a metal ion.

The essence of the present study is based on the following assumption. When a solution of metal ion such as Zn^{2+} is injected into a mixture of a metallochromic indicator (EBT) and a polyaminocarboxylic acid (EDTA) buffered by a buffer such as ammonium ion-ammonia, a transient signal should be produced due to an increase followed by a decrease in absorbance of the M-EBT chelate. Since the conditional formation constant of the M-EDTA chelate is much larger than that of the M-EBT chelate, the rise curve of the signal corresponds to the "instantaneous" formation of M-EBT chelate while the fall curve corresponds to the gradual formation of M-EDTA chelate. The chemical equations describing this sequence can be represented (pH 7.0-11.0) as follows:

$$M^{n+} + HD^{2-} \overset{k_1}{\rightarrow} MD^{n-3} + H^{+} \tag{30}$$

$$MD^{n-3} + HZ^{3-} \overset{k_2}{\rightarrow} MZ^{n-4} + HD^{2-} \tag{31}$$

where M^{n+} represents the metal cations, HD^{2-} the Erichrome Black T ionic species, and HZ^{3-} the EDTA ionic species. It should be noted that the rate of the reaction represented by Equation 30 is much faster than the rate of ligand exchange represented by Equation 31. Finally, the formation of the M-EDTA chelate reaches equilibrium under flow conditions.

In comparison to Equations 20 and 21, it becomes apparent that MD^{n-3} is the monitored species which corresponds to C, M^{n+} corresponds to A, and B and Y correspond to the reagents HD^{2-} and HZ^{3-}, respectively. When $[HD^{2-}]$ and $[HZ^{3-}]$ are present in large excess with respect to the

injected metal concentration, k_1 and k_2 become the pseudo first-order rate constants of the formation and decomposition of MD^{n-3} respectively.

It was the purpose of the present study to investigate the optimum experimental conditions at which these signals are produced, and at which repetitive determinations of Zn^{2+} and Cd^{2+} ions are possible. Polyaminocarboxylic acids, namely EDTA, DCTA, and DETPA (Appendix B.1) and EBT metallochromic indicator (Appendix B.2) were used as the chelating agents; and ammonia-ammonium chloride as the complexing buffer.

VI.3.2. Effects of Different Factors on the Transient Signal

VI.3.2.1. Effect of Erichrome Black T (EBT) Concentration. Variation of the concentration of EBT was mainly governed by the background absorbance of the buffered EDTA-EBT mixture, which increases with increase of EBT concentration following Beer's law. Since the linear relation between the response of the measuring device and the absorbance fails above an absorbance value equal to 1.0. A concentration of EBT equal to 4.37×10^{-5} M was selected as optimum for this indicator; absorbance is then equal to 0.9 at 650 nm.

The wavelength at which there is maximum difference in absorbance between the buffered EDTA-EBT mixture and the M-EBT chelate was found by following the absorption spectra for both at different wavelengths. Though the metal Erichrome Black T chelate has its maximum absorbance at 550 nm, the difference in absorbance between its solution and the background solution is maximal at 645 nm for zinc and at 655 nm for cadmium. Comparison of the spectra showed that a maximum difference between the absorbances at 640 nm for zinc and 660 nm for cadmium, as

has been reported earlier by Scaife [105].

VI.3.2.2. Effect of Polyaminocarboxylic Acid Concentration. Typical variation of the peak height with the concentration of chelating agent is shown in Figure 19. The signal height changes slightly with increase of EDTA concentration, then as expected, starts decreasing at a concentration almost equal to the concentration of injected metal ion. Meanwhile, the signal duration measured by the time elapsed in order to restore the base line, decreases as illustrated in Figure 19 with increase of chelating agent concentration. At a flow rate equal to 42 ml/min, the signal is restored to the baseline after about 27 seconds for an EDTA concentration equal to 4.44×10^{-5} M and an injected amount of metal ion equal to 10^{-3} mmole. Similar behavior has been observed with other chelating agents and at different concentrations of chelating agents and metal ions.

It can be inferred from Figure 19 that an optimum concentration for the chelating agent (EDTA) will be dependent upon the amount of the injected metal ion (Zn^{2+}); in general it should be slightly less than the metal ion amount to insure maximum sensitivity and reproducibility. For example, if 10^{-3} mmole of Zn^{2+} is to be injected into a flow-through cell, the amount of EDTA in the cell should be less than 10^{-3} mmole, so that by washing with EDTA the signal is restored to the base line in a period dependent upon the flow rate as will be discussed later. This state of affairs is not in accord with the conception of having an EDTA concentration greater than the concentration of the injected metal ion where the rates of formation of metal - EBT and metal - EDTA chelates differ, the former being the faster. Accordingly, the rise curve of the signal reflects the rate of formation of metal-EBT chelate, and the

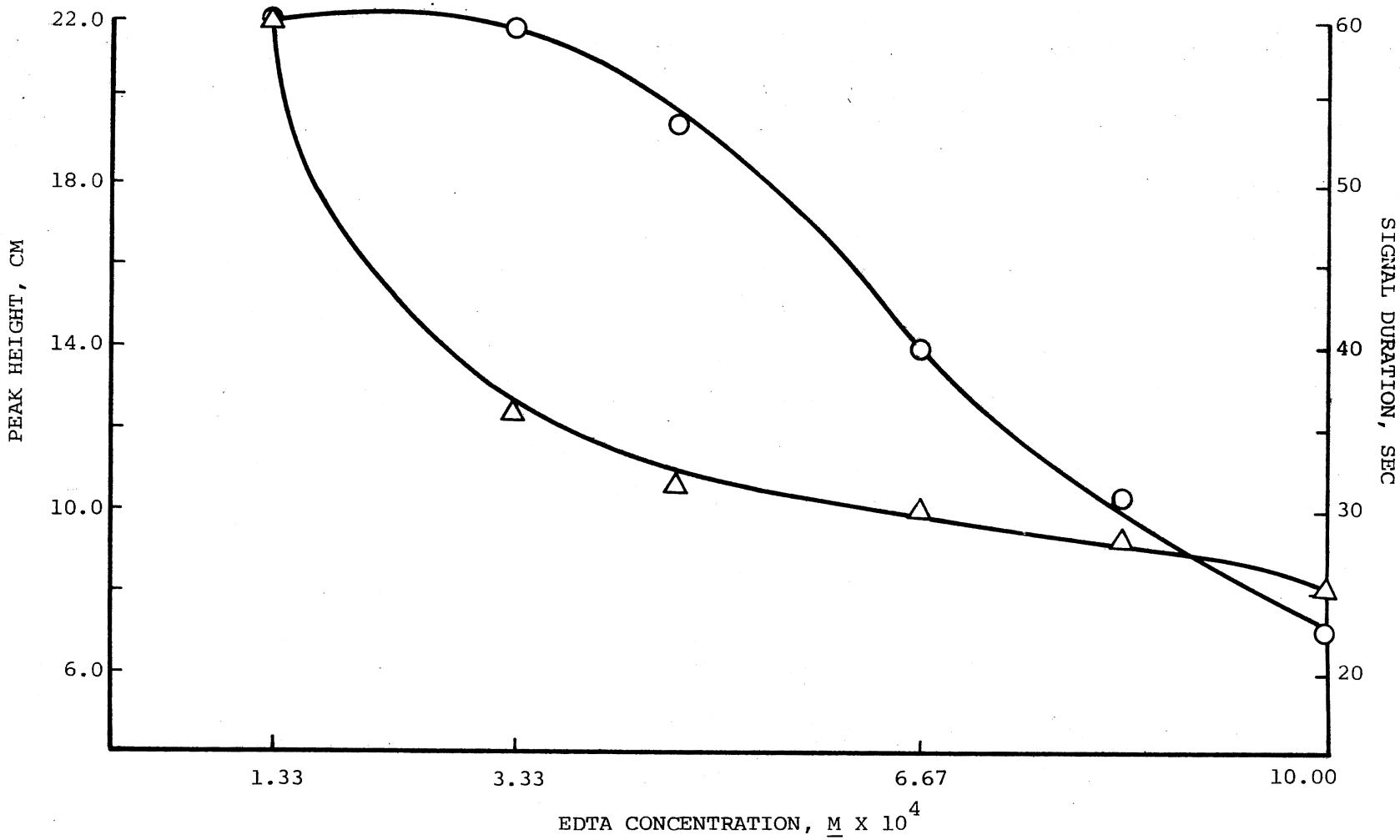

Figure 19. Variation of Peak Height (O) and Signal Duration (Δ) With EDTA Concentration

fall curve reflects the rate of exchange of metal-EBT chelate with metal-EDTA chelate (Section V.3.1). The formation of a stronger metal-acid complex eventually has to take place by breaking the metal-EBT complex.

VI.3.2.3. Effect of pH. At the optimum concentrations of chelating agent metallochromic indicator, the effect of pH of ammonia buffers has been studied. This study of pH deals with different species of the chelating agent, indicator, metal complexes, and accordingly different absorption spectra of the Eriochrome Black T indicator.

The absorption spectra of EBT at different pH values show different absorption maxima for the ionic species H_2D^- (pH ~ 5), HD^{2-} (pH ~ 8), and D^{3-} (pH ~ 13) at 520, 615 and 500 nm, with molar absorptivities approximately equal to 1.2×10^4, 3.0×10^4, and 1.8×10^4 $l \cdot mole^{-1} \cdot cm^{-1}$, respectively [106].

A pH range between 8 and 13 for the reservoir solution was selected for study since the molar absorptivity is largest in this range; however, it is preferable to buffer the reservoir solutions below pH 11, since the free EBT itself (D^{3-}) is yellow-orange above pH 11.5. Thus, the pH range chosen corresponds to the range 10-11.5. It was found that the relation between pH and peak height (Y in cm) could be fitted to a straight line, $Y = 1.87 x - 12.7$, where x is the pH. However, since metallochromic indicators are simultaneously pH indicators, as are their metal chelates, the study of pH effects is rather complex. Theoretically speaking, the best buffer is one which will complex with the metal to the smallest extent over the amount needed to prevent the precipitation of its hydroxide: a pH equal to 10.0 was chosen as the optimum pH.

VI.3.2.4. Effect of Flow Rate. At the optimum chelating agent concentration, EBT concentration, pH, and ionic strength, flow rate variation has a negligible effect on the peak maximum but drastically reduces the signal duration, as illustrated in Figure 20. Meanwhile, at very high flow rates (above 100 ml/min), the peak maximum should be decreased if the peak life is long enough compared to the flow rate. However, a flow rate equal to 42 ml/min was selected as low rate. A flow rate of 70 ml/min or higher is advantageous for repetitive determinations but the tubing life and pulsation are significantly affected at high flow rates.

VI.3.2.5. Effect of Temperature. Though the values of the stability constants of the metal chelates become smaller as the temperature is increased, the effect is not large and amounts to about 0.01 to 0.02 units in the log values per degree centigrade [107]. In general, the values of the constants are temperature-dependent and with few exceptions they become smaller as the temperature increases. However, since the enthalpy change in complexing reactions is small, the effect is not large as mentioned above. Increase of temperature from 25-50^{o}C in 5^{o} increments did not alter either the signal height or signal duration significantly as can be seen in Table XIII. As might be expected, an increase of 25^{o}C decreases the log value of the stability constant by about 0.25 - 0.50 units, i.e., from 16.50 for Zn- and Cd-EDTA complexes to 16.25-16.00 in the logarithms of their stability constants [107]. Thus, variation of temperature had practically no effect on the peak height or the signal duration.

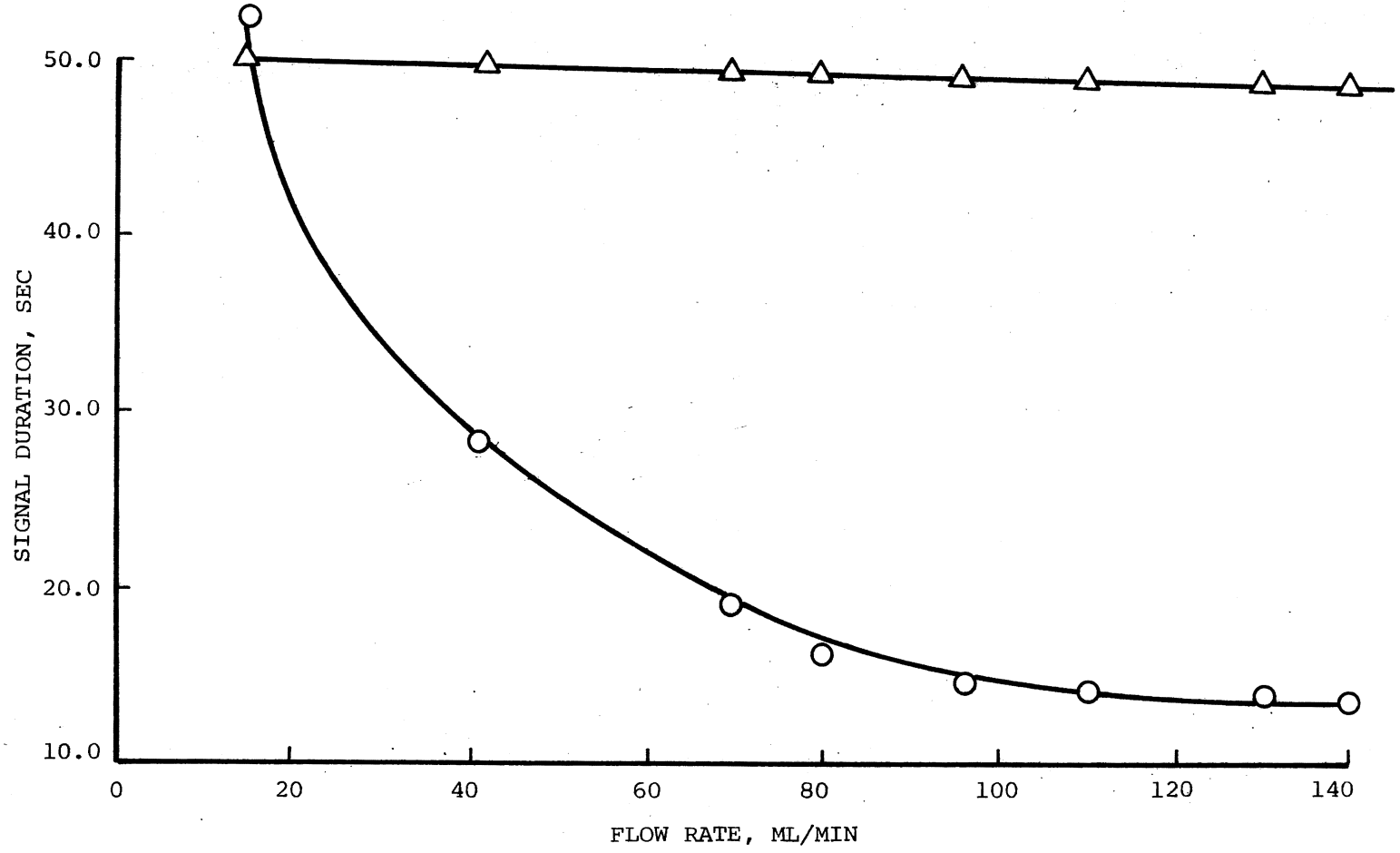

Figure 20. Variation of Signal Height (Δ) and Signal Duration (O) With Flow Rate

TABLE XIII

EFFECT OF TEMPERATURE ON THE PEAK HEIGHT OF THE TRANSIENT SIGNAL

Temperature, ^{o}C	Peak Height, cm
25	15.8
30	15.7
35	15.9
40	15.9
45	16.0
50	16.0

VI.3.2.6. Effects of Other Experimental Conditions. Other experimental conditions such as mV span and chart speed of the recorder, stirring rate in the flow-through cell, and depth of injection have negligible effects on the signal profile. Variations in stirring of the reservoir solution have minimal effects on the transient signals as long as efficient mixing is operative in the reservoir.

VI.3.3. Determination of Zinc(II) and Cadmium(II) Via the Transiently Formed Erichrome Black T Metal Chelates

Table XIV shows some pertinent data for the determination of Zn^{2+} and Cd^{2+} ions via the transient formation of their Eriochrome Black T Chelates. In both cases, the formation and disappearance of the metallochromic indicator-metal chelates was monitored at 650 nm, where maximum difference in absorbance between the free indicator and the indicator-metal chelate was observed. The limit of detection has been chosen conventionally as the amount of the metal ion injected which produces

a peak maximum equal to twice the height of a blank signal, and the range of determination as the linear portion of the working curve. At higher metal ion concentrations deviations from linearity are expected since the amount of metal ion injected will be greater than that of the chelating agent in the cell, referring to the polyaminocarboxylic acid, and hence forms a colored chelate with the metallochromic indicator.

TABLE XIV

USE OF TRANSIENT SIGNALS IN THE SPECTROPHOTOMETRIC DETERMINATION OF MICROGRAM AMOUNTS OF ZINC AND CADMIUM IN AQUEOUS SOLUTIONS

Metal Ion	Limit of Detection, μg	Intercept c, cm	Range of Determination, μg	Slope a, cm/μg
Zn-EDTA	3.0	-0.2	6.5-39.2	0.4
Zn-DCTA	4.0	-0.2	5.0-39.2	0.3_5
Zn-DETPA	5.0	0.1	5.0-32.7	0.2
Cd-EDTA	5.2	-0.3	11.2-67.4	0.2_5
Cd-DCTA	6.9	-0.2	8.6-67.4	0.2_2
Cd-DETPA	8.6	0.3	8.6-56.2	0.1_2

Calibration curves for the determination of Zn(II) and Cd(II) cations, for different chelating agents, are shown in Figures 21 and 22. Linear regression analysis was applied in order to obtain calibration curves for the spectrophotometric analysis, and to check if Beer's law is followed. The differences in slope of the standard curves are

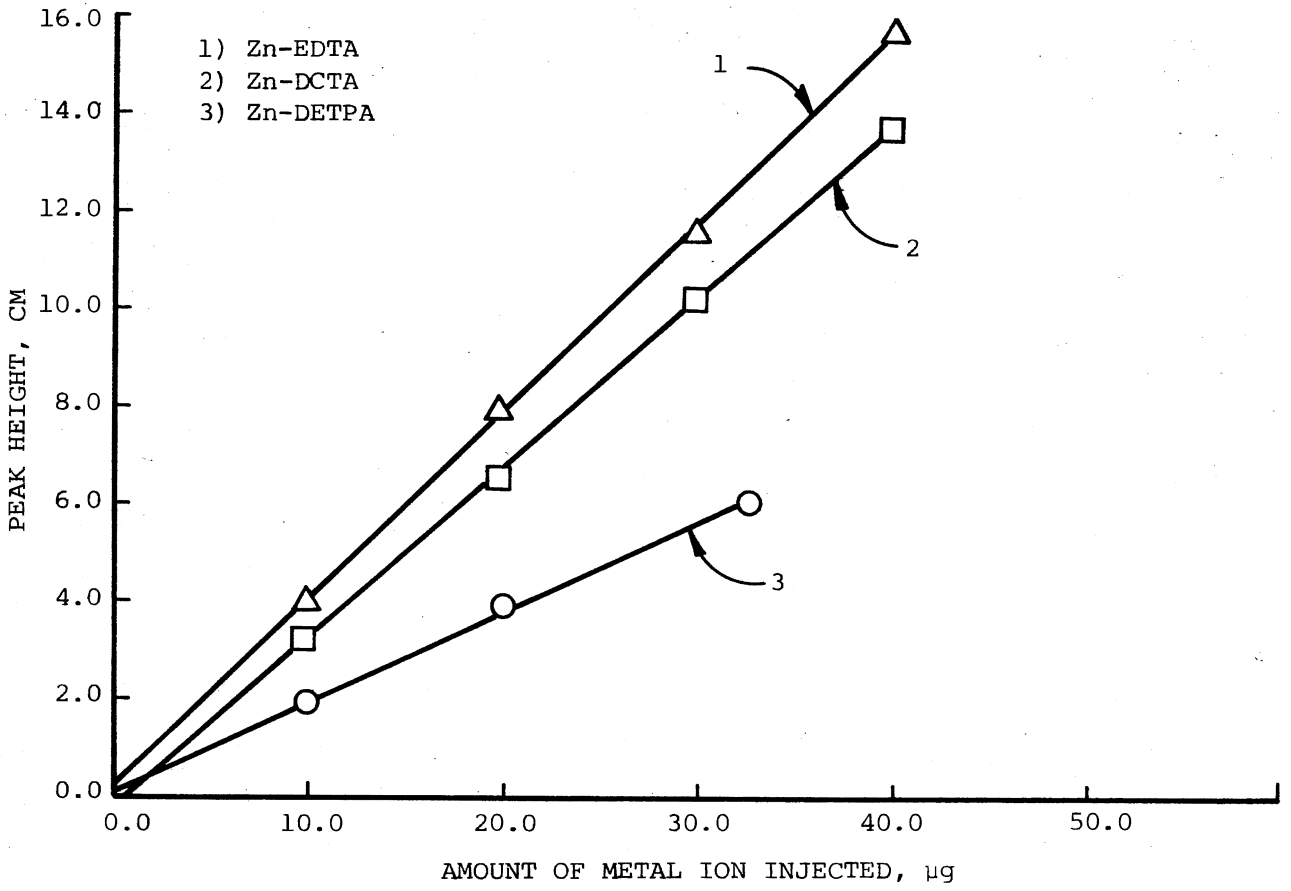

Figure 21. Variation of Peak Height With Metal Ion Concentration

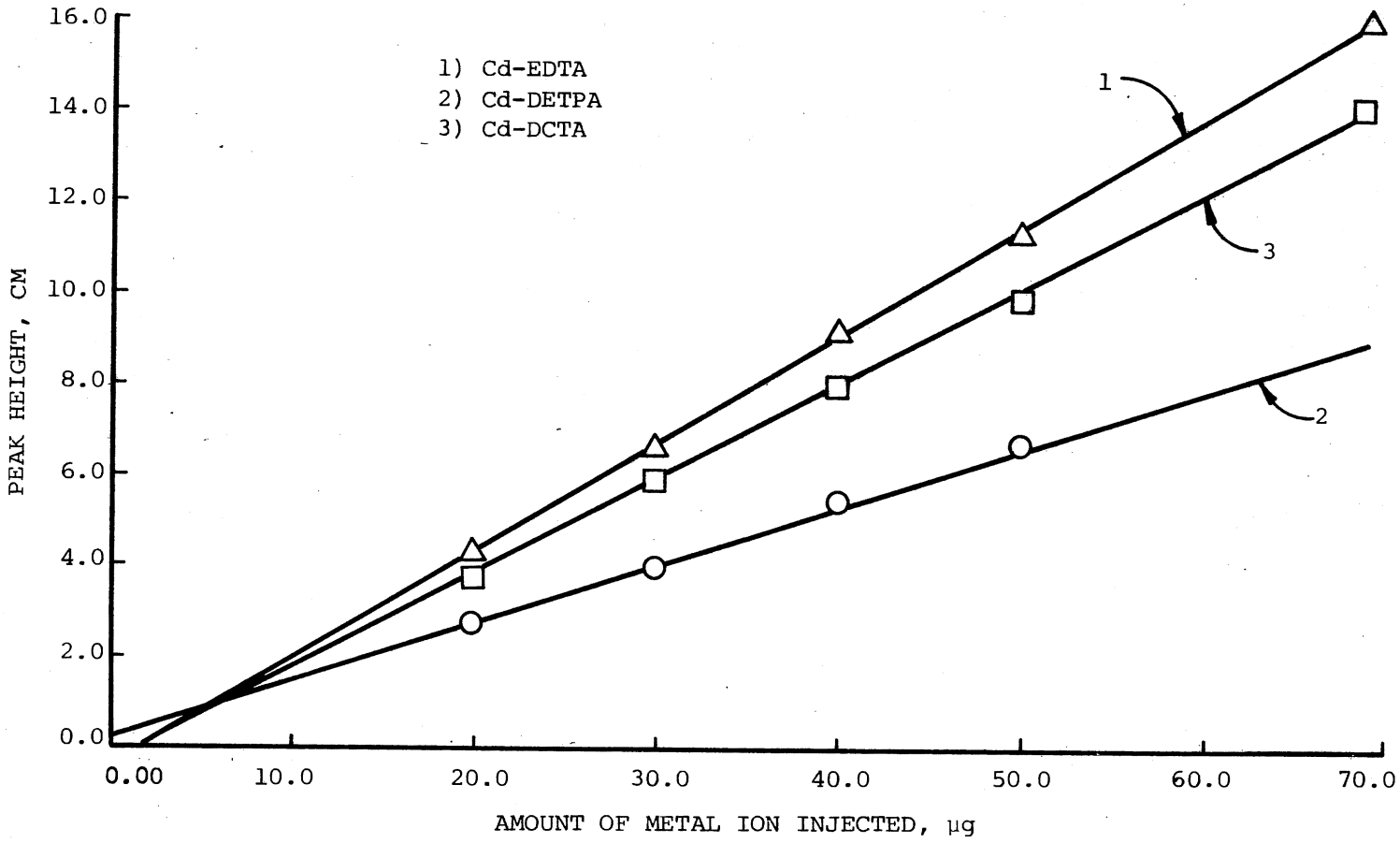

Figure 22. Variation of Peak Height With Metal Ion Concentration

due to the differences in the rates of ligand exchange for the different complex species and reflect the different sensitivities.

Data for repetitive determination of these cations in aqueous solutions are listed in Table XV, where n is the number of injections made which gave signals having the same peak height, but not the same profile, as the signal duration progressively increases with further injections. This is due to the fact that the concentration of the polyaminocarboxylic acid available for chelation with the injected metal ion is progressively decreasing with successive injections. As the Eriochrome Black T-metal chelate has a different color than the free EBT, the baseline is expected to shift progressively with number of injections following the expression [59]

$$A_{b(n)} = \frac{nx}{V_r} \varepsilon b \qquad (32)$$

where $A_{b(n)}$ is the absorbance of the blank after n injections of x mmoles, ε is the molar absorptivity of the colored species, and V_r is the reservoir volume. According to Equation 32, which may be easily derived from Beer's law, large values of V_r will minimize the baseline shift; this has been experimentally confirmed. The average peak height, $\bar{X}$, and the percent relative standard deviation, v_x, are also listed in Table XV (Appendix E.1).

To summarize, zinc and cadmium cations have been determined by injecting their aqueous solutions into a flowing stream of Eriochrome Black T-chelating agent--amonium ion-ammonia buffer, to the order of microgram amounts. The percent relative standard deviation, v_x, which is related to the magnitude of the peak height could be decreased even below its current values by a mechanically controlled injection device.

TABLE XV

APPLICATIONS OF TRANSIENT SIGNALS IN THE REPETITIVE SPECTROPHOTOMETRIC DETERMINATION OF MICROGRAM AMOUNTS OF ZINC AND CADMIUM IN AQUEOUS SOLUTIONS

Metal Ion	Chelating Agent	Number of Injections, n	$\bar{X}$, cm	±Confidence Limits at the 95% Level	v_x
Zn^{2+}	EDTA	40	9.9	0.10	2.6
	DCTA	35	8.6	0.12	3.2
	DETPA	38	5.1	0.056	2.7
Cd^{2+}	EDTA	42	10.5	0.097	2.4
	DCTA	38	9.3	0.13	3.4
	DETPA	39	5.4	0.065	2.8

For each determination 85.0 ml solution was used (chelating agent, 1.82×10^{-4} M; EBT, 4.55×10^{-5} M; $\mu \geq 0.05$; pH = 10,0); other experimental parameters are described in the text; amount of injected metal ion, 0.1 ml of solution (25.0 µg Zn; 43.0 µg Cd); 1.0 cm = 0.044 ΔA.

A host of other metal cations can be determined by the flow injection technique provided that: (a) the formation constant of the metal-polyaminocarboxylic acid chelate is larger than that of the metal-metallochromic indicator chelate by at least four units in their log values; (b) the wavelengths of maximum absorbance for the metal indicator chelate differs from that of the free indicator; (c) if the condition mentioned in (b) fails, any wavelength where maximum difference in absorbance is observed may be selected, and (d) the rate of formation of metal-metallochromic indicator chelate should be faster than the rate of ligand attack, otherwise no transient signal would have been observed.

For each calibration graph, a 60 ml solution was used (EDTA, 3.33×10^{-4} M; EBT, 6.67×10^{-5} M; $\mu \geq 0.05$; pH = 10); other experimental parameters are described in text; values of intercept c and slope a were obtained from the regression line (1.0 cm = 0.044 DA); Zn^{2+}, or Cd^{2+}, solution was injected. Using the expression $|t| = \frac{|c|}{s_c}$, the blank correction was found to be statistically insignificant (Appendix E.1).

As can be seen from Table XIV, the calculated slopes of Zn- and Cd EDTA chelates are larger than those for Zn- and Cd-DETPA; in other words, the determinations are more sensitive for the EDTA than for the DETPA chelates. The table also shows that the determinations for Cd-EDTA are nearly as sensitive as those for Cd-DCTA chelates. Calculation of the "conditional" formation constants for the different metal-polyaminocarboxylic acids and metal-EBT chelates at the experimental conditions from the reported data [108] shows that there are slight differences in the logarithms of their conditional formation constants as given by the expression: $\log K_{MZ} - \log \alpha_{Z(H)} - \log \alpha_{M(A)}$

where the terms have been previously defined. Thus, the different sensitivities can be hardly attributed to different formation constants; on the other hand, these different sensitivites can be attributed to different rates of attack by the polyaminocarboxylic acids.

VI.3.4. Kinetic Studies Related to the Formation and Decay of the Metal-Eriochrome Black T Chelates

On injecting zinc or cadmium cations into a solution containing a chelating agent and Erichrome Black T in the presence of ammonia, various metal ammine complexes; metal chelates, and metal-EBT chelates are formed to various degrees. A typical (time-response) profile for the metal-Eriochrome Black T transient signal shows a steep rise curve representing the formation of the M-EBT chelate, and a fall curve representing the decrease in the concentration of this chelate species into the flow-through cell under flow conditions. The rate of formation of the metal-EBT chelate at time t is a function of the concentration of its species remaining unattacked by the polyaminocarboxylic acid at time t, and will be dependent upon factors of Equation 31. The rate of removal, however, will be dependent on the concentration of the metal-EBT chelate present at time t, and in addition to the factors mentioned above, will be dependent on the concentration of the polyaminocarboxylic acid through the flow-through cell.

The values of response with time for the rise curves could not be obtained because of the extreme rapidity of the formation of the metal-EBT chelates and therefore no data for k_1 are available. The author knows of no values representing this rate constant in the literature, as he is not aware that this flow injection approach has been applied

to similar reactions. However, the time response data for the fall curves were tested for fit to first, second and third-order rate equations, but were found to agree only with first-order kinetics. In order to obtain first-order kinetics over this region of the transient signal profile, it is necessary that the rate of change of concentration of the metal-Eriochrome Black T chelate with time should be solely dependent on its rate of removal from the flow-through cell by the EDTA attack and be independent of its rate of formation. Typical graphs of $\log_e$ (response) against time at various initial concentrations of chelating agent are shown in Figure 23 while calculated values for the first-order rate constant k_2 are given in Table XVI.

It should also be noted that the fall curves for the transient signals follow first-order kinetics at different flow rates. The rate constant k_2' increases with increase of flow rate. For each set of determinations, the rate constant is dependent upon the total amount of the polyaminocarboxylic acid flowing through the cell. The k_2' value is decreasing with decrease of the circulating amount of the polyaminocarboxylic acid (Table XIV). The lag phase, a known kinetic parameter in continuous flow analysis, increases with decrease of the chelating agent. Its value was estimated from extrapolation of the straight portion of the plot to where it intersected the time axis at a time equal to the lag phase. The half wash time, $W_{1/2}$, is another important kinetic parameter in continuous flow analysis, and can be calculated from the relation $W_{1/2} = \frac{1}{k} \ln 2 = \frac{0.693}{k}$ [14].

By using a large reservoir for repetitive injection, the percentage of C_{ss} reached at any given time can be calculated from the expres-

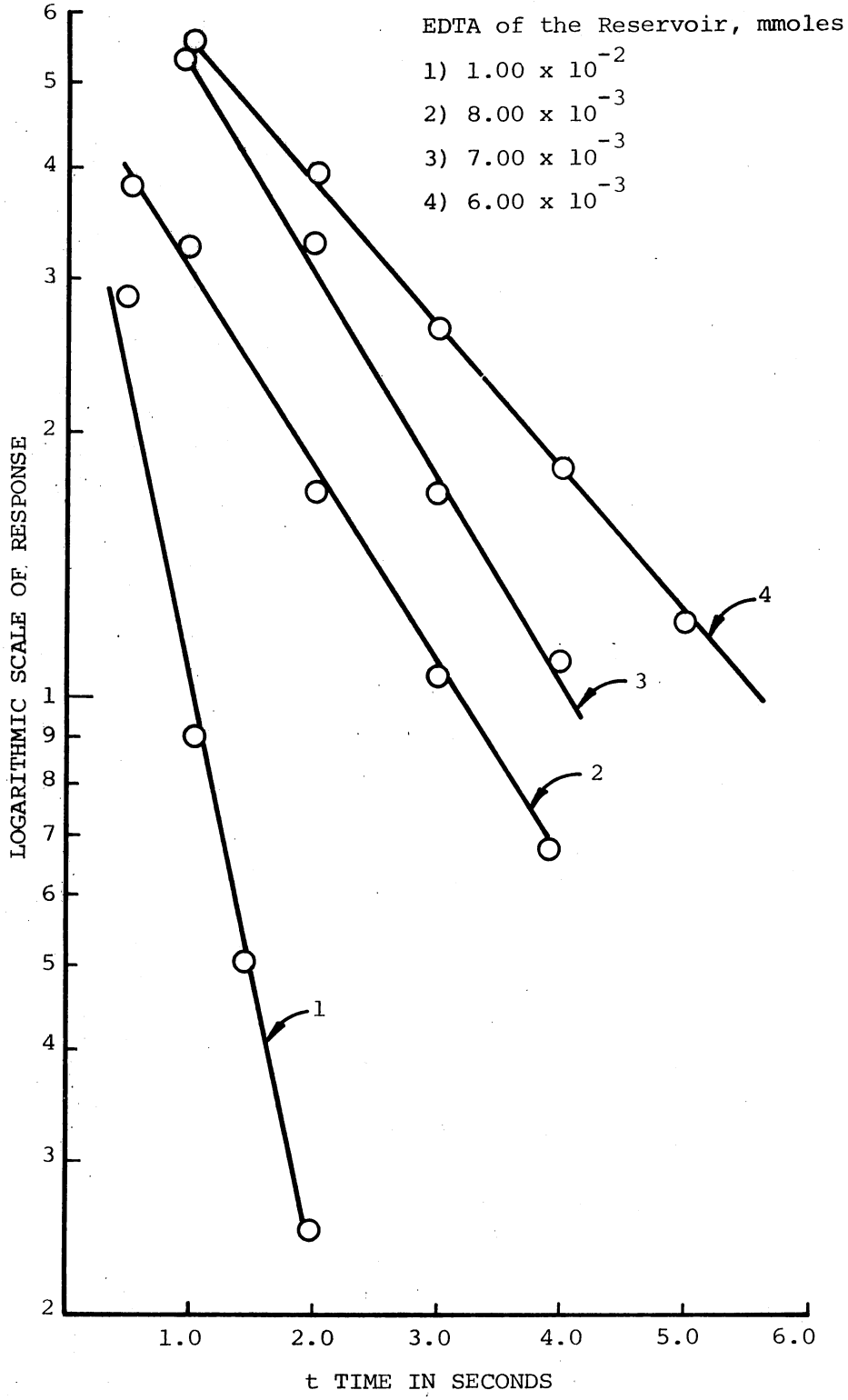

Figure 23. First-Order Plots for the Fall Curves

TABLE XVI

COMPUTATION OF THE FIRST-ORDER RATE CONSTANT FOR THE FALL CURVES OF THE TRANSIENTLY FORMED ERIOCHROME BLACK T CHELATES OF ZINC AND CADMIUM

Total Amount of Polyaminocarboxylic Acid, mmoles	Amount of Acid in Cell, mmoles	k'_2 Sec^{-1} (Zinc)	$W_{1/2}$ Sec	Lag Phase Sec	k'_2 Sec^{-1} (Cadmium)	Lag Phase Sec
EDTA						
1.00×10^{-2}	1.33×10^{-3}	1.61	0.43	0.5	1.60	0.5
8.00×10^{-3}	1.07×10^{-3}	0.63	1.10	1.0	0.60	1.0
7.00×10^{-3}	8.00×10^{-4}	0.36	1.92	1.2	0.32	1.2
DCTA						
1.00×10^{-2}	1.33×10^{-3}	0.89	0.78	0.5	0.92	0.5
8.00×10^{-3}	1.07×10^{-3}	0.45	1.54	1.0	0.50	1.0
7.00×10^{-3}	8.00×10^{-4}	0.39	1.78	1.0	0.42	1.0
DETPA						
1.00×10^{-2}	1.33×10^{-3}	1.18	0.59	0.5	1.25	0.5
8.00×10^{-3}	1.07×10^{-3}	0.76	0.91	1.0	0.80	1.0
7.00×10^{-3}	8.00×10^{-4}	0.77	0.90	2.0	0.81	2.0

For each set of determinations with a specific polyaminocarboxylic acid 30.0 ml solution was used (polyaminocarboxylic acid, 3.33×10^{-4} M; EBT, 6.67×10^{-5} M; $\mu = 0.05$; pH - 10.0); flow rate, 15 ml/min; other experimental conditions are described in the text amount of metal ion injected in mmoles, 10^{-3} mmole.

sion: t in $W_{1/2}$ units = $\frac{t_{in}-L}{W_{1/2}}$, where the terms have been previously defined (Chapter I). For example, substituting the values 0.5, 0.5, and 0.43 seconds for t_{in}, L and $W_{1/2}$, respectively, the times in $W_{1/2}$ units correspond to about 100% of the original steady-state value as read from the chart [14]. The effective number of half-wash times between samples can be calculated from the expression $\frac{t_{bs}-L}{W_{1/2}}$. Again, by substituting the values 1, 0.5 and 0.43 seconds for t_{bs}, L, and $W_{1/2}$, respectively, the effective number is approximately equal to one, which means that 50% of the concentration of any given sample would appear as part of the following sample. When t_{bs} is increased to six seconds, only 1-6% of the preceding concentration would appear.

VI.4. Peak Height and Peak Area Measurements

Considering that the initial concentration of the transient species B is equal to zero at t=0, its concentration at time t is given by Equation 33 (Appendix C).

$$[B] = [A]_0 \frac{k_1}{k_2-k_1} (e^{-k_1 t} - e^{-k_2 t}) \qquad (33)$$

where $[A]_0$ is the initial concentration of the species A which gives the species B, and k_1 and k_2 are the pseudo-first-order rate constants for the rise and fall of the transient signal, respectively. The concentration of B at the peak height can be obtained by differentiation of Equation 33 to give

$$[B]_{max} = [A]_0 \left(\frac{k_2}{k_1}\right)^{\frac{k_2}{k_1-k_2}} \qquad (34)$$

Thus by using values for k_1 and k_2 it is possible to obtain a value for the concentration, and hence the peak maximum. Under steady-state conditions, or if the species B is not transient k_2 approaches zero; then from Equation 34 the peak height value $[B]_{max}$ approaches $[A]_0$ and the highest sensitivity is achieved. The theoretically predicted maximum improvement in peak maximum under these conditions can be calculated by obtaining several values for k_1, k_2 and $[B]_{max}$. However, this steady-state situation mentioned earlier is neither attainable under flow conditions, nor when transient species are formed. Theoretical calculation of percent signal recovery showed that the ratio k_1/k_2 should be equal to 1000 for a 99% recovery [59].

Unlike the situation in the peak measurement methods, the sensitivity in the integration methods is independent of the rate of injection of the sample into the flow-through cell. Equation 33 can also be integrated so as to obtain the peak area value between time zero and time t, to give

$$[B]_{t=0}^{t=t} = [A]_0 \frac{k_1}{k_2-k_1} \left(\frac{e^{-k_2 t}}{k_2} - \frac{e^{-k_1 t}}{k_1}\right)_{t=0}^{t=t} \qquad (35)$$

Again, under steady-state conditions (no flow and/or when the species B is not transient) k_2 approaches zero, the peak area value approaches $[A]_0$, and the highest sensitivity is achieved. By using Equation 35 alone, it is possible to obtain the theoretically predicted variation in the peak area with increasing integration time for a fixed flow rate. In addition, the theoretically predicted values of the ratio of peak area to peak height, at a certain flow rate, can be calculated from Equations 34 and 35.

Generally, the greatest advantage of using an integration technique is realized under conditions when broad peaks are obtained owing to a slow rate of the rise curve; as this rate increases the advantages of integration over peak height measurements rapidly disappear. Naturally, at slower rates of the rise curves, longer integration periods would be advantageous; and for faster rates of the rise curves shorter integration periods could be used. At any rate, the integration circuits applied in the present study perform signal integration until a pre-set level has been achieved. Therefore, a signal integrator with a capability of variation of the integration period was not needed.

Though, generally speaking, it is preferable to measure peak area rather than peak height, since area is less affected by variations in operating conditions, cumulative interferences may adversely affect the precision theoretically obtainable by integration. These interferences are of electronic nature, in general, and can limit the sensitivity of the integrator circuit by baseline drift. However, this type of error can be minimized, in certain circumstances by corrective feedback mechanisms or double-beam instrumentation.

Measurement of both peak height and peak area was done by the techniques mentioned in Table XVII. The precision peak reader circuit shown in Figure 4 was apparently better than the circuit shown in Figure 3, probably because of leakage through the diodes. An electrometer-operational amplifier was used to draw the minimum amount of current. Different combinations of low-leakage capacitors and low-leakage diodes were employed on a trial-and-error basis, taking into consideration the time constant of the circuit, until a peak value which was constant for about seven seconds had been achieved. It was necessary to amplify the

signal considerably in order that the diode could function. As can be seen in Table XVII, there was no practical improvement in the percent relative standard deviation between the two peak height measurements. This is to be expected if the sensitivity of the chart recorder is high, since the peak height measurement with a reader is the digital equivalent to an analog trace. In fact, the reproductibilities of the responses (chart recorder and peak reader) are almost equal.

TABLE XVII

TRANSIENT SIGNAL MEASUREMENT TECHNIQUES

Transient Signal System	Measurement Technique	V_x
Phenothiazines	A millimeter ruler	2.8
Chlorpromazine hydrochloride	Precision peak reader	2.9
Cerium(IV) sulfate	Difference integrator	2.4
	Analog integrator circuit	2.5
Zinc(II) - EDTA-EBT	A millimeter ruler	2.5
Ammonium buffer	Precision peak reader	2.4
	Difference integrator	2.1
	Analog integrator circuit	2.2

For description of measurement techniques, refer to Section IV.4.

Peak area measurements were carried out with the circuits shown in Figure 5 and 6. The familiar difference integrator is shown in Figure 5, where the mV source is adjusted to the base line voltage with opposite

polarity, and T (the time constant) is equal to 0.2 sec. Any change from the base line voltage will be integrated between t=0 and t=t. Thus it was necessary to adjust the mV source to the base line voltage regularly. Another circuit which was used for peak area measurement is the analog integrator circuit shown in Figure 6. Here the mV source need not be adjusted to the base line voltage; it can be set to a value similar in polarity and less than the base line value. The chopper-stabilized operational amplifier draws a minimal amount of current so that the equation of Figure 6 is practically valid. Again, a time constant (0.25 second) much smaller than the rate of the rise curve was used.

Table XVII shows some data for peak area measurements as obtained by the operational-amplifier integrator circuits. In general, the precision as measured by the percent relative standard deviation (v_x) is better than that obtained in the peak height measurements. However, the difference in precision is not remarkable, which is probably due to base line drift. It should be mentioned that integration of transient atomic fluorescence and atomic absorption signals seem to be one of the best methods of obtaining linear and precise analytical working curves [109]. In addition, the sensitivity of peak height measurements is equal to that of peak area measurements in some cases [109]. In the present study, however, linear calibration curves were obtained simply from peak height measurements of the transient signals. It follows that the superiority of the integration technique is not obvious, since the analytical curves are linear.

It should be mentioned that accurate determination of phenothiozines in commercial pharmaceutical preparations were made from peak height

measurements. Mottola et al. have reported the determination of iron(II) in tap and lake waters by measurements of the heights of the transient signals [59].

CHAPTER VII

SUMMARY

Chapter I is an introduction to transient signals in instrumental methods of analysis and the kinetic parameters associated with their profiles (intersection of rise and fall curves). Peak height or peak area measurements of the transient signals are also discussed. Some applications of transient signals, excluding chromatography, are reported in Chapter II, which is mainly a collection of literature information and as such can serve as an overall review.

The experimental apparatus and procedure are described in Chapters IV and V, where the basic components of the apparatus are shown in Figure 1. As can be seen in this figure, the apparatus is simple, easy to set up and inexpensive. The console houses all the plug-in modules and their power supply, and the electronic circuits applied here make use of operational amplifiers and other units available (Figures 3-7).

The main objectives of the present study, as outlined in Chapter III, are adequately detailed in Chapter VI. This chapter is divided into four major parts: the first part deals with the analysis for phenothiazines, the second with the determination of vanadate and dichromate, the third with the determination of zinc and cadmium, and the fourth part deals with measurement techniques.

As reported in Section VI.1 phenothiazines in microgram amounts can be determined via transient species simply by injection of their

aqueous solutions into a cerium(IV) sulfuric acid mixture. Also, successful determination of these phenothiazines in commercial drugs has been accomplished by the same injection technique. In Section VI.1.3, kinetic studies related to the formation and decay of phenothiazine free radicals, using computational and curve-fitting techniques are described. The agreement between the two techniques is quite satisfactory as shown in Figure 13.

In Section VI.2, microgram amounts of vanadate and dichromate have been determined by the injection technique. Kinetic data using computational and curve-fitting methods are reported in Section VI.2.4, a comparison between these methods being shown in Figure 18. Finally, analysis of steel samples (National Bureau of Standards) was carried out following a lengthy procedure for the dissolution of steel and masking some interfacing ions; the results are shown in Table X.

In Section VI.3, determination of microgram amounts of zinc and cadmium is reported via the formation and decay of their Eriochrome Black T chelates. Lag phase, half wash time, and first order rate constants for the fall portions of the signals have also been calculated. It was not possible to calculate the rate constants for the rise portions of the signals because of the rapidity of the reaction.

In Section VI.4, a comparison between the precision of repetitive injections as measured by peak height and peak area was made (Table XVII). Linear working curves have been obtained with peak height measurements; no improvement using peak area measurements is achieved. Probably, the use of more sophisticated measurement techniques, which compensate for baseline drift or instability and noise, would clarify the advantages of peak area over peak height measurements.

In summary, uses of transient signals in the repetitive determination of a variety of chemical species in solutions have been undertaken and are reported in Tables III, VIII, and XV. The percent relative standard deviations can undoubtedly be lowered beyond the obtained values by a mechanically controlled injection system as demonstrated by Mottola et al. [59]. Regarding the kinetics of the formation and decay of the transient signal, it is shown that the signal profile follows consecutive pseudo-first order kinetics with rate constants k_1 and k_2' under present experimental conditions.

Finally, this novel approach to repetitive determinations by injection of the sought-for species into a flow through cell, and monitoring the transient signal obtained should prove useful in industrial quality control and pollution studies. The use of the same reaction mixture eliminates reagent handling, washings between determinations, and excessive consumption of reagents. In addition, determination times are usually in the order of 10 to 20 seconds, which permits analyzing 360 to 180 samples/hour. The approach can also be extended to other monitoring devices such as ion selective electrodes, amperometric measurements, enthalpimetric measurements, conductometric measurements and potentiometric measurements. The technique can also be used for obtaining pseudo first-order rate constants of chemical reactions (Appendix C). A more complicated mathematical treatment is needed by which rate constants for higher-order reactions can be extracted from the transient signal profile. At any rate, mathematical treatments for higher-order reactions are available in the literature [110].

A SELECTED BIBLIOGRAPHY

[1] V. V. S. Eswars Dutt and H. A. Mottola, Anal. Chem., 47, 357 (1975).

[2] J. T. van Gemert, Talanta, 20, 1045 (1973).

[3] J. Ruzicka and E. H. Hansen, Anal. Chim. Acta, 78, 145 (1975).

[4] G. Nagy, Zs Fehér, and E. Pungor, ibid., 52, 47 (1970).

[5] Zs Fehér and E. Pungor, ibid., 71, 425 (1974).

[6] N. G. Anderson, Anal. Biochem., 23, 207 (1968).

[7] C. W. Fuller, Analyst, 99, 739 (1974).

[8] A. A. Frost and R. G. Pearson, "Kinetics and Mechanism," John Wiley & Sons, Inc., New York, 1965, Chapter 8.

[9] C. W. Fuller, Analyst, 100, 229 (1975).

[10] H. L. Kahn and S. Slavin, Atom. Absorption Newsl., 10, 125 (1971).

[11] R. M. Dagnall, B. L. Sharp, and T. S. West, Nature (London), 234, 69 (1971).

[12] D. Ambrose, "Gas Chromatography," Butterworths, London, 1971, Chapter 13.

[13] B. L. Karger, L. L. Snyder, and C. Horvath, "An Introduction to Separation Science," John Wiley & Sons, Inc., New York, 1973, Chapter 5.

[14] R. E. Thiers, R. R. Cole, and W. J. Kirsch, Clin. Chem., 13, 451 (1967).

[15] B. V. L'vov, Spectrochim. Acta, 17, 761 (1961).

[16] H. Massmann, Spectrochim. Acta, 23B, 215 (1968).

[17] G. G. Guilbault, "Practical Fluorescence: Theory, Methods, and Techniques," Marcell Dekker, New York, 1973, Chapter 1.

[18] U. Isacsson and G. Wettermark, Anal. Chim. Acta, 68, 339 (1974).

[19] J. Bartos and M. Pesez, Talanta, 19, 93 (1972).

[20] H. M. Donega and T. E. Burgess, Anal. Chem., 42, 1521 (1970).

[21] J. Aggett and T. S. West, Anal. Chim. Acta, 55, 349 (1971).

[22] R. G. Anderson, I. S. Maines, and T. S. West, ibid., 57, 271 (1971).

[23] R. D. Reeves, C. J. Molnar, and J. D. Winefordner, Anal. Chem., 44, 1913 (1972).

[24] Y. Talmi and G. H. Morrison, ibid., 44, 1455 (1972).

[25] J. E. Cantle and T. S. West, Talanta, 20, 459 (1973).

[26] L. Erdy, O. Weber, and I. Buzas, ibid., 17, 1221 (1970).

[27] W. R. Seitz, W. W. Suydam, and D. M. Hercules, Anal. Chem., 44, 957 (1972).

[28] W. R. Seitz and D. M. Hercules, ibid., 44, 2143 (1972).

[29] I. E. Kalinichenko, Ukr. Khim. Zh., 35, 755 (1969); C. A. 71, 119328u.

[30] A. K. Babko, A. V. Terletskaya, and L. I. Dubovenko, Ukr. Khim. Zh., 32, 728 (1966); C. A. 65, 13405b.

[31] S. Musha, M. Ito, Y. Yamamoto, and Y. Inamori, Nippon Kagaku Zasshi, 80, 1285 (1959); C. A. 55, 5228b.

[32] A. A. Ponomarenko and L. M. Amelina, J. Gen. Chem. USSR, 35, 750 and 2252 (1965).

[33] H. A. Neufeld, C. J. Conklin, and R. D. Towner, Anal. Biochem., 12, 303 (1965).

[34] M. Turowska, Chem. Anal. (Warsaw), 6, 1051 (1961).

[35] K. Weber, Dtsch. Z. Gesamte Gerichtl. Med., 57, 410 (1966).

[36] W. A. Armstrong and W. G. Humphreys, Can. J. Chem., 43, 2576 (1965).

[37] W. S. Oleniacz, M. A. Pisano, M. H. Rosenfeld, and R. L. Elgart, Environ. Sci. Technol., 2, 1030 (1968).

[38] G. E. Ashby, J. Polymer Sci., 50, 99 (1961).

[39] S. P. McGlynn, J. Daigre, and F. J. Smith, J. Chem. Phys., 39, 675 (1963).

[40] G. Oster, N. Geacintov, and A. U. Khan, Nature (London) 196, 1089 (1962).

[41] J. D. Winefordner and M. Tin, Anal. Chim. Acta, 31, 239 (1964).

[42] H. C. Hollifield and J. D. Winefordner, Talanta, 14, 103 (1967).

[43] R. H. Steele and A. G. Szent, Proc. Nat. Acad. Sci., U.S.A., 43, 477 (1957).

[44] W. P. Shiwopiszew, Dokl. Akad. Nauk SSSR, 76, 1198 (1950).

[45] S. Freed, J. H. Turnbull, and W. Salmre, Nature (London) 181, 1731 (1958).

[46] H. A. Moye and J. D. Winefordner, J. Agr. Food Chem., 13, 516 (1965).

[47] H. V. Drushel and A. L. Sommers, Anal. Chem., 38, 10 (1966).

[48] P. B. Hamilton, "Handbook of Biochemistry, Selected Data for Molecular Biology," B-47, The Chemical Rubber Company, Cleveland, 1968.

[49] D. H. Desty and A. Goldup, "Gas Chromatography," R. P. W. Scott, Ed., Butterworths, London, 1960.

[50] L. C. Hansen, W. G. Scribner, T. W. Gilbert, and R. E. Sievers, Anal. Chem., 43, 349 (1971).

[51] S. J. Lyle, Talanta, 2, 293 (1959).

[52] I. M. Kolthoff and L. A. Sarver, J. Am. Chem. Soc., 52, 4179 (1930).

[53] W. M. Clark, "Oxidation-Reduction Potentials of Organic Systems," Williams & Wilkins, Baltimore, 1960.

[54] Advances in Automated Analysis, Technicon International Congress, Vols. I and II (1969), Vol. II (1970), Mediad Inc., New York.

[55] H. U. Bergmeyer and A. Hagen, Z. Anal. Chem., 261, 333 (1972).

[56] N. G. Anderson, ibid., 261, 257 (1972).

[57] E. Sebastiani, K. Ohlo, and G. Riemer, ibid., 264, 105 (1973).

[58] H. Berndt and E. Jackwerth, Spectrochim. Acta, 30B, 169 (1975).

[59] V. V. S. Eswara Dutt, A. Eskander-Hanna, and H. A. Mottola, Anal. Chem, in press.

[60] E. W. Chlapowski, M. S. Thesis, Oklahoma State University, 1974.

[61] H. Hall, B. E. Simpson, and H. A. Mottola, Anal. Biochem., 45, 453 (1972).

[62] J. Blazek, Pharmazie, 26, 388 (1971); C. A. 75, 94235d.

[63] G. Cimbura, J. Chromatog. Sci., 10, 287 (1972).

[64] S. L. Tompsett, Prog. Chem. Toxicol., 5, 151 (1974).

[65] G. A. W. Lucas and C. Fabierkiewicz, J. Forensic Sci., 8, 462 (1963).

[66] F. M. Forrest, I. W. Forrest, and A. S. Mason, Am. J. Psychiat. 118, 300 (1961).

[67] E. G. C. Clarke, "Isolation and Identification of Drugs," The Pharmaceutical Press, London, 1969.

[68] P. Haux and S. Natelson, Am. J. Clin. Pathol., 53, 77 (1970).

[69] N. V. Egorov, T. P. Kazakova and M. I. Shmar'yan, Farmatsiya (Moscow), 23, 72 (1974); C. A. 83, 65518h.

[70] M. Tarasiewicz, Acta Pol. Pharm., 31, 201 (1974); C. A. 82, 64599c.

[71] M. Tarasiewicz and H. Puzanowska-Tarasiewicz, Mikrochim. Acta (Wien) 721 (1973).

[72] J. Kofoed, C. Fabierkiewicz and G. H. W. Lucas, J. Chromatog., 23, 410 (1966).

[73] J. E. Wallace and J. D. Biggs, J. Pharm. Sci., 60, 1346 (1971).

[74] J. Cochin and J. W. Daly, J. Pharmacol. Exptl. Therap., 139, 160 (1963).

[75] T. J. Mellinger and C. E. Keeler, J. Pharm. Sci., 51, 1171 (1962).

[76] A. D. Eagleson, Am. J. Clin. Pathol., 39, 648 (1963).

[77] S. Ebel, B. Dolmeier, M. Fick and H. Kussmaul, Arch. Pharm. 307, 878 (1974); C. A., 82, 129334j.

[78] K. D. Parker, C. R. Fontan and P. L. Kirk, Anal. Chem., 34, 757 (1962).

[79] S. S. Curry, ibid., 40, 1251 (1968).

[80] T. J. Mellinger and C. E. Keeler, ibid., 35, 554 (1963).

[81] J. B. Ragland and V. J. Kinross-Wright, ibid., 36, 1356 (1964).

[82] E. A. Martin, Can. J. Chem., 44, 1783 (1966).

[83] C. Thiery, J. Capette, J. Meunier, and F. Leterrier, J. Chim. Phys. Physiochim. Biol., 66, 134 (1969).

[84] L. A. Gifford, J. N. Miller, D. L. Phillips, D. T. Burns, and J. W. Bridges, Anal. Chem., 47, 1699 (1975).

[85] H. S. Gowda and R. Shakunthala, Talanta, 13, 1375 (1966).

[86] K. T. Lee and I. K. Tan, Mikrochim. Acta (Wien) 93, (1975).

[87] The Pharmacopeia of the United States of America, Eighteenth Revision, Mack Printing Company, Easton, Pa., 1970; American Medical Association Drug Evaluations, Second Edition, Publishing Sciences Group, Inc., Acton, Mass., 1973.

[88] J. S. Fritz and G. H. Schenk, Jr., "Quantitative Analytical Chemistry," Second Edition, Allyn and Bacon, Inc., Boston, Mass., 1966, p. 621.

[89] Physician's Desk Reference, 27th Edition, Medical Economics Company, Oradell, N. J., 1973, p. 1305.

[90] J. P. Candlin and R. G. Wilkins, J. Chem. Soc., 3625 (1961).

[91] F. A. Cotton and G. Wilkinson, "Advanced Inorganic Chemistry," Second Edition, John Wiley & Sons, Inc., New York, pp. 812, 813.

[92] L. A. Sarver and I. M. Kolthoff, J. Am. Chem. Soc., 53, 2902 (1931).

[93] I. M. Kolthoff and L. A. Sarver, Ibid., 52, 4179 (1930).

[94] E. Bishop and L. G. Hartshorn, Analyst, 96, 26 (1971).

[95] A. Berka, J. Vulterin and J. Zyka, "Newer Redox Titrants", Pergamon, London, 1965.

[96] I. M. Kolthoff and R. Belcher, "Volumetric Analysis", Vol. III, Interscience, New York, 1957.

[97] E. Bishop and A. B. Crawford, Analyst. 75, 273 (1950).

[98] V. V. S. Eswara Dutt and H. A. Mottola, Anal. Chem., 40, 1090 (1974).

[99] H. Kaiser, Appl. Chem. 34, 59 (1973).

[100] A. I. Vogel, "Quantitative Inorganic Analysis", Third Edition, Longmans, London, 1961, p. 643.

[101] L. A. Sarver and W. von Fischer, Ind. Eng. Chem., Anal. Ed., 7, 271 (1935).

[102] G. Schwarzenbach and H. Ackermann, Helv. Chim. Acta, 30, 1798 (1947).

[103] G. Schwarzenbach and H. Flascka, "Complexometric Titrations", 2nd English Edition, Methuen & Co., Ltd., London, 1969, p. 15.

[104] G. Schwarzenbach and W. Biedermann, Helv. Chim. Acta, 31, 678 (1948).

[105] D. B. Scaife, Analyst, 88, 618 (1963).

[106] Reference 104, p. 45.

[107] G. Anderegg, Helv. Chim. Acta, 46, 1833 (1963).

[108] Reference 104, Tables 2 and 3, pp. 10 and 11.

[109] P. Schramel, Anal. Chim. Acta, 72, 414 (1974).

[110] C. Capellos and B. H. J. Bielski, "Kinetic Systems", John Wiley & Sons, Inc., New York, 1972.

APPENDIX A

MOLECULAR STRUCTURES OF THE PHENOTHIAZINES USED IN THE PRESENT STUDY (REFERENCE 87)

A.1. Pure Pharmaceutical Preparations

Phenothiazines have the basic structure and numbering shown below

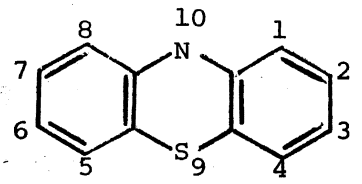

Chlorpromazine hydrochloride, 10-$(CH_2)_3N(CH_3)_2$, 2-Cl

Prochlorperazine dimaleate, 10-$(CH_2)_3$ 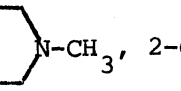 , 2-Cl

Trifluoperazine dihydrochloride, 10-$(CH_2)_3$ 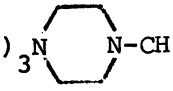 , 2-CF_3

A.2. Propietary Trade Name Pharmaceutical Preparations

These are drug formulations in the form of tablets, capsules, and solutions; in the case of tablets the active drugs are blended with diluents, binders, lubricants, and frequently a disintegrator. Sparine (Promazine hydrochloride) 10-$N(CH_2)_3N(CH_3)_2$; Thorazine (Chlorpromazine hydrochloride); Phenergan (Promethazine hydrochloride) 10-$N \cdot CH_2 \cdot CH(CH_3) \cdot N(CH_3)_2$; Compazine (Prochlorperazine dimaleate).

APPENDIX B

CHEMICAL STRUCTURES OF COMPLEXING AGENTS AND METALLOCHROMIC INDICATORS USED IN THIS STUDY

B.1. Complexing Agents With Carboxymethyl Groups Bound to Several Nitrogen Atoms (Reference 103)

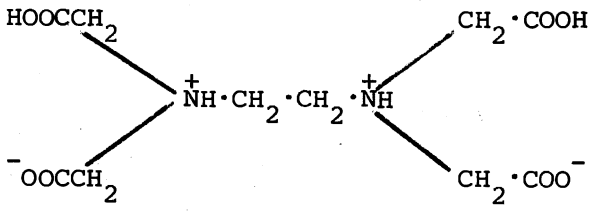

Ethylenediaminetetraacetic acid (EDTA)

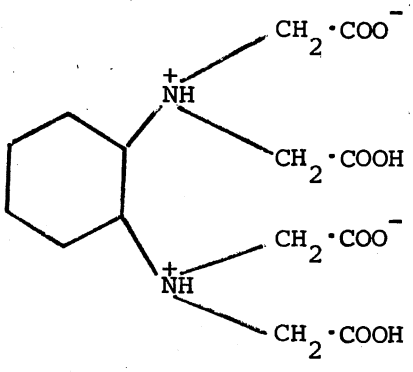

1,2-Diaminocyclohexane-N, N,N', N-tetraacetic acid (DCTA)

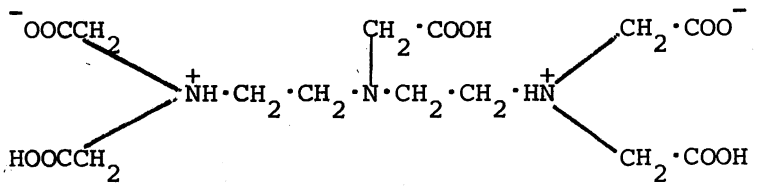

Diethylenetriamine-N,N,N',N',N'-pentaacetic acid (DETPA)

B.2. Metallochromic Indicator (Reference 103)

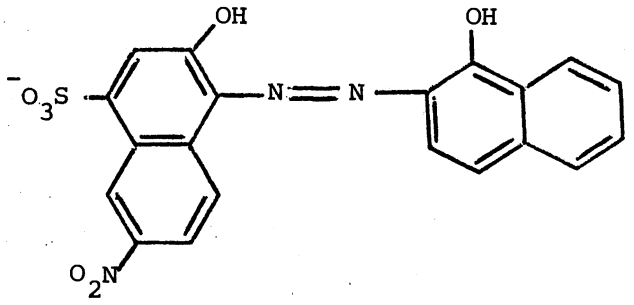

Eriochrome Black T

B.3. Diphenylamine and its Oxidation Products

(Reference 94)

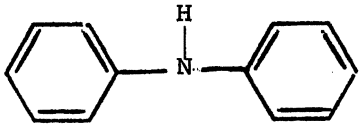

Diphenylamine (DPA)

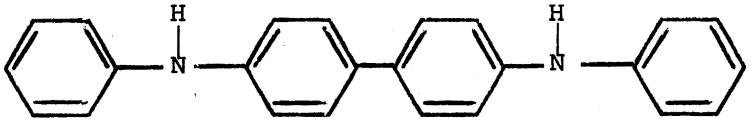

Diphenylbenzidine (DPB)

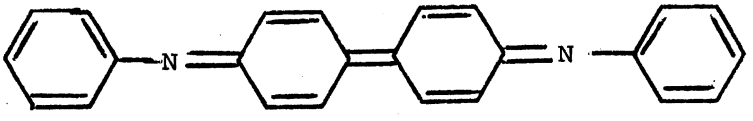

Diphenylbenzidine violet (DPBV)

APPENDIX C

MATHEMATICAL DESCRIPTION OF THE KINETIC SYSTEM FOR THE TRANSIENT SIGNAL (REFERENCES 8 AND 10)

In principle, it is possible to isolate each of the reacting species by adjustment of the concentrations of the other participating species as outlined by Ostwald. Thus, an n-order reaction will behave experimentally as if it were first order, when the concentrations of all other species, except one, are present in large excess.

The reactions under consideration may be considered as first-order consecutive irreversible two stage reactions as follows:

$$A \xrightarrow{k_1} B \xrightarrow{k_2} C$$

where k_1 and k_2 are the rate constants; the concentrations of A, B, and C at time = 0 are $[A]_0$, zero, and zero, respectively, and at time = t are [A], [B], and [C], respectively.

The above mechanism can be described by the following set of equations:

$$-\frac{d[A]}{dt} = k_1[A]$$

$$+\frac{d[B]}{dt} = k_1[A] - k_2[B]$$

$$+ \frac{d[C]}{dt} = k_2[B]$$

which can be solved by two different mathematical operations, the so-called classical and the operational methods. In the latter method which will be developed here, one replaces differentiation by multiplication in which the multiplier is operator S = d/dt.

Substitution of $[A]_0$ for [A] at time zero, when [B] and [C] are equal to zero, yields:

$$\frac{d([A]_0 - [A])}{dt} = S[A]_0 - S[A] = k_1[A]$$

hence,

$$[A] = \frac{S[A]_0}{[S+k_1]}$$

From tables of Laplace transforms:

$$\frac{S}{S \pm a} = e^{\pm at}$$

so that;

$$[A] = [A]_0 e^{-k_1 t}$$

The other differential equations can be solved in a similar fashion, thus:

$$\frac{d[B]}{dt} = S[B] = k_1[A] - k_2[B]$$

hence,

$$[B] = \frac{k_1[A]_0 S}{(S+k_1)(S+k_2)}$$

Substitution values of Laplace transforms in the last equations gives:

$$[B] = [A]_0 \frac{k_1}{k_2-k_1} [e^{-k_1 t} - e^{-k_2 t}]$$

Similarly

$$\frac{d[C]}{dt} = S[C] = k_2[B]$$

hence,

$$[C] = \frac{k_2[B]}{S}$$

Substitution for [B] yields:

$$[C] = k_2[A]_0 \frac{k_1}{k_2-k_1} [e^{-k_1 t} - e^{-k_2 t}]/S$$

After substitution from Laplace transforms, the final form for [C] is:

$$[C] = [A]_0 [1 + \frac{1}{k_1-k_2} (k_2 e^{-k_1 t} - k_1 e^{-k_2 t})]$$

We note from the equation above for [C] that when $k_1 > k_2$,

$$[C] = [A]_0 [1-e^{-k_2 t}]$$

and that when $k_2 > k_1$,

$$[C] = [A]_0[1-e^{-k_1 t}]$$

which illustrates the general principle that the net rate of the reaction is governed by that step which has the smallest velocity constant.

While the concentration of A decreases, the concentration of B increases and reaches a maximum when $d[B]/dt$ is zero, and thereafter decreases exponentially with respect to time. In fact, both concentrations of A and B diminish exponentially with respect to time while maintaining a constant ratio. The time required for the attainment of the stationary state, t_{max}, can be calculated from the relation:

$$\frac{d[B]}{dt} = 0$$

$$k_1[A] = k_2[B]$$

Substitution for A and B by exponential terms gives:

$$k_1 e^{-k_1 t_{max}} = k_2 e^{-k_2 t_{max}}$$

hence,

$$t_{max} = \frac{1}{k_2 - k_1} \ln \frac{k_2}{k_1}$$

The maximum concentration of the intermediate species $[B]_{max}$ can be calculated from:

$$[B]_{max} = \frac{k_1}{k_2}[A]$$

Substitution for [A] yields

$$[B]_{max} = \frac{k_1}{k_2}[A]_0 e^{-k_1 t_{max}}$$

The last equation gives on rearrangement:

$$[B]_{max} = [A]_0 e^{-k_2 t_{max}}$$

which shows that the concentration $[B]_{max}$ becomes smaller as k_2 gets larger.

APPENDIX D

LISTING OF COMPUTER PROGRAMS FOR THE HEWLETT-PACKARD 9820A PROGRAMMABLE CALCULATOR

D.1. Calculation of β_{max} From the Relation:

$$\beta_{max} = \kappa^{\kappa/(1-\kappa)}$$

```
.01→X├
1:
PRT X,X↑(X/(1-X)
);SPC 1├
2:
IF (X+.01→X)>.99
;STP ├
3:
JMP -2├
4:
END ├
R397
```

Output of Program D.1 where values appear as follows: κ/β_{max}

	.140	.280	.420	.560
	.726	.610	.534	.478
$\kappa \rightarrow$	.010	.150	.290	.430	.570
$\beta_{max} \rightarrow$	.955	.715	.603	.529	.475
.020	.160	.300	.440	.580
.923	.705	.597	.525	.471
.030	.170	.310	.450	.590
.897	.696	.591	.520	.468

.040	.180	.320	.460	.600
.874	.686	.585	.516	.465
.050	.190	.330	.470	.610
.854	.677	.579	.512	.462
.060	.200	.340	.480	.620
.836	.669	.574	.508	.458
.070	.210	.350	.490	.630
.819	.660	.568	.504	.455
.080	.220	.360	.500	.640
.803	.652	.563	.500	.452
.090	.230	.370	.510	.650
.788	.645	.558	.496	.449
.100	.240	.380	.520	.660
.774	.637	.553	.492	.446
.110	.250	.390	.530	.670
.761	.630	.548	.489	.443
.120	.260	.400	.540	.680
.749	.623	.543	.485	.441
.130	.270	.410	.550	.690
.737	.616	.538	.482	.438
	.700	.860		
	.435	.396		
	.710	.870		
	.432	.394		
	.720	.880		
	.430	.392		
	.730	.890		
	.427	.390		
	.740	.900		
	.424	.387		
	.750	.910		
	.422	.385		
	.760	.920		
	.419	.383		
	.770	.930		
	.417	.381		

```
.780        .940
.414        .379

.790        .950
.412        .377

.800        .960
.410        .375

.810        .970
.407        .373

.820        .980
.405        .372

.830        .990
.403        .370

.840
.400

.850
.398
```

D.2. A Program for Linear Regression Plotting

```
0:
PRT "LINE THROUGH
H "," POI
NTS"┤
1:
SPC 1;PRT "
X","      Y";0→C→
Z┤
2:
ENT "X=?",X;IF
FLG 13=0;ENT  "Y=
?",Y;PRT  X→RC,Y→
R(C+10);C+1→C;
SPC 1;JMP 0┤
3:
ENT "Y  INTERCEPT
",A, "SLOPE",B┤
4:
PRT "Y  INTERCEPT
",A,"SLOPE",B;
SPC 2┤
5:
ENT "XMAX",R50,"
XTIC",R51,"YMAX"
,R52,"YTIC",R53┤
```

```
6:
SCL 0,R50,0,R52;
AXE 0,0,R51,R53┣
7:
C-1→Z┣
8:
LTR RZ,R(Z+10),3
21;PLT "O";IF (Z
-1→Z)>-1;JMP 0┣
9:
0→X;R50/50→Z┣
10:
PLT X,BX+A;IF (X
+Z→X)≤ .9R50;JMP
0┣
11:
PEN :ENT "AGAIN=
1",Z;IF Z=1;GTO
5┣
12:
END |
R354
```

D.3. A Program for Curve Fitting of the Transient Signal

```
O:
O→C;CFG 13;PRT "
CURVE FIT FOR.."
;SPC 1;PRT "A*K1
/(K2-K1)*";FXD 3
┣
1:
PRT " (EXP(-K1X)
-";PRT "     EXP
(-K2X))";SPC 1;
PRT "       X";
PRT "       Y"┣
2:
ENT "X=?",RC;IF
FLG 13=0;ENT "Y=
?",R(C+20);PRT R
C,R(C+20);C+1→C;
SPC 1;JMP 0┣
3:
ENT "START K1",X
,"STP K1",Y,"K1
STEPS",Z;(Y-X)/Z
→R51┣
4:
11:
R50+1→R50;IF R50
>C;JMP 2┣
12:
JMP -2┣
13:
IF R56≤R57;R56→R
57;R61→R71;R62→R
72;R60→R70┣
14:
IF (R60+R55→R60)
≤R54;GTO 9┣
15:
IF (R62+R52→R62)
≤B;GTO 8┣
16:
IF (R61+R51→R61)
≤Y;DSP R61;GTO 7
┣
17:
PRT "A=",R70,"K1
=",R71,"K2=",R72
,"SUM OF ERROR S
```

```
ENT "START K2",A
,"STP K2",B,"K2
STEPS",Z;(B-A)/Z
→R52┤
5:
ENT "START A",R5
3,"STP A",R54,"A
 STEPS",Z;(R54-R
53)/Z→R55┤
6:
1E99→R57;X→R61┤
7:
A→R62┤
8:
R53→R60┤
9:
0→R50→R56┤
10:
(R60R61/(R62-R61
)*(EXP (-R61RR50
)-EXP (-R2RR50)
)-R(R50+20))↑2+R
56→R56┤
72))┤
24:
IF Y≤X;JMP -1┤
25:
STP ┤
26:
END ┤
R288
QR",R56;SPC 9┤
18:
0→R77;ENT "CLOSE
R LOOK=1",R77;
IF R77=1;GTO 3┤
19:
ENT "XMAX",X,"YM
AX",Y,"XTIC",A,
YTIC",B┤
20:
SCL 0,X,0,Y;AXE
0,0,A,B;C→Z┤
21:
IF 0≤(Z-1→Z);
LTR RZ,R(Z+20),3
21;PLT "X";JMP 0
┤
22:
0→Y;.01X→A┤
23:
PLT Y+A→Y,R70R71
/(R72-R71)*(EXP
(-YR71)-EXP (-YR
```

APPENDIX E

DEFINITION OF STATISTICAL PARAMETERS*

E.1. Statistical Description of Experimental Data

$\bar{X}$	Arithmetic mean of a series of measurements $\Sigma X_i/n$
X_i	Value of the ith measurement
n	Total number of measurements
s^2	Variance of sample $\sum_i (X_i-\bar{X})^2/n$
s	Standard deviation of a sample $\sqrt{s^2}$
v_x	Percent relative standard deviation $100s_x/\bar{X}$
t	Student's t $(\bar{X}-m)/s_{\bar{x}}$
$s_{\bar{x}}$	Standard deviation of the population of means $s_x/\sqrt{n}$
s_x^2	Estimated variance of the population $\sum_i (X_i-\bar{X})^2/(n-1)$

E.2. Choice of Sample Size

m	Estimated population mean $\bar{X}\pm t_{f,\alpha}s_{\bar{x}}$
p	A chosen predetermined factor $(t_{f,\alpha}s_{\bar{x}})/\bar{X}$
α	Probability that the tabulated value of t will be exceeded for a sample with f degrees of freedom
f	Degrees of freedom, usually (n-1)

---

*From H. L. Youmans, "Statistics for Chemistry," Charles E. Merrill Publishing Co., A Bell & Howell Company, Columbus, Ohio, 1973.

$\sqrt{n}$ Acceptable sample size $(t_{f,\alpha} s_x)/(p\bar{x})$

E.3. Treatment of Divergent Data

Q A statistical test for rejecting a measurement at a certain confidence level d/w

d Difference between the questionable datum and the datum nearest in magnitude to it

w Range of the sample data

E.4. Linear Regression Analysis

y A function of $x_i = ax+c$

a Value of the slope

c Intercept of the straight line with the y axis

s_c Standard deviation of c

VITA

Adel Hanna Eskander-Hanna

Candidate for the Degree of

Doctor of Philosophy

Thesis: USE OF TRANSIENT EFFECTS IN THE REPETITIVE DETERMINATION OF A VARIETY OF CHEMICAL SPECIES IN SOLUTIONS

Major Field: Chemistry

Biographical:

Personal Data: Born in Cairo, Egypt, November 15, 1943, the son of the late Hanna Eskander-Hanna and Fourtinée Gerges Yacoub; single.

Education: Graduated from El-Tewfikiah Secondary School, Cairo, Egypt, in June 1959; received the Bachelor of Science degree in chemistry with Second Class Honors from the Faculty of Science, Cairo University, in May, 1963; received the Master of Science degree in chemistry, Ain Shams University, Cairo, Egypt, in May, 1968; received the Master of Science degree in chemistry, Clarkson College of Technology, Potsdam, New York, in August, 1971; and completed the requirements for the Doctor of Philosophy degree from Oklahoma State University in July, 1976.

Professional Experience: Demonstrator, Chemistry Department, Faculty of Science, Ain Shams University, Cairo, Egypt, 1963-1969; Research Assistant, Chemistry Department, Clarkson College of Technology, Potsdam, N.Y., 1969-1971; Graduate Instruction Assistant, Research Assistant, Teaching Assistant, Department of Chemistry, Oklahoma State University, Stillwater, Oklahoma, 1972-present; Also Gulf Summer Fellow, 1973 and CONOCO Summer Fellow 1976.

Professional Organizations: American Chemical Society, Phi Lambda Upsilon (Honorary Chemical Society), and American Association of University Professors.